

Matériaux pour la Géologie de la Suisse

## GEOPHYSIQUE

No 19

Publiés par la Commission Suisse de Géophysique  
Organe de la Société Helvétique des Sciences Naturelles,  
subventionnée par la Confédération

# A NEW GEOMAGNETIC SURVEY OF SWITZERLAND

Un nouveau levé géomagnétique  
de la Suisse  
Eine neue geomagnetische Landesaufnahme  
der Schweiz

GASTON FISCHER  
P.-A. SCHNEGG  
JEAN SESIANO

En Commission  
chez Kümmerly & Frey, Geographischer Verlag, Berne  
Paul Attinger S.A., Neuchâtel  
1979

# Table of contents

	page		page
List of Tables . . . . .	3	<b>CHAPTER V</b>	
List of Figures . . . . .	3	<b>Contour Tracing of Geomagnetic Maps . . . . .</b>	22
List of Maps . . . . .	3	<b>CHAPTER VI</b>	
Editor's Preface . . . . .	5	<b>The New Reference Station of Neuchâtel</b>	
Résumé . . . . .	6	VI.1. General Layout and Situation . . . . .	23
Zusammenfassung . . . . .	6	VI.2. Station Equipment . . . . .	23
Summary . . . . .	7	<b>CHAPTER VII</b>	
Foreword . . . . .	7	<b>User-Related Problems</b>	
<b>CHAPTER I</b>		VII.1. The Compass Theodolite . . . . .	26
<b>Introduction . . . . .</b>	9	VII.2. Meridian Convergence . . . . .	26
<b>CHAPTER II</b>		VII.3. Secular Variation . . . . .	27
<b>Historical Notes on Geomagnetic Measurements in</b>		VII.4. The Influence of Altitude . . . . .	27
<b>Switzerland</b>		<b>CHAPTER VIII</b>	
II.1. Earliest Records . . . . .	10	<b>Discussion of the Maps</b>	
II.2. The Brückmann Survey . . . . .	10	VIII.1. Map Presentation . . . . .	30
II.3. Recent Surveys . . . . .	10	VIII.2. The Main Anomalies . . . . .	30
II.4. The Regensberg Observatory . . . . .	11	<b>Acknowledgements . . . . .</b>	32
<b>CHAPTER III</b>		<b>Notes . . . . .</b>	33
<b>A New Portable Vector Magnetometer for Geomagnetic</b>		<b>References . . . . .</b>	34
<b>Surveys</b>		<b>Caption to Table VI . . . . .</b>	36
III.1. Principle of the New Magnetometer . . . . .	13	<b>Table VI . . . . .</b>	37
III.2. Construction and Operation . . . . .	14	<b>Map Captions . . . . .</b>	43
III.3. Adjustments and Calibrations . . . . .	15	<b>Maps . . . . .</b>	00
III.4. Two Sources of Errors . . . . .	16		
III.5. Sensitivity and Frequency Response . . . . .	17		
<b>CHAPTER IV</b>			
<b>The New Survey</b>			
IV.1. Basic Strategy . . . . .	18		
IV.2. Network of Survey Stations . . . . .	18		
IV.3. Selection of Survey Stations . . . . .	18		
IV.4. Temporal Variations and the Reduction			
of Field Data . . . . .	18		

## List of Tables

No.		page
Ia	Isolated absolute field measurements at Regensburg.	11
Ib	Yearly averages of the field elements at Regensburg.	12
II	Example of data scatter, arising mainly through the time-reduction procedure.	16
III	Example of AMOS data record.	23
IV	Example of table of hourly means derived from AMOS.	24
Va	Field elements and their gradients at $\varphi = 47^\circ \text{ N}$ , $\lambda = 8^\circ \text{ E}$ , for epoch 1978.0.	28
Vb	Field elements versus altitude at $\varphi = 47^\circ \text{ N}$ , $\lambda = 8^\circ \text{ E}$ , for epoch 1978.0.	28
VI	List of survey sites with measured field elements reduced to epoch 1978.0.	36–42

## List of Maps

The maps are collected at the end of the present report. The map captions are on page 43 and on the back flap.

No.	
1	Declination.
2	Inclination.
3	Amplitude or total intensity.
4	Declination against map North.
5	Horizontal component or horizontal intensity.
6	Vertical component or vertical intensity.
7	Declination anomalies.
8	Inclination anomalies.
9	Amplitude anomalies.
10	Survey sites.

## List of Figures

No.		page
1	Representation of the geomagnetic field vector.	9
2	Declination at Regensburg from 1945 to 1970.	11
3a	Geometrical rotation to find the magnetic axis of a directional sensor.	13
3b	Geometrical rotation of a directional sensor to find the direction of the field.	13
4a–b	Two views of the new vector magnetometer.	14
5	Geometrical construction to illustrate the effects of a levelling error of a vector magnetometer.	15
6a–c	Comparison of the field variations at Fürstfeldbruck and Dourbes.	19
7a–d	Magnetogrammes at Dourbes and Neuchâtel.	20
8	Geometrical sketch to illustrate the convergence of the meridians.	26

## Editor's Preface

The present publication, entitled "A New Geomagnetic Survey of Switzerland", is Report No. 19 of the "Contributions to the Geology of Switzerland – Geophysical Series". It contains a complete account of the detailed work carried out by the Observatoire Cantonal of Neuchâtel between 1972 and 1978, aimed at establishing a new geomagnetic survey of the country as part of the current systematic "Geophysical Survey of Switzerland".

Prerequisite for this comprehensive geomagnetic survey was the design and construction of a new vector magnetometer which facilitated and speeded up the field measurements considerably. A significant increase in station density as compared to the previous survey (1930/31) was achieved in four field seasons (1974–1977), thereby providing data to trace the secular variation across the country for the first time. Another part of this project was the setting up of a new geomagnetic reference station for Switzerland; the new station near Neuchâtel became fully operational in the summer of 1977 and will now provide data for time reduction to anyone in need of geomagnetic reference observations.

The Swiss Geophysical Commission is greatly indebted to Dr. Gaston Fischer and his collaborators, Drs. P.-A. Schnegg and J. Sesiano, for having taken the initiative of realizing this important project. They have provided the necessary instrumentation for the new geomagnetic survey and carried out the extensive field measurements in a remarkably short time. The outcome of this work is the present report with its 10 maps, for the content of which the authors accept sole responsibility.

Special thanks for financial support are due to the Swiss Federal Office of Science and Research, the Swiss National Science Foundation, the Swiss Academy of Natural Sciences, the Topographical Survey of Switzerland and last – but not least – to the Canton of Neuchâtel, which has carried the major burden of the present project.

Zurich, May 1979

In the name of the  
Swiss Geophysical Commission  
The President:



Prof. Stephan Mueller

Un nouveau levé des éléments du champ magnétique terrestre a été exécuté en Suisse. On a mesuré la déclinaison  $D$ , l'inclinaison  $I$  et l'amplitude ou intensité totale  $F$ . La détermination de  $F$  s'est faite au moyen d'un magnétomètre à protons, alors qu'on a mesuré les angles  $D$  et  $I$  à l'aide d'un nouveau magnétomètre vectoriel. Le principe de fonctionnement de ce nouvel instrument consiste à faire tourner une sonde de «fluxgate» dans le champ terrestre. L'orientation de l'axe de rotation est ajustée jusqu'à disparition de tous signaux alternatifs, ce qui se produit lorsque cet axe est parallèle au champ. Un clinomètre fournit aussitôt l'inclinaison, tandis que la déclinaison est déterminée au moyen d'un théodolite à gyroscope.

Les éléments  $D$ ,  $I$  et  $F$  ont été mesurés à environ 450 endroits du pays et des régions avoisinantes de l'étranger. La réduction des mesures a été réalisée sur la base de données des observatoires de Fürstfeldbruck et de Dourbes. Les courbes de niveau des éléments géomagnétiques ont été calculées par un principe de minimalisation du carré de la courbure moyenne. Dans ce rapport on présente des cartes à l'échelle 1:1 250 000 des éléments  $D$ ,  $I$  et  $F$ , ainsi que de  $D_K$  (déclinaison relativement au nord de carte),  $H$  (composante ou intensité horizontale),  $Z$  (composante ou intensité verticale) et des anomalies  $\Delta D$ ,  $\Delta I$  et  $\Delta F$  par rapport à un champ normal.

Les nouvelles cartes sont discutées tant du point de vue de leur utilisation que de celui de leur signification géologique et géophysique. Des cartes à l'échelle 1:500 000 et sur fond tectonique de  $D$ ,  $I$  et  $F$  seront probablement mises en vente par le Service Topographique Fédéral au cours de l'année.

Eine neue Landesaufnahme der erdmagnetischen Feld-elemente ist in der Schweiz durchgeführt worden. Gemessen wurden die Deklination  $D$ , die Inklination  $I$  und die Amplitude oder Totalintensität  $F$ . Ein Protonenmagnetometer diente zur Bestimmung von  $F$ , während die Winkel  $D$  und  $I$  mittels eines Vektor-Magnetometers von neuer Konzeption gemessen wurden. Das Arbeitsprinzip dieses neuen Instrumentes besteht darin, dass eine «Fluxgate»-Sonde im Erdfeld gedreht wird. Die Orientierung der Drehachse wird verstellt, bis alle Wechselsignale verschwinden. Dies trifft ein, sobald die Drehachse parallel zum Erdfeld steht. Ein Klinometer liefert sogleich die Inklination, wobei die Deklination mit einem Kreiseltheodolit gefunden wird.

Die  $D$ -,  $I$ -,  $F$ -Elemente sind an etwa 450 Orten der Schweiz und der angrenzenden Gebiete des Auslandes vermessen worden. Die Zeitreduktion der Daten erfolgte mit Hilfe der Observatoriumswerte von Fürstfeldbruck und Dourbes. Isolinienkarten sind nach einem Prinzip kleinster mittlerer quadratischer Krümmung bestimmt worden. Im vorliegenden Bericht findet man Karten im Massstab 1:1 250 000 der Elemente  $D$ ,  $I$  und  $F$ , sowie von  $D_K$  (Deklination gegenüber Kartennord),  $H$  (Horizontalkomponente beziehungsweise Horizontalintensität),  $Z$  (Vertikalkomponente oder Vertikalintensität) und auch von den Anomalien  $\Delta D$ ,  $\Delta I$  und  $\Delta F$  gegenüber einem Normalfeld.

Die neuen Karten wurden inbezug auf ihre Anwendung und auf ihren Zusammenhang mit geologischen und geophysikalischen Merkmalen diskutiert. Karten von  $D$ ,  $I$  und  $F$  im Massstab 1:500 000, auf einem tektonischen Untergrund, werden voraussichtlich noch dieses Jahr von der Eidgenössischen Landestopographie zum Verkauf gebracht.

## Summary

A new survey of the geomagnetic field has been carried out in Switzerland. The elements measured are the declination  $D$ , the inclination  $I$ , and the amplitude or total intensity  $F$ . This last parameter was determined with a proton magnetometer, whereas the angles  $D$  and  $I$  were obtained with a new vector magnetometer. This new instrument works on the principle of rotating a fluxgate sensor in the Earth's magnetic field. The axis of rotation is then adjusted until all varying periodic signals disappear. This occurs when the axis of rotation lies in the direction of the Earth's field. A clinometer immediately yields the inclination, while declination is found with a gyroscope and a theodolite.

The elements  $D$ ,  $I$ , and  $F$  have been surveyed at about 450 sites in Switzerland, and abroad in a strip along the country's borders. Time-reduction of the data was effected with the help of the observatory recordings from Fürstentfeldbruck and Dourbes. Contours of the geomagnetic elements were calculated on a principle of minimum integrated squared curvature. This report presents maps with a scale of 1:1 250 000 displaying the elements  $D$ ,  $I$ , and  $F$ , as well as  $D_K$  (declination with respect to map North),  $H$  (horizontal component or intensity),  $Z$  (vertical component or intensity), and the anomalies  $\Delta D$ ,  $\Delta I$ , and  $\Delta F$  with respect to a normal field.

The new maps are discussed from the point of view both of their use and of their geological significance. It is expected that maps of  $D$ ,  $I$ , and  $F$ , with a scale of 1:500 000 and on a tectonic background, will be published in the current year and sold commercially by the Topographical Survey of Switzerland.

## Foreword

The reader unfamiliar with Swiss geography is referred to a detailed map (e.g. the 1:500 000 or 1:300 000 National Maps of the Topographical Survey of Switzerland) to locate the many places mentioned in this report.

**References** are given by the authors' names and year, whereas superscript numbers refer to the **Notes**.

**Equations, Figures, and Maps** are referred to by Arabic numbers in the text, whereas Roman numbers are used for **Chapters** and **Tables**. Individual **Sections** are described with a Roman/Arabic number combination to identify the chapter.

**Angles** are always expressed in sexagesimal degrees ( $D$ ), minutes ( $M$ ), and tenths of minutes ( $m$ ). They are always written in the form  $DD^\circ MM.m$ , for example  $62^\circ 31.7$  (except in Table VI where the notation  $DD.MMm$  is used, i.e. 62.317 for the example above).

## CHAPTER I

### Introduction

The decision to undertake a new geomagnetic survey of Switzerland was taken essentially for two reasons. The first concerns station density, the second has to do with secular variation. The original Brückmann survey (BRÜCKMANN 1930, 1931) had an average station density of one station per 308 km<sup>2</sup>. But this density was by no means uniform; it was higher in the anomalous areas of the cantons of Vaud and Ticino, and accordingly lower elsewhere. As a consequence several large anomalies were left undetected, especially in the cantons of Valais and Graubünden. Even though the existence of some of these anomalous areas was later mentioned occasionally in the literature and was known to the Topographical Survey of Switzerland, these anomalies were never charted. Nor were they indicated in any of the geomagnetic maps published by Brückmann's successors up to 1973. Several of these successors improved the data in particular areas, but not until the present survey was any attempt made to follow secular variation in various parts of the country. For all the declination maps issued or published between 1931 and 1973 it was assumed that over the entire country secular variation was uniformly the same as at Regensburg, where a reference station had been set up by BRÜCK-

MANN (1930). This of course is not true and has led, especially in the westernmost regions of Switzerland, to increasing errors which for the 1972.5 map amounted to 15 arc-minutes (cf. Sec. VII.3).

A corollary to the survey work was the project to establish a new geomagnetic reference station, because the Regensburg station was falling into disuse. Unfortunately, our own new station became fully operational only in the Summer of 1977 and we had, therefore, to turn to the geomagnetic observatories of Fürstfeldbruck, near Munich, and of Dourbes, in southern Belgium, to obtain the necessary data for time-reduction. The new reference station will nevertheless be described briefly in Ch. VI of the present report, as it provides now the data for time-reduction required by users of the new survey. This station can be considered as part of the new geomagnetic service of Switzerland.

Work for the survey began in 1972 with the construction of a new vector magnetometer described in Ch. III. Early in 1974 the field equipment was completely assembled and a preliminary survey of the entire country, with a rather coarse triangular mesh of about 30 km, was carried out in that year. A first set of new although still provisional maps of the elements  $D$ ,  $I$ , and  $F$  (cf. Fig. 1) was made available to the Swiss Topographical Survey and the Swiss Federal Air Office at the end of 1974.

Other chapters of this report will be devoted to a brief historical review (Ch. II), the survey work itself, including data reduction (Ch. IV), map production (Ch. V), some notes addressed to users of the survey (Ch. VII), and a short discussion of the geological implications of the new geomagnetic maps (Ch. VIII).

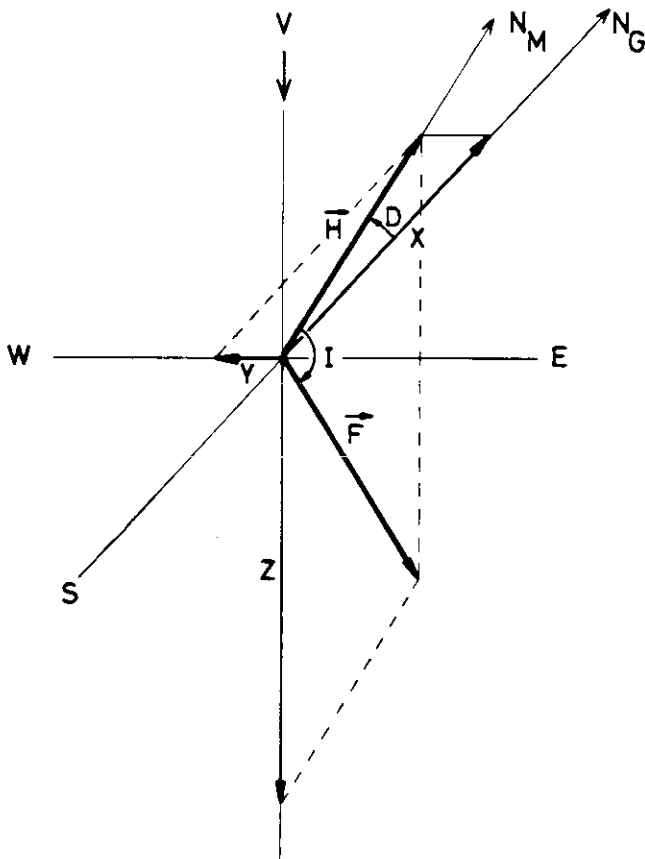


**Figure 1.** Several different representations of the geomagnetic field vector  $F$  are in usage. The modern tendency is to give  $F$  by its orthogonal components ( $X$ ,  $Y$ ,  $Z$ ). More traditionally  $F$  was given in terms of its horizontal and vertical components,  $H$  and  $Z$  respectively, and its declination  $D$  (angle between magnetic North  $N_M$  and geographic North  $N_G$ ). It is also very useful to introduce the horizontal and vertical vectors  $H$  and  $Z$ , as for example in this figure for  $H$  and in Fig. 5 for  $H$  and  $Z$ . In the present report we speak mainly in terms of the parameters that were measured in the survey, i.e., declination  $D$ , amplitude  $F$ , and inclination  $I$  (angle between  $F$  and the horizontal plane). Note that in Switzerland the vector  $F$  points downward and slightly west of geographic North, implying that component  $Y$  and declination  $D$  are negative. All other components are positive. If, in the above situation,  $D$  is given by a positive number it must be stated that it refers to a **westerly declination**.

## Historical Notes on Geomagnetic Measurements in Switzerland

### II.1. Earliest Records

A very exhaustive listing of geomagnetic measurements performed in Switzerland before 1900 has been published by MAURER (1907). We refer the interested reader to this bibliography, from which only a few events of that early period will be mentioned here.

The first declination measurements on record in Switzerland are probably those quoted by WOLF (1858); they were carried out in Basel in 1531. This is even earlier than the first recorded but anonymous measurements of 1540 in Great Britain (MALIN). In the 18th and 19th centuries occasional declination and inclination determinations were made in Basel, Geneva (Genève) and Zurich, mostly by foreign scientists, e.g. HUMBOLDT and GAY-LUSSAC (1808), because they expected to observe large anomalies connected with the Alps. The first reliable measurements of all the vector components were made by WILD and SIDLER (1859) in Bern.

Between 1888 and 1892 BATELLI (1889, 1892 a, 1892 b) carried out the first survey of the magnetic elements over the entire territory of Switzerland and published the first maps (BATELLI 1892 b). But Batelli's work apparently suffered from inadequate data reduction to compensate for random temporal variations (cf. Sec. IV.4). Furthermore, Batelli all but completely failed to observe the important Jorat anomaly which extends over a large area around Lausanne (cf. Maps 1–9).

MAURER (1885 a, 1885 b) and the Dutch scientists VAN RIJCKEVORSEL and VAN BEMMELEN (1896, 1899) tried without success to find a relationship between altitude and magnetic field (cf. Sec. VII.4), with measurements in the areas respectively of the Säntis and the Rigi.

### II.2. The Brückmann survey

The events from 1900 to 1930 that preceded and finally led to the Brückmann survey have been discussed in much detail by BRÜCKMANN (1930) himself. From that period we only mention BRÜCKMANN's (1913) unsuccessful attempts at establishing a correlation between geomagnetic field and altitude, at which occasion Brückmann even set up a temporary reference station in Grindelwald.

In 1927 BRÜCKMANN (1930) established a permanent reference station at Regensberg near Zurich, where horizontal, vertical and total intensities, as well as declination, were recorded continuously (cf. Fig. 1). A year later a complete survey of the country was started. BRÜCKMANN's (1930, 1931) survey stations usually correspond-

ed to geodetic reference points. Stations in Germany (Tülingen, north of Basel), France (Annemasse, east of Geneva), Italy (Domodossola), and Austria (Bregenz) secured integration of the new survey into the international network. The approximately square mesh size of the survey was about 40 km, but the anomalous regions of the Upper Valais (Gomsertal), of the Ticino, and around Lausanne subsequently received more attention, with a measurement site every 13 to 18 km.

The survey was completed in 1931. 134 stations had been visited; at most of these declination, inclination, and horizontal intensity had been measured. BRÜCKMANN (1930, 1931) published tables of all his data and maps of the elements D, I, H, Z (cf. Fig. 1) for epoch 1931.5. The elements X, Y, Z and total intensity F were also tabulated. CADISCH (1932) soon gave a cursory geological interpretation of the new maps.

A few years later BRÜCKMANN (1933) anticipated secular variation and published a declination map for epoch 1935.5. But in this new map declination was referred to the rectangular or kilometric x, y coordinates of the maps rather than to geographic North (cf. Sec. VII.2).

### II.3. Recent Surveys

MERCANTON and WANNER (1943, 1945) carried out a detailed survey of the Jorat anomaly (cf. Maps 1–9). The vertical component Z was measured at 211 sites distributed mainly over the entire Canton of Vaud, but with an especially high density around Lausanne, although no data could be obtained over Lake Geneva (Lac Léman), into which the anomaly obviously extends. MERCANTON and WANNER (1946, 1948) then measured horizontal intensity H at 165 sites and declination D at 90 sites, for the most part different from the ones visited during the Z survey. The possible origin of the anomaly was carefully investigated, and it was concluded that it could only be due to some fairly magnetic intrusion at a depth of several kilometers, oriented about S 60° W, i.e. roughly parallel to the Alpine arc in that area. Such a model could also fit the gravimetric measurements of NIETHAMMER (1921). DE LORIOLE (1962) extended the Z survey to the south of Lake Geneva (Lac Léman), into France. More recently, MEYER DE STADELHOFEN, SIGRIST, and DONZÉ (1973) surveyed the Jorat anomaly again, this time measuring total field F and extending the survey over the waters of Lake Geneva and again into France on the south shore. Their results improved upon but essentially confirmed the model proposed by MERCANTON and WANNER (1946, 1948). It is worth stressing, however, that present geologic knowledge in the Jorat is very cursory at depths beyond about two kilometers. There is thus



no geological evidence speaking for or against the proposed model at this time.

WEBER, GASSMANN, NIGGLI, AND RÖTHLISBERGER (1949) surveyed the Locarno anomaly (cf. Maps 1-9) in detail during 1944 and 1945. Horizontal and vertical components, H and Z, were measured at 178 sites and detailed maps published for epoch 1944.5. Here interpretation was reasonably straightforward and obviously connected with the Ivrea body, with which both orientation and width of the anomaly agree. But the survey only covered the very small part of the Ivrea body that projects into Switzerland, in the Locarno-Brissago area. No serious model calculation was attempted, however (cf. Sec. VIII.2).

WANNER (1947) using the MERCANTON and WANNER (1946, 1948) data, as well as some 20 new declination measurements in the Cantons of Ticino and Graubünden published a somewhat improved declination map for 1948.0. GRÜTER (1965) then synthesized all available data and in collaboration with the Topographical Survey of Switzerland issued the set of maps most widely known today of declination D, and horizontal and vertical intensities H and Z, for epoch 1962.5. But we shall see proof in Sec. VII.3 that this map is still based essentially on BRÜCKMANN's (1930) data. Provisional but really new maps of D, I, and F have been published only recently by FISCHER and SCHNEGG (1977).

In 1970 an aeromagnetic survey of total intensity F for parts of the Swiss Jura and Plateau was made by the Compagnie Générale de Géophysique (Paris) for the SHELL Petroleum Company and a map has been published and analyzed by BITTERLI (1970). A similar aerial survey over part of the same area was carried out in 1959 and discussed by SCHWAB (1960).

II.4. The Regensburg Observatory

There is ample evidence that in the early days of the Regensburg station the reference data was used by Brückmann and others in their survey work to effect the temporal reduction to a given epoch. It seems, however, that no table of annual means or other records were published or stored away for safekeeping. The only absolute values published are those for 1931.5 and 1940.75, as shown in Table Ia. At the time of Wanner's 1940.75 declination measurement the Regensburg station was in fact being enlarged and modernized (WANNER 1939). But no other such measurements appear to have been made.

Table Ia - The geomagnetic field elements at Regensburg from isolated absolute measurements reduced to specified epochs<sup>1</sup>. D<sub>w</sub> signifies that declination is westerly. Units are sex. degrees and minutes for D<sub>w</sub> and nT<sup>10</sup> for the other elements.

Epoch	D <sub>w</sub>	I	F	H	Z	X	Y
1931.5	7° 26.0						
1940.75	5° 53.2						
1975.5	2° 30.8	63° 11.1	46849	21134	41811	21114	-924

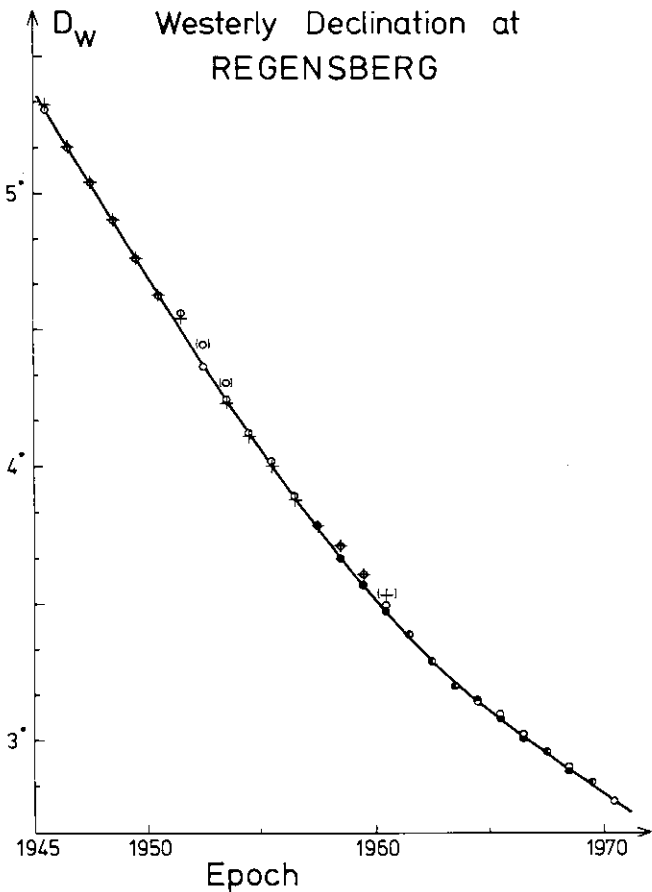


Figure 2. Westerly declination at Regensburg from 1945 to 1970. The source of the various data points is given in Note n° 1. The data point nearest to the curve traced is listed in Table I, except for 1951 where we arbitrarily chose the curve intercept, since both data points were quite far off the curve.

In 1945 the first annual means seem to have been computed and recorded. These means, listed in Table Ib and Fig. 2 were obtained from different sources<sup>1</sup> which did not always agree. We decided, therefore, to plot all declination data obtained on a graph and traced the apparently fitting curve of Fig. 2, choosing for Table Ib the data points closest to the curve, except for 1951, where the value given in Table Ib is deduced from the curve.

After 1970 annual means were no longer computed. At the close of 1975, operation ceased completely and the station was finally dismantled<sup>2</sup>.

**Table Ib** – The geomagnetic field elements at Regensburg<sup>1</sup>.  $D_w$  signifies that declination is westerly.  $\langle \rangle$  means yearly average.  $\Delta D_w$  is the annual decrease of  $\langle D_w \rangle$ . Units are sex. degrees and minutes for  $D_w$  and I, and nT<sup>10</sup> for the other elements.

Year	$\langle D_w \rangle$	$\Delta D_w$	$\langle I \rangle$	$\langle F \rangle$	$\langle H \rangle$	$\langle Z \rangle$	$\langle X \rangle$	$\langle Y \rangle$
1943			63° 24.5	45926	20558	41068		
1945	5° 18.5	8.4						
1946	5° 10.1	7.5						
1947	5° 02.6	8.4						
1948	4° 54.2	8.3	63° 26.6	46069	20597	41208	20522	-1760
1949	4° 45.9	8.3						
1950	4° 37.6	7.6						
1951	4° 30.0	8.1						
1952	4° 21.9	7.1						
1953	4° 14.8	7.3	63° 25.3	46209	20675	41326	20618	-1531
1954	4° 07.5	7.4						
1955	4° 00.1	7.2						
1956	3° 52.9	5.6			20703			
1957	3° 47.3	7.3	63° 25.4	46311	20719	41418	20674	-1369
1958	3° 40.0	5.8	63° 25.0	46341	20737	41442	20695	-1326
1959	3° 34.2	5.7	63° 24.7	46364	20752	41461	20712	-1292
1960	3° 28.5	5.3	63° 25.0	46407	20763	41501	20725	-1259
1961	3° 23.2	5.8	63° 23.5	46432	20795	41514	20759	-1228
1962	3° 17.4	5.4	63° 22.3	46452	20820	41525	20786	-1195
1963	3° 12.0	3.2	63° 21.5	46474	20840	41544	20808	-1163
1964	3° 08.8	4.1	63° 20.4	46501	20865	41557	20834	-1145
1965	3° 04.7	3.8	63° 19.0	46523	20891	41569	20861	-1122
1966	3° 00.9	3.5	63° 18.5	46543	20906	41583	20877	-1100
1967	2° 57.4	3.6	63° 18.1	46561	20920	41597	20892	-1079
1968	2° 53.8	3.4	63° 17.0	46589	20945	41615	20918	-1058
1969	2° 50.4	3.8	63° 15.7	46619	20974	41634	20948	-1039
1970	2° 46.6							

## A new portable Vector Magnetometer for Geomagnetic Surveys<sup>3</sup>

### III.1. Principle of the New Magnetometer

With the advent of the portable, highly accurate, and relatively inexpensive proton magnetometer<sup>4</sup>, accurate and detailed surveys of the amplitude  $F$  of the Earth's magnetic field vector  $\mathbf{F}$  have become extremely easy. When it comes to measuring the direction of this vector, specifically and with reference to Fig. 1, declination  $D$  and inclination  $I$  with the same sort of accuracy, one still faces a very difficult task. Many types of instrument have been proposed (for a review cf. PRIMDAHL 1970, and SERSON and PRIMDAHL 1972) but in general they are either very cumbersome and expensive or they are of very low accuracy. Instruments of the "fluxgate" type<sup>5</sup> are available at low cost, but they suffer from two main defects: the geometric axis of the sensor probe in general coincides only roughly with the sensor's magnetic axis, and the electronics are subject to erratic drifts which prevent the use of the instrument as a reliable null indicator<sup>5</sup>.

Let us imagine a device that can rotate a fluxgate sensor around an arbitrary axis, at a speed slower than the frequency response of the instrument, e.g., one rotation in 1 or 2 seconds. When the sensor is in rotary motion one can visualize its magnetic axis as sweeping the surface of a circular cone. The axis of the cone coincides with that of the rotary movement imposed, but the angle at the apex of the cone is usually not accurately known. Obviously the sensor samples all the field components over the conical surface it sweeps. This results in a signal with strong AC components, except for two limiting situations, where for simplicity of the present argument we assume that the field to be measured, i.e., in particular the Earth's magnetic field  $\mathbf{F}$ , is constant in time and locally uniform:

- No AC signals will be generated **if the sensor's magnetic axis is parallel with the rotation axis**. This is true no matter what direction the field actually assumes, and this property can be used, if one wishes, to identify the sensor's magnetic axis. This situation is represented in Fig. 3a.
- When the magnetic axis of the sensor is not parallel to the axis of rotation, no AC signal will be observed **if the axis of rotation coincides with the direction of the field to be measured**. Clearly, in this second situation, the field components over the circular cone swept by the sensor are all of the same magnitude. This is the property which we are using to identify the direction of  $\mathbf{F}$ . Fig. 3b depicts this situation diagrammatically.

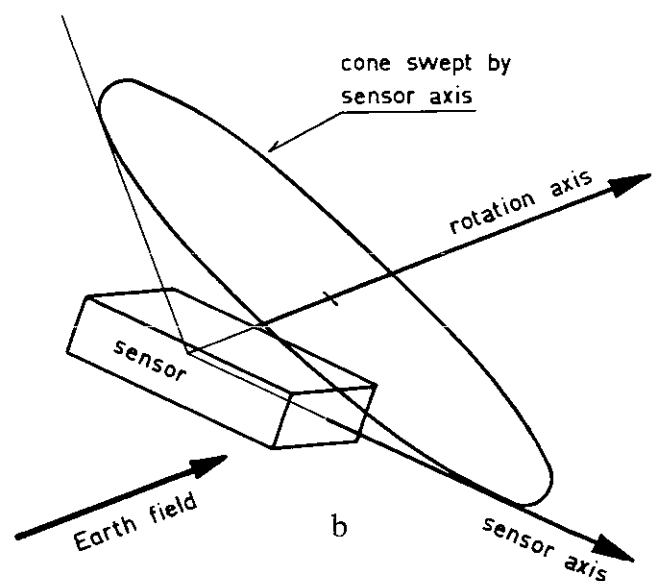
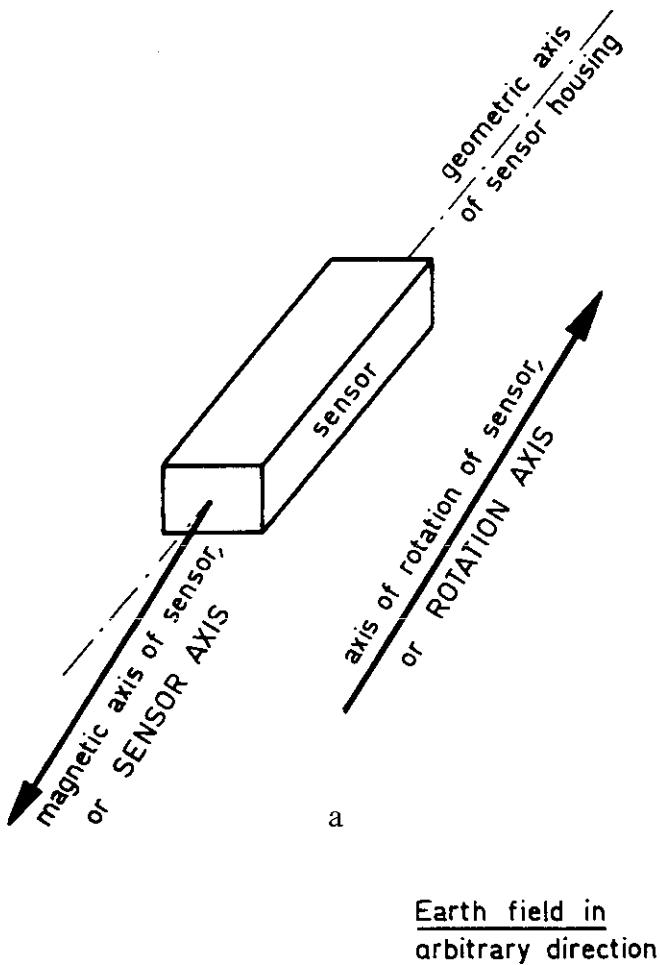


**Figure 3.** Two geometries in which no AC signals are induced during rotation of a fluxgate sensor in a uniform steady magnetic field. In situation (a) the magnetic sensor axis is parallel to the rotation axis. In (b) the rotation axis is parallel to the ambient field.

Obviously in situation (b) the highest sensitivity will be achieved when the cone swept by the sensor's magnetic axis is as obtuse as possible, meaning that the sensor should be placed approximately at a right angle to the rotation axis, as suggested by Fig. 3 b. It is worth remarking at this point that the disappearance of all AC signals will also take place when the sensor is not rotated at a uniform speed, for example in an alternating rotation only partway around a full turn, as long as the portion of conical surface swept by the sensor is truly circular.

Our method therefore consists in finding the orientation of the rotating shaft which corresponds to the limiting situation described above under (b), and is thus a modern version of the classical "earth inductor". The orientation of this rotating shaft is then coincident with the direction of **F**. What must be done next is to measure the inclination of the shaft and its declination with respect to geographic North. In Sec. III.2 we shall describe how this can most easily be carried out.

Fluxgate sensors rotating with spacecraft on which they are mounted have been used in space exploration (see, e.g., NESS 1970). The rotation of the platform allows sampling of the field in various directions, but is not controlled with the aim specifically of aligning the axis of rotation with the prevalent field in order to derive the field direction with the highest possible accuracy.

### III.2. Construction and Operation

The instrument we have built is a vector magnetometer working on principle (b) discussed in the previous section

and is shown in Fig. 4. We see in this figure that the rotating mechanism of the magnetometer is supported like a seesaw on a yoke in the form of an inverted two-pronged fork. The inclination of rotating axis (G) can be adjusted by rotation around the seesaw shaft (F). Rotating axis (C) carries a fluxgate-type sensor<sup>6</sup> (D), but because of the cable joining sensor and metering cabinet it is preferable, to avoid sliding contact problems, not to rotate the sensor continuously in the same sense. We have chosen a rotation over about 200°, back and forth in approximately two seconds, with a lever and excenter mechanism (B) driven by a miniature DC motor (A). The inverted fork can be pivoted about a vertical axis, so that the rotating sensor shaft (C) can be oriented in any direction. The entire mechanism fits on a non-magnetic theodolite base (I) and tripod (J).

In field operation, the orientation of rotating shaft (C) is adjusted until all AC signals disappear. When that happens, rotating shaft (C) is parallel to the Earth's field vector **F**. Inclination *I* can then be determined with a precision clinometer (E), which, as Fig. 4 shows, is mounted on the seesaw with rotating shaft (C). Also mounted on the seesaw is a small telescope (M) which can be tipped in a vertical plane parallel to the rotating sensor shaft (C).

After inclination has been recorded a surveyor's ranging pole is driven into the ground, at a distance of between 20 and 100 meters, in the exact center of the telescope's viewing field. Depending on the topography at the survey site, the telescope can be aimed in the direction of magnetic North or magnetic South, whichever is more suitable. The ranging pole carries a solid flag with a scale and two mark-

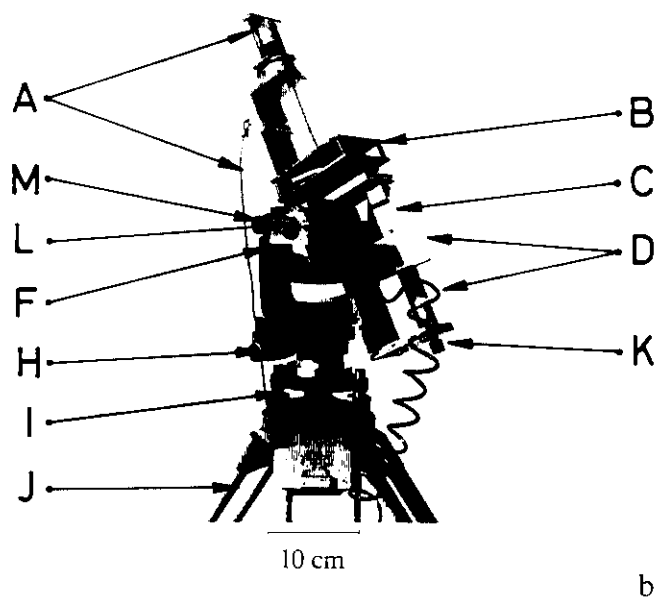
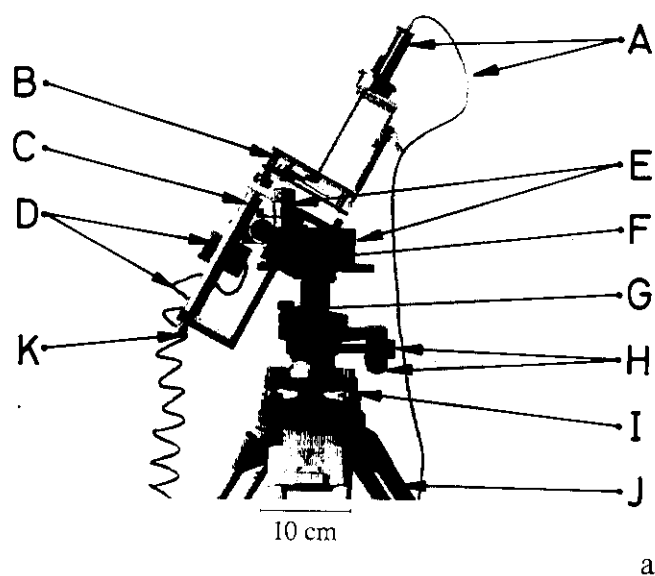


**Figure 4.** Two views of the new vector magnetometer. (A) Motor in its  $\mu$ -metal housing and cable to the battery (6V, 200 mA). (B) Mechanical inverter with lever and excenter. (C) Rotating axis carrying the sensor. (D) Sensor and cable joining it to the metering cabinet. (E) Precision clinometer with micrometer levelling screw. (F) Horizontal seesaw shaft. (G) Micrometer screw for inclination

adjustment. (H) Clamping and micrometer screws for declination adjustment. (I) Theodolite base with levelling screws and water level (for coarse prelevelling). (J) Tripod. (K) Mirror at the end of the sensor-carrying rotating axis. (L) Mirror at the extremity of the telescope (M) tipping shaft. The telescope tipping shaft mount carries a very sensitive water level for accurate levelling.

ers separated by the parallax between rotating shaft (C) and telescope (L). The magnetometer is then removed from the base and replaced by a theodolite<sup>7</sup>. Declination  $D$ , which is the azimuth of the ranging pole with respect to true North, can then be found by triangulation. The accuracy of this declination measurement is essentially determined by the original positioning of the rotating sensor shaft (C), and amounts to about one minute of arc or better.

An easy way of obtaining declination  $D$  without having to carry out any triangulation is to use a theodolite coupled to a gyroscope<sup>8</sup>. This has the great advantage that one can work where no reference targets are available, e.g., in forest clearings or in moderate fog, as long as one can see a ranging pole at about 20 meters. With this instrument we have surveyed the geomagnetic field at as many as ten different sites in one day, measuring the  $D, I, F$  elements three times at each site with an interval of about 30 minutes between the first and second reading (the time required to determine true North with the gyroscope), and a few minutes between second and third readings.

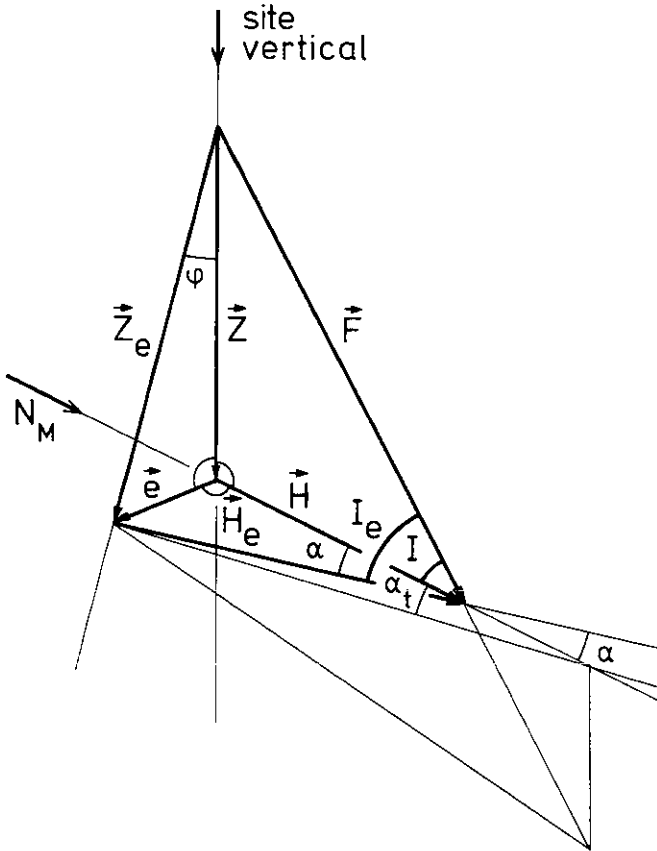


**Figure 5.** Consequences of a levelling error in a plane perpendicular to the horizontal vector  $\mathbf{H}$ . The tilt  $\varphi$  away from the true vertical is fully described by the tilt or error vector  $\mathbf{e}$ . It is seen that the effect of the tilt is to decompose the field vector  $\mathbf{F}$  into vectors  $\mathbf{H}_e$  and  $\mathbf{Z}_e$  instead of  $\mathbf{H}$  and  $\mathbf{Z}$ . Declination  $D$  is affected by a first-order angle  $\alpha$ , whereas there is only a second-order effect on inclination  $I \cong I_e$ .

The magnetometer we have described enables the determination of absolute values of declination  $D$  and inclination  $I$  without requiring calibration at a geomagnetic observatory. All that is needed are two theodolites with autocollimation attachments such as to permit certain calibrations and adjustments during construction. These will be discussed in the following section.

### III.3. Adjustments and Calibrations

Levelling of the magnetometer is achieved with the levelling screws (I) of the base and a sensitive water level, hidden by telescope (M) in Fig. 4a, ensuring verticality of the fork's pivot axis to within 0.1 minute. As will be shown below, this levelling must be carried out with care, since errors in verticality can result in rather large declination errors. Horizontality of the seesaw shaft (F) can be guaranteed to 0.1 minute by proper machining. Inclination clinometer (E) is calibrated by autocollimation with a theodolite, reflecting the reticle on mirror (K) cemented to the end of the rotating sensor shaft (C). Accuracy of this calibration is better than one arc-minute and our working range goes from  $56^\circ$  to  $73^\circ$  inclination<sup>9</sup>, but other ranges can be achieved by slight changes in construction.

Parallelism of the tipping plane of telescope (M) with the vertical plane through rotating sensor shaft (C) is again achieved by autocollimation. Here, both mirror (K) at the end of sensor shaft (C) and mirror (L) at the end of the telescope tipping shaft are necessary, as well as two theodolites. The error of parallelism between these two vertical planes is a few tenths of a minute.

The driving force is provided by a miniature DC motor (1.2 VA, 7500 RPM under load). A 250-fold reducing gear, visible in Fig. 4 below motor (A), brings the speed down to one turn every two seconds, before excenter mechanism (B) transforms this rotation into an alternating motion. Motor (A) is about 35 cm away from fluxgate sensor (D), at which location it produces a field of less than 10 nT<sup>10</sup>. This was measured with a proton magnetometer, the motor being at rest. When the motor rotates it generates AC fields. At first these prevented operation of the proton magnetometer at the short distance of 35 cm. Since these AC fields might also perturb proper operation of the fluxgate sensor, they have been eliminated by means of a  $\mu$ -metal photomultiplier shield which completely surrounds the motor. Effectiveness of this shield was easily demonstrated since the proton magnetometer could again function correctly at the fluxgate sensor location (D) when the motor was operating.

Let us now look at the consequences of an error of levelling on a particular measurement. When the magnetometer is not level, the fork's pivoting axis is not vertical. But this fork axis can be tilted away from the vertical in two directions with greatly different consequences. If the tilt is within the vertical plane which contains the field vector  $\mathbf{F}$  [i.e., the  $(\mathbf{F}, \mathbf{H})$  plane of Fig. 1], the measurement will not suffer at all, for this tilt will automatically be compensated for by some additional rotation around the seesaw shaft when the AC signals are nulled. Since the clinometer (E)

is mounted rigidly on the seesaw shaft (F) it will read the correct inclination irrespective of an initial tilting error within the (F, H) plane. Obviously, no error will affect the measurement of declination either in this situation.

Things are quite different when the fork axis is tilted away from the vertical in a direction at right angles to the vertical plane through F. With reference to Fig. 1 this is a tilt in a plane perpendicular to H. Let us assume, as in Fig. 5, that the error of levelling takes the fork axis away from the vertical by a small angle  $\varphi$ . The magnetometer's rotating sensor shaft (C) can still be adjusted to take the direction of F, for which all AC signals disappear. But now the telescope can only be tipped around in a plane through F which slants by the angle  $\varphi$  away from the vertical. This can be described more simply, saying that the seesaw shaft (F) has been tilted away from horizontal by an angle  $\varphi$ . With reference to Figs. 1 and 5 we see that the vectors Z and H are the vertical and horizontal components of field vector F. But the tilted fork axis is along  $Z_e$ , and  $H_e$  is along the horizontal direction of the tilted plane spanned by F and  $Z_e$ . Auxiliary vector e is in the direction of the horizontal projection of seesaw shaft (F), and its length is a direct measure of the amount of tilt. In effect this vector completely characterizes the tilt perpendicular to H. It is clear from Fig. 5 that  $\alpha$  represents the deviation from the correct declination angle D whereas  $(I_e - I)$  is the inclination error which will result from the levelling error.

Looking at Fig. 5 we can write the following equations:

$$e = Z \operatorname{tg} \varphi. \quad (1)$$

$$e = H \operatorname{tg} \alpha. \quad (2)$$

$$Z_e = Z / \cos \varphi. \quad (3)$$

$$H_e = H / \cos \alpha. \quad (4)$$

From these equations we deduce that

$$\operatorname{tg} \alpha = \operatorname{tg} \varphi \cdot \operatorname{tg} I \quad (5)$$

and

$$\operatorname{tg} I_e \cong \frac{\cos \alpha}{\cos \varphi} \cdot \operatorname{tg} I \quad (6)$$

In the latitudes we are considering,  $\operatorname{tg} I$  is finite, and since we expect  $\varphi$  to be very small (less than 0.1 arc-minute), equations (5) and (6) can be approximated by

$$\alpha \cong \varphi \cdot \operatorname{tg} I. \quad (7)$$

$$\operatorname{tg} I_e \cong \operatorname{tg} I. \quad (8)$$

From this we conclude that inclination is quite insensitive to all levelling errors. Not so declination, however. In Switzerland  $I \cong 63^\circ$ , so that  $\operatorname{tg} I \cong 2$ , and we see that a levelling error of one arc-minute could lead to an error twice as large in declination.

In the preceding evaluation of the consequences of levelling errors, we assumed implicitly that the measurement of declination was being carried out on level ground and

that the telescope was pointing in the direction of vector  $H_e$ . When the measurement takes place on sloping ground the telescope may have to be pointed away from horizontal. Fig. 5 then shows that equations (5) and (7) must be replaced by

$$\alpha_i \cong \operatorname{tg} \alpha_i = \operatorname{tg} \varphi \cdot \operatorname{tg} I_i \cong \varphi \cdot \operatorname{tg} I_i, \quad (9)$$

where  $I_i$  is the angle between F and the telescope's optical axis. Errors due to faulty levelling will therefore increase when ground slopes up toward north, and decrease if it slopes down toward north. The reverse naturally holds if the telescope has to be aimed south.

#### III.4. Two Sources of Errors

In a recent geomagnetic survey of Baden-Württemberg (south-western Germany), FARKAS (1973) also used a Wild gyroscope<sup>8</sup> to determine geographic North. Farkas carefully studied the accuracy that can be expected through proper use of the gyroscope. He concluded that the inner error (systematic instrumental errors plus random scatter) amounts to about  $\pm 12$  arc-seconds, in good agreement with the manufacturer's claim of  $\pm 20$  arc-seconds, and well within the range of  $\pm 1$  arc-minute that we estimate as overall accuracy for our declinations.

An outer source of errors must be mentioned: the local deviations from the vertical (in German: Lotabweichungen) which are generally unknown at our survey sites. These deviations affect the operation of the gyroscope, as well as our vector magnetometer (cf. Sec. III.3). In Switzerland the largest deviations from the vertical are about  $\pm 20$  arc-seconds (ELMIGER 1971, GURTNER 1978), but are usually smaller. Their effect on the gyroscope is considered to be negligible by FARKAS (1973), who claims that gyroscopic North (i.e. the north direction identified by the gyroscope) is essentially the same as geodetic North. This opinion is not shared by R. SCHWEN-DENER, who believes that gyroscopic North is dependent on the east-west component of the deviation from the vertical, and is therefore rather close to astronomic North. But even in this second case the resulting error will only be of the order of 0.1 arc-minute.

**Table II** – Reduction of test site data measured at various dates to a common reference time  $t_0$ , arbitrarily chosen as epoch 1977.0. The site is Frochoux ( $x = 210.250$  km,  $y = 567.100$  km). Units are sex. degrees and minutes for D and I, and nT<sup>10</sup> for F.

Date	$D_{1977.0}$	$I_{1977.0}$	$F_{1977.0}$
18.04.75	2° 51.3	62° 42.1	46739
13.08.75	2° 51.5	62° 42.1	46740
16.05.76	2° 50.6	62° 41.7	46740
10.03.77	2° 51.7	62° 40.9	46740
13.04.77	2° 51.8	62° 41.9	46735
04.10.77	2° 52.6	62° 41.9	46730

The effects on the magnetometer are similar. Inclination  $I$  is only affected by the component of the deviation from verticality in the direction of magnetic North, the direction of vector  $\mathbf{H}$ . Typically this is 0.1 arc-minute again, and therefore again at the sensitivity threshold of the magnetometer. The influence on the measurement of declination  $D$  can be deduced from the discussion in Sec. III.3, where it was shown that only the deviation in the plane perpendicular to vector  $\mathbf{H}$  matters, and can therefore lead to an error of 0.2 arc-minute. But since  $\mathbf{H}$  is perpendicular to the magnetic east-west direction, it is this component of the deviation from the vertical that affects the determination of magnetic North. If the gyroscope behaves as R. SCHWENDENER believes, rather than according to FARKAS (1973), the effects of the deviation from the vertical on the gyroscope and on the vector magnetometer are opposite in sign, and of the same order. The effect on the gyroscope depends on latitude, whereas the effect on the magnetometer depends on the angle between the field vector  $\mathbf{F}$  and the direction toward which the telescope must be aimed on the ranging pole target (cf. Sec. III.3 and Fig. 5).

In conclusion we can say that errors attributable to the local deviations from the vertical are just small enough that they can be overlooked. They are about an order of magnitude smaller than the overall errors that must, for the main part, be attributed to the procedure of time-reduction (cf. Table II) to be discussed in Sec. IV.4.

### III.5. Sensitivity and Frequency Response

The sensitivity of the new vector-magnetometer is best demonstrated by the gradual reappearance of AC signals after they have been suppressed by the alignment procedure carried out in determining the direction of the field vector  $\mathbf{F}$ . Unless the field is exceptionally stable it usually

takes only 10 to 20 seconds for AC signals at the rotation frequency to appear again as a consequence of the slow ( $< 0.5$  Hz) components of the fluctuations of  $\mathbf{F}$ .

When the magnetometer is correctly aligned with the direction of a stable field  $\mathbf{F}$ , AC signals can also be observed as soon as the magnetometer alignment is changed by about one tenth of a minute of arc in inclination and about two tenths in declination. These sensitivity thresholds can be achieved only if the fluxgate sensor<sup>5,6</sup> is itself sufficiently sensitive, and should be compared with the sensitivity of one nT for the measurement of  $F^4$ . According to Fig. 1

$$\begin{aligned} H &= F \cos I, \\ Y &= X \tan D. \end{aligned} \quad (10)$$

Let us calculate what changes in  $H$  and  $Y$  correspond respectively to 0.1 arc-minute in  $I$  and 0.2 arc-minute in  $D$ . In Switzerland  $F \cong 47\,000$  nT,  $X \cong 21\,300$  nT,  $I \cong 63^\circ$ , and  $D < 4^\circ$ . Therefore,

$$\begin{aligned} \Delta H &= F \sin I \Delta I \cong 1.2 \text{ nT}, \\ \Delta Y &\cong X \Delta D \cong 1.2 \text{ nT}. \end{aligned} \quad (11)$$

We see that the sensitivity threshold is of the same order for the measurement of all field components, even though in the measurements of the angles  $D$  and  $I$  the accuracy is as much as 5 to 10 times lower than in the measurement of the amplitude  $F$ . The frequency response of the vector-magnetometer is limited by the speed of rotation of the fluxgate sensor, and therefore lies around 0.2 Hz.

Observatory instruments based on principles similar to the ones embodied in our field instrument should be capable of achieving higher accuracies and sensitivities. Such an instrument has recently been built by USHER and REID (1975).

## The New Survey

### IV.1. Basic Strategy

The main guiding principles that govern the strategy involved in the present geomagnetic survey of Switzerland derive essentially from factors such as the type of instruments available, the desire for speed and for a small team, the selection of suitable measuring sites in relation to topography, industrial activity, and population density. The problems related to data reduction, to compensate for the temporal variations, also played an important role in determining our strategy. We also wanted to carry out a complete preliminary survey in the first year, with a very coarse mesh, in order to get quickly a general impression about the geomagnetic field over the entire country. In this chapter we therefore discuss in turn the network of survey stations, the selection of stations, and the data reduction and processing.

### IV.2. Network of Survey Stations

The survey was carried out in three phases. In the first phase (1974) the entire country was surveyed with a coarse grid, of triangular mesh roughly 25 km to the side, corresponding to approximately 130 stations. For the second phase (1975 and 1976) a station was chosen inside each triangle and the area surveyed was extended beyond the country's borders to ensure proper matching with the geomagnetic maps of Switzerland's neighbours. Together the first two phases correspond to a grid with triangular mesh of about 15 km to the side, with a total of close to 350 stations. The last phase (1977) was reserved to the confirmation of weak anomalies revealed in the preceding phases and to a more detailed study of the strongly anomalous Alpine areas. On the whole, the survey covers an area of approximately 60 000 km<sup>2</sup> with a total of 450 stations, corresponding to an average triangular mesh of 12.4 km to the side. An equivalent square network would have a mesh size of 11.5 km, but we should note that there are only 4 nearest neighbours in a square mesh against 6 for a triangular network. Our station density is therefore about one per 130 km<sup>2</sup>.

Table VI lists all the stations surveyed, with their (x, y) coordinates (cf. Sec. VII.2) and the observed but reduced field elements.

### IV.3. Selection of Survey Stations

Because of the large number of survey stations, it would have been very difficult to establish fixed survey points, identified for example with pillars. But the flexibility of our instrumentation puts very few limitations on the sites that can be accepted, as long as they are accessible by car<sup>11</sup>. Since azimuth determinations are made with a

gyroscope (see Ch. III), we require no triangulation references and can work in conditions of very low visibility. In a geomagnetic survey the coordinates of a measuring station do not need to be known with high accuracy. It is not necessary, therefore, to establish the geomagnetic survey sites at geodetic reference points. This is an advantage because such reference points are often magnetically perturbed because of the proximity of buildings or roads. With the survey maps at scales of 1:25 000 or 1:50 000 it is possible to identify the station locations to within  $\pm 20$  m.

The survey stations were checked for freedom from artificial perturbation with the proton magnetometer<sup>4</sup>, since anything that perturbs the natural field will generally perturb all its elements. In most areas a site was accepted only if within a radius of 50 m the total field gradient was less than 0.1 nT/m<sup>10</sup>. This can be compared with an average N-S gradient of only 0.003 nT/m in Switzerland (cf. Table Va). In perturbed areas of the Alps the natural gradient often reaches values of 0.1 nT/m or more, so that stations with gradients of up to about 0.3 nT/m had occasionally to be accepted.

Already in the very early phases of the survey, it was found that in mountain areas, sediment-filled valley floors often yielded very good sites. Most other good sites were found in the middle of large smooth meadows or fields. Observations like these strongly influenced the selection criteria for subsequent phases of the survey.

Thanks to the very strict selection criterion of less than 0.1 nT/m uniformity for most stations, a displacement of 100 m can change  $F$  by 10 nT at most, and declination and inclination combined by no more than 0.75 arc-minute. Our belief is that sites which satisfy a uniformity criterion of a few nT per 100 m, and where measurement can be repeated within a radius of 100 m, qualify as repeat stations for secular variation measurements.

### IV.4. Temporal variations and the reduction of field data

Data reduction is possible because, as has long been observed, temporal variations are often highly synchronous over distances of several hundred kilometers (see e.g. GARLAND 1971). Fig. 6 gives an example of this observation. The main reasons behind the high degree of synchronism are twofold: (1) the sources of the variations are at great distances in the ionosphere (see e.g. GARLAND 1971 and WIENERT 1970), and (2) for distances at the surface which are short compared to the Earth's radius the electrical conductivity is mainly a function of depth. But it is well known today that good synchronism cannot be expected in the vicinity of tectonic features



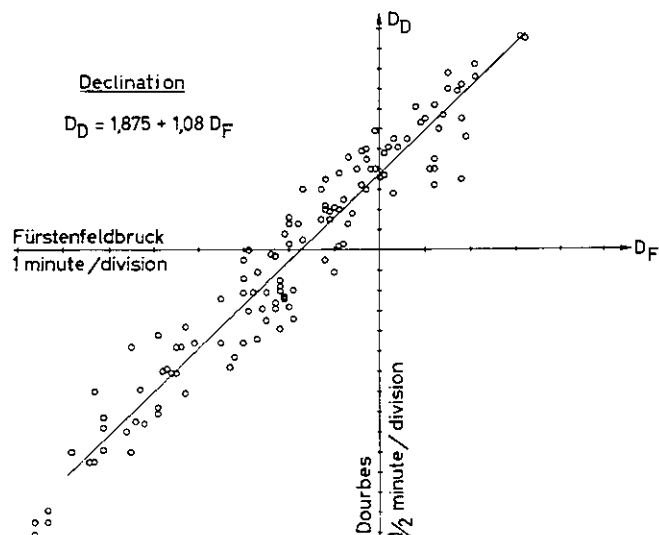


Fig. 6a

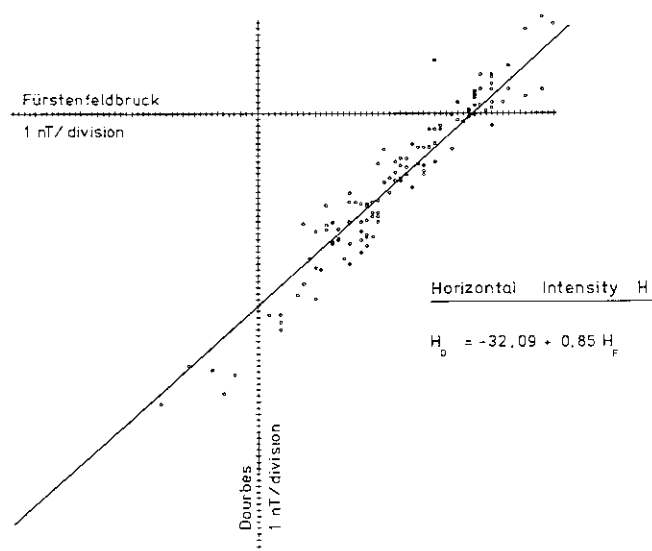


Fig. 6b

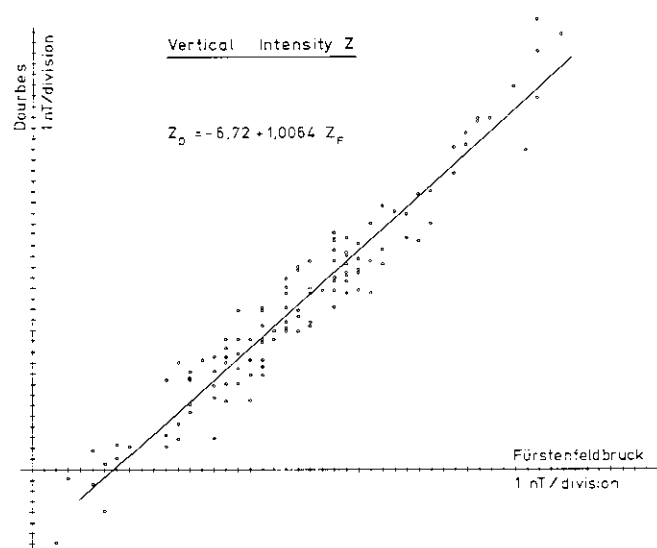


Fig. 6c

exhibiting high lateral conductivity contrasts, such as an ocean coast (see, e.g. FISCHER, SCHNEGG, and USADEL 1978, or FISCHER 1979), or a steeply plunging geological layer of high conductivity in an otherwise low conductivity matrix (see, e.g., WEAVER AND THOMSON 1971). The distances  $d$  from the conductivity discontinuity to which synchronism is perturbed depend on the spectral periods contained in the variations (see, e.g., Figs. 7a–d), and on the ground resistivities on both sides of the discontinuity. This distance  $d$  can be expressed in km as

$$d_{km} = k \sqrt{\rho_{\Omega m} T_{sec}}, \quad (12)$$

where  $\rho$  is the specific resistivity in  $\Omega m$ ,  $T$  the period in seconds, and  $k$  a dimensionless function which varies with the resistivity ratio or contrast. For very large contrasts,  $k$  levels off at about 1.5. It is unity for a resistivity ratio of 10, and vanishes as the resistivity ratio disappears. Typically, for periods of one hour and resistivities of 40 and 400  $\Omega m$ ,  $d = 400$  km and 1200 km on the low and high resistivity sides of the fault. In practice the situation is fortunately not as serious as the above example suggests. Resistivity contrasts can sometimes be very high, but they are generally limited to formations of at most a few hundred meters thickness and several kilometers in lateral extension. Nevertheless, data reduction must be considered a major source of error in any geomagnetic survey, at least at times of magnetic disturbances. Close proximity of two stations ensures good synchronism of their variations only if no conductive fault bisects the two locations. Since the variation gradients are largest near a fault, two distant stations, both remote from the bisecting fault, will exhibit a better synchronism than two close stations separated by the fault. In our opinion uncertainties introduced by data reduction make it illusory to claim an absolute accuracy for reduced data better than about 10 nT for  $F$  and one or two arc-minutes for  $I$  and  $D$ , respectively. This is clearly demonstrated by the data of Fig. 6 and Table II. Table II in fact makes it possible to separate, for reduced data, the scatter which is of instrumental origin from scatter arising through the time-reduction process. Since  $F$  is measured with an accuracy of 1 nT, the  $\pm 5$  nT scatter is about 10% instrumental and 90% due to reduction. For inclination the scatter is probably less than  $\pm 0.6'$ , which according to equations (10) and (11) corresponds to about  $\pm 7$  nT. If reduction is again held responsible for a scatter of about  $\pm 5$  nT, the instrumental scatter is  $\pm 2$  nT. The scatter in inclination is therefore approximately 30% instrumental and 70% due to reduction. The  $\pm 1'$  scatter in declination corresponds to about  $\pm 12$  nT, of which  $\pm 5$  nT may be attributed to reduction (42%),  $\pm 5$  nT to the magnetometer (42%), and  $\pm 2$  nT to the gyroscope (16%). These figures probably give a fair evaluation of the accuracy possible with the new vector magnetometer (cf. Ch. III).

**Figure 6.** Comparison of variations of (a) declination, (b) horizontal intensity, and (c) vertical intensity at Fürstenfeldbruck (near Munich) and Dourbes (southern Belgium). These two observatories are separated by 550 km. Perfectly synchronous variations would lead to points on straight lines with unit slope. The scatter of the points gives an idea of the errors resulting from the process of data reduction. In general synchronism improves when site separation decreases.

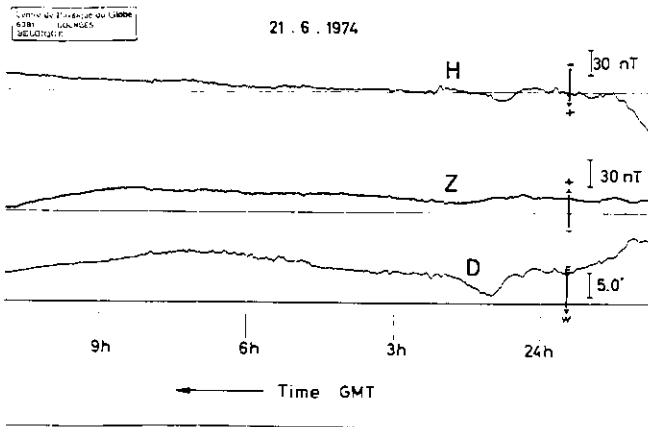


Fig. 7a

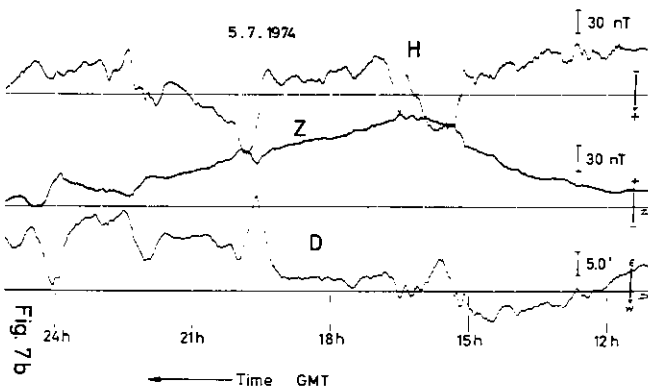


Fig. 7b

**Figure 7.** Magnetogrammes of the geomagnetic field elements D, H, Z in Dourbes on (a) a magnetically quiet day and (b) a magnetically perturbed day. Magnetogrammes of element X, Y, Z at the new reference station near Neuchâtel, on (c) a quiet day and (d) a perturbed day. Figure 7d in effect corresponds to conditions of a small magnetic storm. Note the high sensitivity of recordings (c) and (d). To maintain the high sensitivity we record only the last two digits (e.g. 87 when  $x = 21287$ ). When the end of the scale is reached, the recorder makes a + or -  $100 \text{ nT}^{10}$  jump to the other scale end. This feature, known as "scale expander", is clearly visible in Fig. 7d. It may require a careful inspection of the trace to keep correct track of the hundreds digit during a magnetic storm. But a simultaneous digital recording provides insurance against tracking errors arising from the scale expansion.

Notwithstanding the unavoidable errors associated with data reduction, we have followed the standard practice of reducing our field data with observatory data. As has been said in the Introduction (Ch. I) the reduction was performed with data from the geomagnetic observatories of Fürstfeldbruck near Munich and Dourbes in the south of Belgium<sup>12</sup>. Assuming then that variations at the survey station and at the reference observatory are synchronous, data reduction is effected according to the following formula:

$$F_{\text{stat}}(1978.0) = F_{\text{stat}}(t) - F_{\text{obs}}(t) + F_{\text{obs}}(1978.0). \quad (13)$$

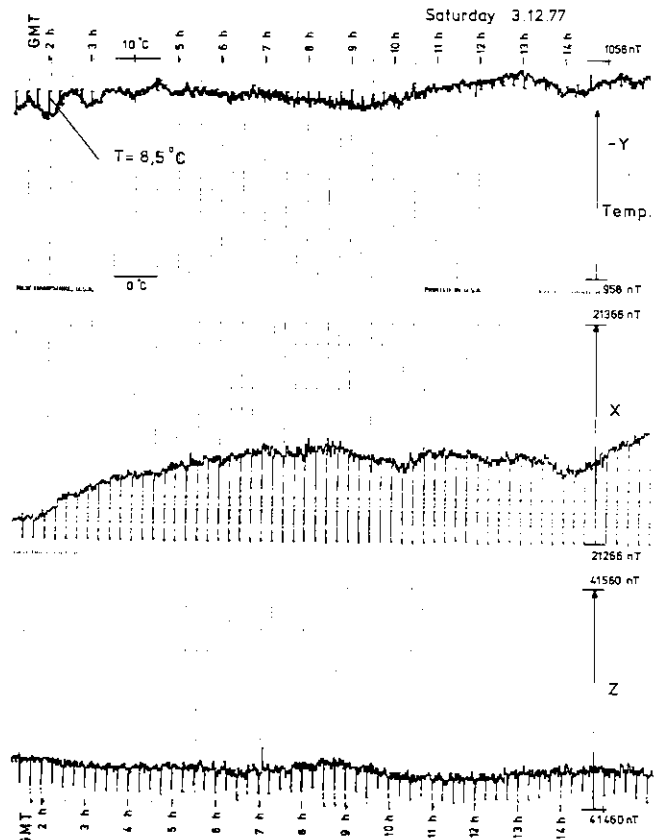


Fig. 7c

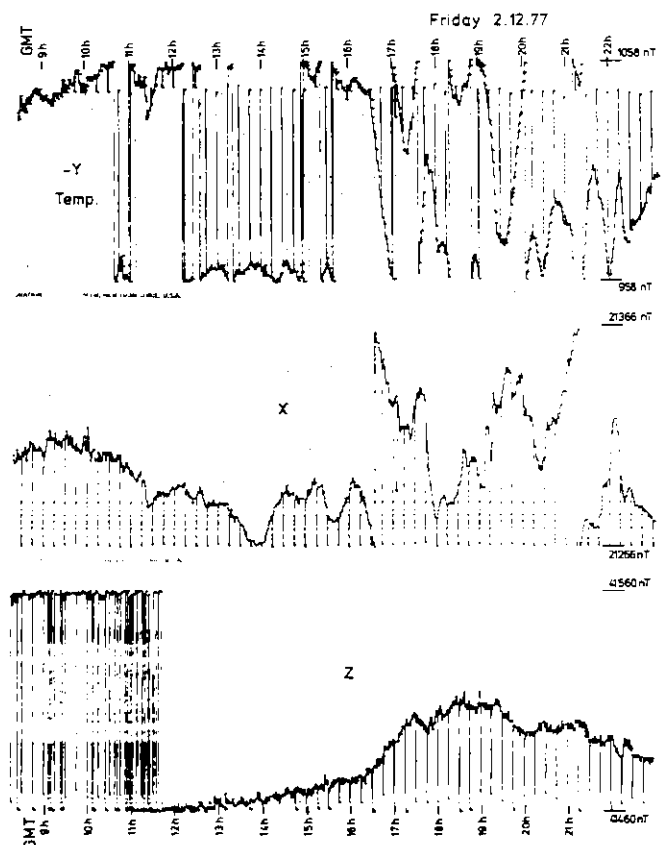


Fig. 7d

where  $\mathbf{F}_{\text{stat}}(t)$  and  $\mathbf{F}_{\text{obs}}(t)$  refer to the geomagnetic field measured respectively at the field station and at the observatory, at the same instant  $t$ . For  $t$ , which represents the times at which measurements are made in the field, we always choose integral minutes of UTC (cf. Sec. VI.2).

Equation (13) means that reduction is made to epoch 1978.0, i. e. midnight of January 1st, 1978. But  $\mathbf{F}_{\text{obs}}(1978.0)$  is not an instantaneous value; it is an average value of the field at the beginning of the year, derived from the observatory's yearly means. These yearly means are thus assumed to represent the average field at mid-year.

## Contour tracing of geomagnetic maps

With the survey data collected and reduced to a common epoch, various contour maps can be traced. There are many well-known methods by which to calculate the contours of a function known at isolated points. We have chosen a procedure based on what may be called a two-dimensional spline, working on a principle of minimum curvature (see e.g. BRIGGS 1974).

Let us describe with  $(x, y)$  the coordinates of a given map point. In accordance with the Swiss military kilometric coordinates (cf. Sec. VII.2),  $x = 200$  km in Bern and increases to the north, whereas  $y = 600$  km in Bern and increases to the east. The passage from  $(x, y)$  to longitude  $\lambda$  and latitude  $\varphi$ , and vice versa, is a simple matter (see e.g. BOLLIGER 1967). We call  $E_i(x_i, y_i)$  the measured and reduced field element  $E$  at survey site  $(x_i, y_i)$ . To calculate the contours of a given field element  $E$ , where for example  $E = D, I$ , or  $F$ , a surface of minimum integrated squared curvature is forced to pass through the data points  $E_i(x_i, y_i)$  in the three-dimensional space  $(E, x_i, y_i)$ . This surface is then intersected by horizontal planes at evenly spaced constant values of  $E$ , for example at values of declination  $D$  from 5 to 5 arc-minutes, as in Map 1, and similarly for  $I$ , shown in Map 2. For  $F$ , represented in Map 3, we choose a spacing of 50 nT.

The surface  $E(x, y)$  of minimum squared curvature which satisfies the condition that

$$E(x_i, y_i) = E_i \quad (14)$$

is given by the differential equation

$$\frac{\partial^4 E}{\partial x^4} + 2 \frac{\partial^4 E}{\partial x^2 \partial y^2} + \frac{\partial^4 E}{\partial y^4} = \sum f_i \delta(x-x_i, y-y_i), \quad (15)$$

where  $\delta(x-x_i, y-y_i)$  is the Dirac delta-function, defined by the following properties:

$$\begin{aligned} \delta(x-x_i, y-y_i) &= \infty & \text{when } x = x_i \text{ and } y = y_i, \\ \delta(x-x_i, y-y_i) &= 0 & \text{everywhere else.} \end{aligned} \quad (16)$$

and

$$\iint_{S_i} \delta(x-x_i, y-y_i) \cdot dx dy = 1. \quad (17)$$

$S_i$  being a small surface element of arbitrary finite size but completely enclosing survey site  $(x_i, y_i)$ .

Equation (15) applies to a uniform, plane, elastic surface, subjected to small vertical deformations by a set of vertical point forces  $f_i$ . In the present problem the forces  $f_i$  are

unknown, but the deformations  $E_i$  at the points  $(x_i, y_i)$  are prescribed. In principle the problem could be solved by calculating first the forces  $f_i$  required to produce the prescribed deformations  $E_i$ . From equation (15), the solution  $E(x, y)$  over the entire area of interest could then be derived. BRIGGS (1974) has shown that this surface minimizes the integrated squared curvature  $C(E)$ :

$$C(E) = \iint \left( \frac{\partial^2 E}{\partial x^2} + \frac{\partial^2 E}{\partial y^2} \right)^2 dx dy. \quad (18)$$

From this condition Briggs has derived an iterative numerical method of solution, based on finite difference equations, in which the forces  $f_i$  need not be determined explicitly.

Successive iterations yield  $[E(x, y)]_n$  at the nodes of a regular fine grid. The set of prescribed values  $E_i(x_i, y_i)$  forms a random network, but in each iteration these values contribute to the determination of the nearest grid node value, which is calculated as intercept of a plane  $E(x, y)$  laid through the measuring site and the two nearest neighbours of the node on the far side of the survey site. In each iteration the integrated squared curvature  $C(E)$  is evaluated to monitor convergence of the process. To start the process an initial situation must be established, but the final result is independent of the initial situation. A good initial choice saves computer time, since fewer iterations are necessary to achieve a preset decrease of  $C(E)$  between successive iterations.

For our maps a square grid of approximately 4.4 km grid spacing was chosen. The initial situation was established with the following set of rules:

- 1) For nodes with a survey site  $(x_i, y_i)$  within a distance of  $a/\sqrt{2}$ , i.e. half a mesh diagonal, the node-value chosen is the measured value  $E_i$ .
- 2) Nodes with survey sites within a range of distances comprised between  $a/\sqrt{2}$  and  $5a$  are given a node-value weighed according to the inverse square distances of the sites.
- 3) Nodes with no measurements within a range of  $5$  grid constants receive the value of the nearest survey site.

About 50 to 60 iterations were generally found to suffice. The grid was then ready for contour tracing, which was done by linear interpolation between neighbouring nodes. Plotter-drawn contours therefore were polygonal. The final smoothing was achieved while drafting the maps.

## The New Reference Station of Neuchâtel

### VI.1. General Layout and Situation

The new geomagnetic reference station is situated in the Bois de l'Hôpital, on a small hill in a protected forest north of the town of Neuchâtel. The site is on the gently sloping lower reaches south of the Chaumont anticline, on Jurassic limestone. This is a reasonably good although certainly not the most ideal location from the point of view of geomagnetic variations (cf. Sec. IV.4) and closeness of the town; but proximity to the Observatory has some decided advantages.

Our station comprises two similar wooden huts, one of which is on the hilltop and houses only the magnetic sensors. The second hut is 40 m distant at about 10 m lower altitude and gives shelter to power supply and electronic equipment. The 4 by 4 m floors contain a one square meter hole or pit at their center. In the top hut the hole is 2 m deep with a flat bottom, where a triaxial fluxgate head is rigidly fixed on a short piece of aluminium pipe cemented into the ground. The pit is plugged with styrofoam to provide a relatively stable temperature environment for the fluxgate sensors. A proton magnetometer sensor is attached under the roof of the hut, about 4 m away from the fluxgate head to reduce interference. It is placed inside a cubic aluminium shield of about 60 cm to a side. An underground plastic pipe ( $\varnothing_i = 8$  cm) leads all cables to the second hut.

This second hut also has a square hole in the center of its floor. Here the pit is 2.5 m deep and the bottom is taken up by a round cement cylinder, 90 cm high, anchored to the rock. The flat cylinder top is destined to receive a set of seismic sensors.

The coordinates of the station, as given by the location of the magnetic sensors, are as follows:

$$\begin{aligned} \text{kilometric} \quad x &= 206.140 \text{ km} \\ y &= 562.665 \text{ km}, \\ \text{geographic} \quad \lambda &= 06^\circ 56' 57''.9 \text{ E of Greenwich} \\ \varphi &= 47^\circ 00' 23''.7 \text{ N} \end{aligned} \quad (19)$$

The altitude is 600 m above mean sea level.

Access to within about 60 m of the station by car is possible practically all year round, by an unsurfaced forest road. The nearest houses or residential roads are 270 m away. Linear distance to the Observatory is 700 m, although by road the distance is about 3.5 km.

### VI.2. Station Equipment

The magnetometer system of our station is an AMOS Mk II from EDA<sup>13</sup>. We have modified it somewhat to suit our requirements. The proton magnetometer has a resolution of 0.2 nT and an accuracy of 0.4 nT. Its temperature dependence is practically linear from  $-15$  to  $+35^\circ\text{C}$  and amounts to  $-0.028$  nT/ $^\circ\text{C}$ . The fluxgates have resolutions of 1 nT. Long-term drifts are a few nT per year and temperature coefficients are about 1 nT/ $^\circ\text{C}$ . These figures are much lower than for portable instruments since the electronics involved in an observatory instrument do not have to satisfy severe volume, weight, and power limitations, and can therefore be more refined.

**Table III** – Example of an AMOS data record. The data is presented in the sequence sY0sX0sZ0F0 after sampling every minute, as described in Section V.2. The components X,Y,Z, each of which is allocated 6 significant digits and its sign s, are given in nT<sup>10</sup>. F is expressed with 7 digits, to a tenth of an nT. The record is 15 minutes long and is terminated by a sequence of 3 control voltages with sign, day (083) and time (2045) information, and a station identification code including the year (012197874). Note that F differs from  $\sqrt{X^2 + Y^2 + Z^2}$  by an amount varying around 25 nT. This is so because the X,Y,Z data are not absolute, but require corrections and occasional calibrations.

```
-0022730+0212910+041510004668270
-0022740+0212930+041512004668200
-0022730+0212920+041514004668350
-0022730+0212940+041514004668510
-0022720+0212920+041512004668270
-0022710+0212900+041510004668150
-0022720+0212920+041512004668080
-0022730+0212920+041514004668480
-0022720+0212920+041515004668550
-0022730+0212940+041514004668430
-0022730+0212920+041513004668390
-0022710+0212920+041514004668710
-0022720+0212910+041514004668560
-0022720+0212910+041510004668110
-0022720+0212910+041512004668450
+0000010+0749390-004840008320450
12197874*
```

The sensors sample the various field elements at precise moments determined by a central control and quartz clock unit. The clock is monitored by the Swiss HBG radio time-signals to follow UTC (see e.g. BONANOMI and SCHUMACHER 1976a and b).

The proton magnetometer samples F for one second every minute, between seconds 59 and 60 = 00 of every UTC minute. The digital data is temporarily stored. The fluxgate system samples X, Y, and Z at a rate that can be set manually from once every second to once every 60 seconds, but the first sampling always occurs between seconds 00 and 01. Sampling time for each component is 45 ms and takes place at the following moments: X from 00.005 to 00.050, Y from 00.105 to 00.150, and Z from 00.205 to 00.250 sec. The (X, Y, Z) information is available in analog form but is also A/D converted and enters a FIFO buffer memory (First In – First Out). In standby operation sampling occurs only once per minute. At the close of every record, the length of which can be adjusted manually but which is set at 15 minutes in standby operation, three control voltages are also sampled and A/D converted. With these voltages continuous monitoring of power voltage and temperature – for example temperature at the fluxgate head – is possible from the observatory situated in the town.

The reference station being in a forest reserve, no power or telephone connections are available. Because of the lack of power the data cannot be recorded at the site itself. A one-way radio link with the Observatory solved this problem. The coded station data is sent by means of an FM modulated 42.8 MHz directional beam to the Observatory, where it is decoded and recorded analogically and digitally. In standby operation data enters the FIFO memory in the sequence Y,  $\emptyset$ , X,  $\emptyset$ , Z,  $\emptyset$ , F,  $\emptyset$ , and is transmitted around 01 second of UTC. At the close of every record, i.e. every 15 minutes, the above sequence is followed by the three control voltages, day and time information, and a station identification code. Table III is an example of a complete standby data record.

Power requirement at the station has been reduced to about 14 W. The transmitter itself needs only 0.5 W and only less than 100 mW are radiated. To generate the necessary power a 24 W thermoelectric generator<sup>14</sup> working on propane gas has been installed. Stability and reliability of this generator are such that no batteries are needed as buffers. To insure adequate power for the power surges required during the polarizing cycles of the proton magnetometer, a 14 Ah Ni-Cd battery has been shunted across the power supply line. Propane consumption is

TABLE IV – Example of a table of corrected hourly means of component X, computed from the magnetic tape record. Units are nT<sup>10</sup>.

NEUCHÂTEL		X = 21000. + TABULAR VALUE																								DEC 1977	
GMT	0	1	2	3	4	5	6	7	8	9	10	11	12	13	14	15	16	17	18	19	20	21	22	23	24	MEAN	
1	. 433	433	433	434	436	437	435	436	435	434	434	437	439	443	438	435	430	435	427	412	413	421	418	422	.	431	
2	. 426	432	451	470	444	427	405	407	408	411	405	392	389	372	383	385	364	311	294	322	316	368	392	366	.	389	
3	. 367	374	384	393	397	401	404	405	407	403	403	405	403	402	400	410	413	415	416	418	419	420	414	421	.	404	
4	. 417	415	414	415	419	421	425	425	419	414	408	408	413	415	415	421	408	408	402	389	387	399	393	400	.	410	
5	. 410	418	419	420	417	416	419	426	424	416	419	415	416	417	423	423	427	428	428	424	423	424	420	419	.	420	
6	. 427	421	427	434	438	442	443	442	437	425	422	424	430	433	434	433	433	433	431	428	430	427	427	426	.	431	
7	. 428	425	427	429	431	432	431	430	428	426	423	425	429	435	438	439	439	438	435	430	426	427	436	437	.	431	
8	. 436	433	433	436	437	440	441	438	431	423	418	419	425	432	437	438	437	436	435	434	433	434	435	434	.	433	
9	. 435	435	436	440	441	437	438	434	434	431	426	421	423	427	433	434	434	436	436	434	435	436	435	436	.	434	
10	. 435	436	436	435	436	436	436	438	436	436	431	429	429	434	434	439	442	444	446	448	446	444	443	435	.	437	
11	. 434	432	449	437	440	424	411	407	413	401	368	354	330	334	363	379	359	381	399	401	394	415	405	407	.	397	
12	. 409	419	433	432	420	418	409	414	415	413	409	408	414	398	404	413	416	415	411	402	410	418	421	418	.	414	
13	. 420	424	438	426	427	428	431	435	438	437	429	425	424	415	409	406	420	414	406	416	425	424	424	424	.	424	
14	. 425	426	424	424	427	425	424	427	428	418	412	414	422	427	427	420	421	424	427	429	432	431	430	431	.	425	
15	. 432	430	431	429	434	435	436	437	430	418	412	415	416	420	427	427	431	433	433	429	431	431	433	432	.	428	
16	. 432	434	435	436	439	441	439	439	438	434	428	428	434	437	435	424	416	400	399	409	413	417	421	412	.	427	
17	. 415	417	416	412	413	435	415	411	413	416	418	420	423	427	430	432	430	433	434	435	431	428	425	428	.	423	
18	. 427	427	427	430	434	430	432	436	437	438	435	432	435	437	438	438	436	434	434	435	436	436	436	436	.	434	
19	. 435	435	435	437	438	440	439	441	440	436	434	437	440	439	438	437	439	447	446	443	442	441	439	439	.	439	
20	. 438	439	442	443	445	448	448	450	452	448	442	436	434	428	426	426	429	429	430	431	433	435	436	437	.	438	
21	. 436	437	438	441	444	447	448	451	454	450	448	447	441	437	431	429	433	440	444	442	435	431	426	428	.	440	
22	. 435	436	436	439	440	445	443	444	448	442	435	433	432	429	428	433	436	435	435	434	437	440	439	440	.	437	
23	. 444	441	440	442	447	451	455	457	458	452	445	442	432	431	430	437	442	444	446	444	443	439	430	428	.	443	
24	. 431	433	435	439	442	446	449	450	449	447	442	439	438	436	435	435	438	439	440	441	443	442	443	443	.	441	
25	. 442	441	440	441	443	446	449	451	450	448	447	450	450	446	445	444	443	440	439	429	426	430	430	430	.	442	
26	. 439	445	439	437	441	443	446	448	450	449	446	447	450	447	445	442	441	443	432	430	432	435	436	444	.	442	
27	. 444	438	434	440	443	443	447	447	443	436	437	439	441	441	437	434	434	435	436	438	438	438	437	437	.	439	
28	. 439	439	440	443	443	448	448	448	445	436	433	430	434	245	327	446	448	451	436	416	443	415	413	426	.	425	
29	. 438	428	428	435	440	440	444	444	442	439	436	435	435	440	442	439	437	439	434	436	436	435	439	436	.	437	
30	. 430	427	431	435	437	440	440	439	430	424	425	432	434	435	437	435	436	439	439	440	437	438	442	446	.	435	
31	. 439	439	440	441	444	447	446	444	439	432	430	439	434	433	437	440	443	444	443	437	435	436	435	438	.	439	
MEAN:																											
ALL DAYS:		429	429	432	434	435	436	435	435	434	430	426	425	426	419	424	428	428	427	426	424	425	427	427	427	.	429

about 1.5 kg/day. The 10 W spare power is to be utilized when the new seismographic station is installed. The analog data from the three seismic channels will be "multiplex-coded" and sent to the Observatory by a separate FM transmitter with a different carrier frequency.

At the Observatory the analog graphic recordings provide real-time information on geomagnetic activity, whereas the digital magnetic tape records are especially suitable

for subsequent data processing, like compensating for drifts related to aging or temperature changes, computation of averages or data reduction. All of these operations of course require that occasional absolute measurements be performed. These are carried out with the new vector magnetometer (cf. Ch. III), which is itself compared about once a year with standards of the Fürstfeldbruck Observatory. Table IV gives an example of hourly means computed for an entire month.

## User-Related Problems

### VII.1. The Compass Theodolite

By far the most common user interest will be for declination  $D$  and the corresponding Map 1. As the map suggests,  $D$  varies appreciably with position and we have also seen that it varies with time. Whereas the map enables the user to overcome position dependence, time dependence can only be compensated for by carrying out the procedure implied in equation (13) with the appropriate reference data. The new station in Neuchâtel, where map users can obtain the necessary reference data, has been set up for that purpose. The compass theodolite<sup>15</sup> is probably the most appropriate tool to solve problems of orientation with magnetic declination<sup>16</sup>. Its own intrinsic accuracy of  $\pm 1$  arc-minute is the same as that claimed for the declination map and it may therefore represent the cheapest means of determining absolute azimuths to  $\pm 2'$  without the need for any reference targets. To use the compass theodolite properly some precautions are necessary, however. The first of these has to do with magnetic perturbations. A ton of iron, for example a car, should be at a distance of at least 20 m. The same is true for a twelve inch steel pipe (extended structures are known to perturb more than concentrated ones). The easiest way to check a site is a quick survey with a proton magnetometer<sup>4</sup> (cf. Sec. IV.3). If such an instrument is not available it will be wise to avoid features of terrain that suggest hidden pipes or dikes, or other structures of reinforced concrete. If the compass theodolite has to be set up on a manifestly perturbed site, the thing to do is to aim at that site and at the target from an auxiliary site which is not perturbed. Moving then to the perturbed site, the azimuth of the target can be found with reference to that of the auxiliary site, which was determined first.

In the unclamped position the horizontal circle of the compass theodolite can rotate on a pin. It orients itself with respect to magnetic North under the torque exerted on a magnetic needle fixed under the circle. This horizontal circle should therefore be clamped, but during clamping care should be exercised to avoid all magnetic perturbations, as for example with magnetic frames of glasses. The time when clamping is effected is the time to which the data will be reduced if the temporal variations are to be compensated. The positioning of the magnetic needle under the circle is not particularly accurate, consequently the circle zero does not in general line up exactly with magnetic North. The deviation can be as much as  $\pm 20$  arc-minute and an initial calibration is therefore necessary.

When an accuracy of  $\pm 10'$  is sufficient, Figs. 7a and 7c show that time reduction of the theodolite readings is generally not required to compensate for the fluctuations, unless these readings have been made during strong mag-

netic activity such as is displayed in Figs. 7b and 7d. Fortunately rapid fluctuations of declination beyond  $\pm 10'$  are not too frequent. The simplest means of verifying the absence of strong magnetic activity would again be the proton magnetometer<sup>4</sup>. For times beyond a year or two from the epoch of a declination map, it will nevertheless be necessary to correct the theodolite readings for secular variation, the long-time trend of the average field elements at a given location, as demonstrated by Fig. 2 (cf. also Sec. VII.3).

### VII.2. Meridian Convergence

In Sec. II.2 and in Ch. V we already mentioned the system of rectangular kilometric plane coordinates ( $x, y$ ) of the Swiss system of geoid projection (see e.g. BOLLIGER 1967). The  $x$ -coordinate axis through Bern Observatory is identical with the local meridian, whereas the local lati-

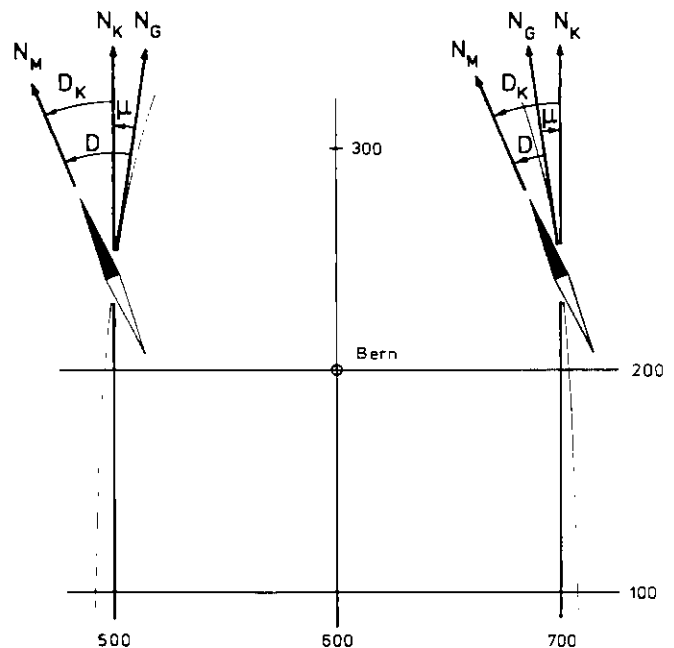


**Figure 8.** Sketch of the pattern of the meridians (thin lines converging toward north) with respect to the orthogonal kilometric coordinate network of the Swiss topographic maps. Also sketched is the present westerly direction of magnetic North  $N_M$ . At any given place geographic North  $N_G$  is parallel to the local meridian. Because of the meridian convergence  $\mu$  toward  $N_G$ , it is seen that declinations  $D_K$  with respect to grid North or map North  $N_K$  differ from declinations  $D$  with respect to geographic North  $N_G$ .  $D_K$  is larger than  $D$  east of Bern, and smaller than  $D$  west of Bern. The reverse would be true for easterly declinations  $D$ . Such easterly declinations will probably occur in the east of Switzerland in about 15 years' time, and in the west in perhaps 30 years.



tude line is only tangent to the y-coordinate in Bern. In the so-called civilian system, the origin of coordinates x and y is precisely Bern Observatory. To avoid confusion, the military system attributes  $x = 200$  km and  $y = 600$  km to this origin, with the result that over the entire area of Switzerland  $x < 300$  km and  $y > 480$  km. In what follows we always use this military system.

The system of geoid projection, which preserves angles, forms the basic grid of the system of surveyor maps of the Topographical Survey of Switzerland. For the map user it is often more practical to refer his azimuth to the local x-axis or ordinate rather than to the local meridian. It is important, therefore, to be able to calculate the angle between these two lines and to specify clearly whether the declination quoted refers to grid North (x-coordinate axis) or geographic North. Fig. 8 shows how these two declinations are related,  $D$  referring to geographic North and  $D_K$  to kilometric grid North (sometimes this is also called map North). Note that for the westerly declinations  $D$  of today one has

$$D_K < D \quad \text{west of Bern,} \quad (20)$$

$$D_K > D \quad \text{east of Bern.}$$

In 15 or 20 years from now some declinations in Switzerland may have become easterly, as suggested by Fig. 2, and we can see with reference to Fig. 8, that relations (20) may not hold any longer.

The accepted practice is to express easterly declinations with positive numbers, and correspondingly westerly declinations are given a negative sign. The relationship between  $D$  and  $D_K$  can then be expressed unambiguously as follows:

$$D_K = D - \mu, \quad (21)$$

where  $\mu$ , the so-called angle of convergence of the meridians, is expressed in arc-minutes to better than  $0.1'$  and with the appropriate sign by

$$\mu = 0.57607 (y - 600) + 9.65 \cdot 10^{-5} (x - 200) (y - 600) + 23 \cdot 10^{-9} (x - 200)^2 (y - 600) - 8 \cdot 10^{-9} (y - 600)^3 \quad (22)$$

An equivalent formula gives  $\mu$  in terms of  $\lambda$  and  $\varphi$ . Whereas Map 1 is a representation of  $D$ , Map 4 gives the contours of  $D_K$ .

### VII.3. Secular Variation

Secular variation is the slow change from year to year of the average field or its elements, typified for example by the changing declination in Regensburg shown in Table I and Fig. 2. Over the past several hundred years this slow change never exceeded about  $10'$  a year in declination (MAURER 1934). For inclination the yearly change was even less and for  $F$  it has remained below  $100$  nT/year. In general secular variation is sufficiently uniform over vast areas, that it can be considered to obey the rule of synchronism assumed for the fast variations (cf. Sec. IV.4)

during the 3 or 4 years required to carry out a survey in a country with dimensions of a few hundred kilometers only. For longer periods of time this does not remain true. In the recent past western Europe has seen a decrease in the east-west gradient of declination. This decrease is quite evident in a comparison of the maps of BATELLI (1892), BRÜCKMANN (1931), and our Map 1. Along the latitude through Bern the gradient was about  $39'$  per  $100$  km in 1892,  $35'$  per  $100$  km in 1931, and  $30'$  in 1978 (cf. Table Va). On the average the east-west declination gradient has therefore been decreasing by about one arc-minute per hundred kilometers and per decade in western Europe.

It is evident from the above that a declination map cannot be updated with a uniform secular correction, even for a small country like Switzerland. Repeat measurements at a few stations distributed throughout the country are necessary every 5 or 10 years to follow secular variation properly. This secular correction is easy to apply if the geomagnetic field is first separated into a normal and an anomalous part (cf. Sec. VIII.1). In a first approximation the anomalous part can be considered as time-independent, its origin resting entirely in magnetic features of a complex geology. The normal field has no small scale features, but is assumed to be responsible for secular variation.

The assumption of a time-independent anomalous field is certainly justified for periods as long, perhaps, as 50 years, but for longer periods this may not be true. The magnetization of rocks causing the anomalous field has two components, a remanent component and an induced component. While the first component is obviously constant in time, the second component is induced by a normal field which changes slowly, both in intensity and direction and it will therefore itself be changing slowly. The anomalous field should not, therefore, be considered as absolutely constant in time. Future surveys, or a regular updating of various portions of the maps, must therefore be envisaged.

### VII.4. The Influence of Altitude

In the historical part (Ch. II) we mentioned several early attempts to find a correlation between the field elements or their variations with altitude. We know today why these attempts could not but fail, for the vertical gradients are very small, both for  $F$  and its temporal variations. In the vicinity of a strong but very localized anomaly these gradients become large, in vertical as well as in horizontal directions.

To give an idea of the gradients expected for  $F$  in unperturbed areas we can look at the predictions of any reasonably good global scale geomagnetic field model like IGRF<sup>17</sup> or AWC-75<sup>18</sup>. In Table V we give gradients of the various field elements as well as the values of the field components predicted by AWC-75 for 1978.0 and those derived from our survey for the point of coordinates  $47^\circ\text{N}$ ,  $8^\circ\text{E}$  of Greenwich ( $x = 205.443$  km,  $y = 642.618$  km). For AWC-75 the field elements quoted are for the zero level of the International Reference

**Table Va** – Field elements and their gradients at  $\phi = 47^\circ\text{N}$ ,  $\lambda = 8^\circ\text{E}$  (i.e.  $x = 205.443$  km,  $y = 642.618$  km) at epoch 1978.0. Units are sex. degrees and minutes for D and I, and  $\text{nT}^{10}$  for F. For the gradients they are minutes or  $\text{nT}$  per 100 km.

Epoch:	D			I			F		
1978.0	map	AWC-75	normal	map	AWC-75	normal	map	AWC-75	normal
Element E	$-2^\circ 24$	$-2^\circ 41.4$	$-2^\circ 23.4$	$62^\circ 42$	$62^\circ 39.9$	$62^\circ 43.4$	46,750	46,693	46,760.5
dE/dx	-6.3	-4.9	0	50.5	49.3	50	288	272	280
	D increases northward			I increases northward			F increases northward		
dE/dy	30.3	29.4	30	1.3	1.8	0	66	49	60
	D decreases eastward			I increases eastward			F increases eastward		
dE/dz	-	12.5	-	-	8.1	-	-	2135	-
	D increases upward <sup>1</sup>			I decreases upward			F decreases upward		

map: Data from our survey (cf. Maps I–III).

AWC-75: Data from reference field AWC-75 for 1978.0. (cf. Note No. 18)

normal: Normal field chosen in deriving the residual Maps 7, 8, and 9.

Spheroid<sup>19</sup>, which is close to the local sea level. The excellent agreement between measured and model values both for the field elements and their horizontal gradients suggests that the AWC-75 model predictions for the vertical gradients are close to what would be observed. Obviously these vertical gradients are small and justify our decision to ignore them when computing Maps 1 to 4. In fact, these maps refer to surface data and are therefore especially suited for ground-level work.

Just as the effect of altitude upon the field elements can be ignored, so can its effect upon the temporal variations. In the time-reduction process, described in Sec. IV.4, any effect of altitude can therefore be safely ignored.

Table V is worthy of a few comments. The large northward and upward gradients of F are of global nature; the same is true for the northward gradient of I. These features are characteristic of a single central dipole field. But such a field would have no vertical inclination gradient. If the single dipole were axial, i.e. lined up with the Earth's rotation axis, there would also be no declination. For declination to appear it is sufficient to have a non-axial central dipole. But if we assume that the present geomagnetic North pole, at approximately  $77^\circ\text{N}$ – $102^\circ\text{W}$  just north of Bathurst Island in Canada, is due to a non-axial central dipole only, then declination in Switzerland should amount to about  $18^\circ\text{W}$ , i.e.  $D = -18^\circ$ . The large deviation from this value, and the rather important vertical inclination gradient predicted by AWC-75, not only point to the inadequacy of any single dipole model of the Earth's geomagnetic field, but are related to the presence of a large-scale anomaly covering the eastern Atlantic, all of Europe and western Africa. While this anomaly is not of global scale it has probably been a stable feature over the past century or longer, like other well-known large-scale anomalies (COX 1975).

The fact that western Europe is situated in the middle of an anomaly of continental or larger dimensions has implications for the behaviour of the geomagnetic field at higher altitudes. With increasing height the Earth's geomagnetic field should look more and more like the field of a single dipole. Therefore, those features characteristic of a single dipole field will gradually take the upper hand. This explains why with increasing altitude the westerly declination should increase and the vertical inclination gradient should decrease, as correctly predicted in Table V by the AWC-75 model field. An aeromagnetic survey of the field amplitude F is presently under way in Switzerland<sup>20</sup>. There is little doubt that this survey will confirm a decrease of F of about 21  $\text{nT}$  per km with altitude. This value also corresponds to the gradient expected for a central dipole. However, the data of Table Vb indicate that

**Table Vb** – Field elements as a function of altitude, at  $\phi = 47^\circ\text{N}$ ,  $\lambda = 8^\circ\text{E}$  (i.e.  $x = 205.443$  km,  $y = 642.618$  km), computed for AWC-75<sup>18</sup> model at 1978.0 epoch. Units are kilometers for altitude, degrees and minutes for D and I, minutes per 100 km for dI/dz, and  $\text{nT}^{10}$  for F.

Altitude	D	I	dI/dz	F
0	$-2^\circ 41.4$	$62^\circ 39.9$	8.1	46 693
1	$-2^\circ 41.6$	$62^\circ 39.8$	-	46 672
3	$-2^\circ 41.8$	$62^\circ 39.7$	-	46 629
5	$-2^\circ 42.1$	$62^\circ 39.5$	-	46 587
10	$-2^\circ 42.7$	$62^\circ 39.1$	8.0	46 480
20	$-2^\circ 44.0$	$62^\circ 38.3$	7.9	46 269
50	$-2^\circ 47.9$	$62^\circ 36.0$	7.7	45 642
100	$-2^\circ 54.3$	$62^\circ 32.2$	7.3	44 622
200	$-3^\circ 06.7$	$62^\circ 25.2$	6.7	42 670
500	$-3^\circ 41.6$	$62^\circ 08.3$	4.8	37 451

an aeromagnetic survey at heights of 5000 m or less would have difficulty observing the small changes expected for the normal D and I. But it would be interesting to follow the behaviour of D and I with altitude in regions with highly localized strong anomalies.

The northward D-gradient and the eastward I-gradient are probably also connected with the large-scale anomaly described above, but these gradients are smaller and it is quite conceivable that they may reverse their signs within a few decades.

## Discussion of the Maps

### VIII.1. Map Presentation

In addition to Maps 1 to 4, of D, I, F and  $D_K$ , mentioned before, we have established a number of other maps, to follow standard practice on the one hand, and to facilitate the interpretation of anomalies on the other. We should also like to call attention to the fact that Map 1 is the only one where the contours extend all the way to the map frame. This was done at the request of the Swiss Federal Air Office to insure a good overlap with foreign declination maps. Since the numerical declination data between neighbouring countries often disagree by several arc-minutes, we have not used absolute foreign declination data in extrapolating the isogonic lines beyond Switzerland's borders. Instead, we have taken over the isogonic line-pattern of these maps. This procedure is especially reliable in the present case because, as Map 10 and Table VI show, we have surveyed an important strip around the entire country to facilitate the matching procedure. We have not attempted a similar extrapolation with the other elements, in part because the necessary data is not available for all the countries bordering ours.

Maps 5 and 6 are representations of H and Z, i.e., horizontal and vertical components respectively. Traditionally these representations were the ones most often used in past modelling attempts or interpretative work. The advent of the proton magnetometer<sup>4</sup> with the resulting ease and accuracy it affords for measurements of the amplitude F, has of course changed the situation. Most inversion or modelling programmes are now concerned with amplitude or total intensity data F.

Maps 7, 8, and 9 are so-called anomaly or residual maps. Such maps are obtained after subtracting from the observed field a somewhat arbitrary "normal field", i.e., a field that might prevail if there were no anomalies. Reference field AWC-75<sup>18</sup> (cf. Sec. VII.4) would have been an acceptable choice as a normal field, but we see in Table Va that whereas the field gradients of observed field and AWC-75 are well matched, there is some discrepancy between the actual values of D and F. Furthermore, the overall geomagnetic field pattern in Switzerland is surprisingly regular in comparison, for example, with that of Belgium (DE VUYST, KOENIGSFELD, and LAHAYE 1962), a country of similar size but much simpler topography. More specifically, it is seen in Map 1 that the isogonic lines form a reasonably regular north-south pattern, the isoclinic lines of Map 2 an even more regular east-west array, whereas the isodynamic lines of Map 3 are directed mainly east-west, with a slight south-easterly component. We have, therefore, chosen a normal field of the form indicated in Table Va. Our normal declination has an east-west gradient of 30' per 100 km and no north-south

gradient. Our normal inclination has a 50'/100 km north-south gradient, but is constant along an east-west abscissa. F has gradients of 280 nT/100 km to the north and 60 nT/100 km to the east. The actual normal value of the three elements at the (47°N, 8°E) reference point of Table Va is of little significance. The values quoted result from the particular origin chosen for the normal field in the (x, y) coordinate system.

As one would expect if the normal field is suitably chosen, the residual Maps 7 to 9 exhibit large areas free of any contours. Maps 2 and 8, of inclination I and residual inclination  $\Delta I$ , seem to indicate that inclination is less perturbed by local anomalies than the other field elements. A good example is the Jorat anomaly around Lausanne. We believe that this behaviour follows from the relative orientations of the normal field, directed essentially north-south but inclined at about 62°, and of the geological features causing the local anomalies. These features are all related to the Alpine arc, whose orientation in Switzerland is essentially east-west. The perturbing bodies are therefore mostly thin structures elongated in a direction at right angles to the normal field (cf. Sec. VIII.2), a situation especially apt at producing large declination anomalies while perturbing inclination only slightly. This explanation is strongly supported by almost identical field patterns observed in Austria (PÜHRINGER, SEIBERL, TRAPP and PAUSWEG 1975), where similar conditions prevail as in Switzerland. In Belgium, on the other hand, the hills of the Brabant are a region of moderately strong geomagnetic perturbations, but the geological features causing these perturbations are randomly oriented with respect to the normal field. Consequently inclination and declination are seen to be equally perturbed (DE VUYST, KOENIGSFELD, and LAHAYE 1962).

### VIII.2. The Main Anomalies

It is not our purpose here to attempt a detailed geological interpretation of our data. However, one cannot fail to notice on all maps that the Alps contain several highly perturbed areas. Ultimately these perturbations will have to be explained in geological and geophysical terms. But not all of the Alps are perturbed: in particular the range from the eastern end of Lake Geneva (Lac Léman) to the western edge of the Aar Massif is very regular. We note that this is a vast crystalline area covered by various sedimentary bodies, which is, therefore, essentially non-magnetic. The Jura chain also is surprisingly little perturbed. But three large anomalous zones are particularly evident on the maps, and will now be discussed briefly.

The Jorat anomaly around Lausanne has already been considered at some length in Sec. II.3. The additional information contained in our declination and inclination data could perhaps lead to improvements in the models already proposed, but this is perhaps not warranted while no geological evidence is available to support or refute such model calculations. Some features of this anomaly are quite interesting: it is well isolated from any other anomaly, reasonably large in extent ( $50 \times 50$  km), and of very high symmetry. As was said in the preceding Section, this is a consequence of the highly regular shape of the intrusive body causing the anomaly, and of its orientation almost at a right angle to the normal field (cf. MEYER DE STADELHOFEN, SIGRIST, and DONZÉ 1973).

The entire triangle between Mont-Blanc, Oberalppass and Varese is perturbed. Within this area one can distinguish at least three separate features connected with separate geologic entities. The most prominent of these, of course, is the Ivrea body stretching in a south-westerly arc away from Locarno, along the Insubric Line. This anomaly has been the subject of a large number of geological and geophysical studies. We can only mention a few of them here, concentrating on those involving magnetic measurements. ALBERT (1974) measured a series of vertical component profiles, whereas several others surveyed the total field and the magnetism of rocks (WEBEL 1973, GALLAY 1975, WAGNER et al. 1978, H. SCHWENDENER 1978). Albert proposed a structural model which agrees fairly well with recent seismic measurements (BERCKHEMER et al. 1968). Our data cover only the 80 easternmost kilometers of this area. Comparison of our data with that of ALBERT (1974) is not very straightforward, probably because our point density is much lower. But our data reveal a very strong increase of the anomaly at its eastern end, the Locarno area, confirming the high  $Z$  values found by WEBER et al. (1949) and suggesting a rather abrupt termination of the Ivrea Body. This aspect is particularly evident on Maps 2 (inclination), 5 (vertical component), and 8 (inclination anomaly). The western end of the Ivrea body, which occurs around Ivrea itself, appears to behave similarly according to ALBERT's (1974) data, whereas the seismic study (BERCKHEMER et al. 1968) suggests that the anomaly should taper off more gradually in the west since there the intrusive body plunges to greater depths. Vector measurements could help resolve that question.

The second feature of the triangle mentioned above is a series of weak anomalies stretching along the Simplon–Furka–Oberalp axis. As suggested elsewhere (FISCHER and SCHNEGG 1977), this is probably connected with large ultrabasic masses at depths of a few kilometers, but of which some lenticular projections reach upward and have, for example, been found during construction of the Gotthard railway tunnel<sup>21</sup>.

The last feature within the Mont-Blanc–Oberalppass–Varese triangle is the region in Italy, just south of the Valais, i.e. the Piedmont part of the Pennine Alps, but including the area of Zermatt in Switzerland. This is a highly perturbed area because of the presence of many magnetite-rich bodies of metamorphic ophiolites (serpentine, gabbro, prasinite). This region is also covered in part by the studies of WEBEL (1973), GALLAY (1975), and WAGNER et al. (1978).

The third large perturbed zone is in the south-eastern part of Graubünden. While two main focal points stand out, the Oberhalbstein (area of Bivio, Piz Platta, and Tiefencastel) on the one hand and the Val Poschiavo on the other hand, the entire zone is strongly perturbed by magnetite bearing rocks. The Oberhalbstein is a metamorphic basic and ultrabasic volcanic zone, in which a dense amplitude survey has recently been carried out by WOLFENBERGER (1977), who also attempted a model calculation. But the area is so strongly perturbed and on such a short scale that the model results are probably not very significant. Comparison with our much lower density survey is completely meaningless in this case. In that area, especially near Lake Lunghin (Lunghin-See, or Läggh dal Lunghin), declination anomalies exceeding  $\pm 20$  degrees have been reported by STAUB (1950), the  $40^\circ$  swing of the magnetic needle taking place over a distance of only about 2 km. The Poschiavo anomalous area, in which an amplitude survey agreeing quite well with ours has been carried out recently by HERZIG (1977), extends west of the Italian border, but does not reach the bottom of the Valtelina valley itself. Here a large serpentine formation causes the anomaly, with declination deviations of up to  $6^\circ$  (STAUB 1950). The Valtelina valley floor is left unperturbed because the serpentine body stops by way of a fracture about 10 km north of the center of the valley.

Finally, we should like to mention a few weak anomalies strewn along the Jura chain in the north of Switzerland, particularly in the areas of the Chasseral, of Basel, and near Bevaix, just north of Lake Neuchâtel.

A rather extensive list of the geomagnetic anomalies known in Switzerland up to 1950 was published by STAUB (1950) and mentions all the large-scale anomalies which we have discussed in the present Section. Also mentioned are many very local anomalies that we did not attempt to observe. However, our measurements in the Blenio valley do not confirm the large-scale anomaly apparent on the maps of BRÜCKMANN (1931, 1933), as well as on all the maps published thereafter. Our present maps take account of all the sites surveyed, excepting a single site in the Cleuson valley (Valais), where a very localized anomaly mentioned previously (FISCHER and SCHNEGG 1977) was detected. The perturbed Cleuson site has purposely been omitted from Table VI and Map 10.

## Acknowledgements

It is impossible to mention the many people who have, in one way or another, helped us carry out the present survey. Financial help came from three different sources: the Canton of Neuchâtel, our employer, the Swiss National Science Foundation, with a big equipment grant especially for the new reference station, and the Geophysical Commission of the Swiss Academy of Natural Sciences, which helped finance field-work and the construction of the reference station, and covered the costs of printing the present report.

Important assistance came from the firm of Wild-Heerbrugg during construction of the new vector magnetometer (especially from Messrs. Piske, R. Schwendener, and

Loher); from the Swiss Federal Air Office through Mr. Donau who transported us and our equipment onto the Aar and Aletsch glaciers, and from the Topographical Survey of Switzerland, which provided all the necessary survey maps and helped in drawing the new geomagnetic maps. Dr. K. A. Wienert (Fürstfeldbruck) and Prof. A. De Vuyst (Dourbes) graciously furnished all the reference material necessary to carry out the time-reduction of the field data. Dr. F. S. Barker Jr. (U. S. Naval Oceanographic Service) provided the AWC-75<sup>18</sup> model data and Prof. J. P. Schaer (University of Neuchâtel) gave geological advice. Miss Wüthrich of our Observatory carefully typed this report.

## Notes

<sup>1</sup> Our sources for the Regensberg geomagnetic data quoted in Table I and Fig. 2 have been: 1) The Topographic Survey of Switzerland (open circles in Fig. 2); 2) The World Data Center A (WDC-A) in Boulder, Colorado, USA (Dr. K. L. Svendsen) who supplied a table (closed circles) as well as copy of a 1960 letter from Dr. Lugeon (a former director of the Swiss Institute of Meteorology) to the US Dept. of Commerce (crosses); 3) some relics of the former Regensberg station (1931.5 and 1940.75); 4) our own measurements (1975.5). The World Data Center CI in Edinburgh also gave us information, some of which is included in Table Ib.

<sup>2</sup> Table I and Fig. 2 contain all the Regensberg data that could be secured. The authors would, of course, welcome the missing yearly means of the period 1927–1945, but in his brief historical review GRÜTER (1964) leaves little hope that these means were ever computed.

<sup>3</sup> This new vector magnetometer was built by FISCHER (1973, 1975) and first described in some detail in a recent French publication (FISCHER and SCHNEGG, 1977).

<sup>4</sup> The proton magnetometer calls on a property of atomic nuclei. It is, therefore, practically unaffected by temperature variations and can be considered a highly accurate absolute instrument. Most portable models weigh about 4 to 5 kg, have a sensitivity and accuracy of 1 nT<sup>16</sup>, and cost around Sw. Fr. 6000.–. These instruments now all have a digital display. Upon depressing a single button a preprogrammed sequence of operations is initiated which culminates, about 2 seconds later, in a display of total field F. Proton magnetometers are not directional, except as concerns their sensitivity. They usually require that the field to be measured be fairly uniform. Our instrument stops performing correctly in field gradients larger than about 500 nT/m.

<sup>5</sup> Fluxgates are vector-magnetometers operating on an ingenious induction method. They yield a signal proportional to the field component along the sensor axis. The zero of fluxgates or similar directional magnetometers is usually at mid-scale. But a null reading does not, in general, correspond to a vanishing field, either because of drifts of the electronics, or because the “zero-offset” circuitry cannot be switched off. For the new vector magnetometer described in Ch. III this is of no consequence.

<sup>6</sup> The sensor mounted on our vector magnetometer is not a fluxgate. The manufacturer calls it “variable- $\mu$  magnetometer”. It works on a principle somewhat different from the fluxgate, but is used in the same manner. The sensitivity of this instrument is about 20 nT<sup>10</sup> per cm of the scale.

<sup>7</sup> Our theodolite is a Wild T16E (Wild-Heerbrugg, CH-9435 Heerbrugg, Switzerland) with a modified (non-magnetic) and larger than standard base.

<sup>8</sup> Our gyroscope is a Wild GAK1.

<sup>9</sup> This range is chosen in view of surveying Switzerland. It is in fact appropriate for most latitudes between 40 and 60 degrees north in Europe and Asia. By changing the water level tilt other ranges can be chosen.

<sup>10</sup> In accordance with the SI system of units we express the field in nT (nanotesla). One nT is equivalent to one  $\gamma$  (gamma), i.e. to 10<sup>−5</sup> Gauss.

<sup>11</sup> For areas inaccessible by car we have assembled a lighter portable system comprising a proton magnetometer<sup>4</sup>, a digital fluxgate magnetometer without offset<sup>5</sup> for the vertical component, and a Wild TO compass theodolite<sup>7</sup>. This system has been used occasionally in parallel with our standard equipment to test it.

<sup>12</sup> The observatories of Fürstentfeldbruck and Dourbes were chosen because they are both reasonably close to Switzerland and are known to be among the best for the reliability of their data and the quality of their service.

<sup>13</sup> E.D.A. Instruments Inc., 1 Thorncliffe Park Drive, Toronto, Canada M4H-1G9.

<sup>14</sup> Global Thermoelectric, P.O. Box 459, Bassano, Alberta, Canada T0J-0B0.

<sup>15</sup> The Wild TO is the only commercial compass theodolite known to the authors (cf. Notes 7 and 11).

<sup>16</sup> Among the possible applications of magnetic declinations we can cite: (a) Navigation on lakes. (b) Aerial navigation, especially for small aircraft with little or no modern electronic navigational equipment. (c) Travel on glaciers and in forests. (d) Orienting directional transmitting or receiving antennas. (e) Orienting sun dials. (f) Orienting artillery guns. (g) Determining the orientation of planned buildings with the help of a compass theodolite. (h) Surveying of caves and constructing medium-length tunnels or galleries, using a compass theodolite. (i) Determining the orientation of geologic structures and of rock samples to be collected.

<sup>17</sup> IGRF stands for International Geomagnetic Reference Field. cf. ESSA Technical Report C & GS 38, by E. B. Fabiano and N. W. Peddie, a publication of the US Dept. of Commerce: Grid values of total magnetic intensity – 1965. Updated versions of IGRF for 1970 and 1975 are probably available now.

<sup>18</sup> AWC-75 is a reference field similar to IGRF produced by the US Oceanographic Office, Bay St Louis, Mississippi, USA. We are grateful to Dr. F. S. Barker of the above office (Geomagnetism Data Branch, Code 3523, NSTL Station, Mississippi, USA 39511) for the grid-values at various altitudes of the field elements in the area of Switzerland.

<sup>19</sup> See “International Ellipsoid” in Transactions of the International Astronomical Union (1966), or IAGA Bulletin no. 28 (1969): World Magnetic Survey.

<sup>20</sup> An aeromagnetic survey of field amplitude or total intensity F is presently under way in Switzerland. This project is being carried out by the Institute of Geophysics of the Swiss Federal Institute of Technology in Zurich, under the responsibility of Dr. E. Klingelé.

<sup>21</sup> See e.g. the geological profile of the railway tunnel by F. M. Stapff and E. Ambühl, reproduced on the map “Gotthardpass” published by the Swiss PTT with the brochure “Gotthardstrasse, Andermatt-Airolo” (Bern, 1951, now out of print).

## References

- ALBERT, G. (1974): Die magnetische Anomalie der Ivrea-Zone. *J. Geophys.*, Vol. **40**, pp. 283–301.
- BATELLI, A. (1889): Misure Assolute degli Elementi del Magnetismo Terrestre nella Svizzera. Eseguito nel 1888 e nel 1889. *Annali dell'Ufficio Centrale Meteorologico e Geodinamico Italiano*, Vol. **11**, 2nd Series, Part 3, pp. 29–167.
- BATELLI, A. (1892a): Sur les Variations Séculaires des Eléments Magnétiques en Suisse. *Arch. des Sciences Phys. et Natur.*, Genève, 3rd Period, Vol. **28**, pp. 202–235.
- BATELLI, A. (1892b): Carta Magnetica della Svizzera. *Annali dell'Ufficio Centrale Meteorologico e Geodinamico Italiano*, Vol. **14**, 2nd Series, Part 1, pp. 83–88, plus two maps.
- BERCKHEMER, H. and German Research Group for Explosion Seismology (1968): Topographie des "Ivrea-Körpers" Abgeleitet aus Seismischen und Gravimetrischen Daten. *Schweiz. Mineralog. und Petrograph. Mitteil.*, Vol. **48**, n° 1, pp. 235–246.
- BITTERLI, P. (1972): Erdölgeologische Forschungen im Jura. *Bull. Ver. Schweiz. Petrol.-Geol. u. -Ing.*, Vol. **39**, pp. 13–28. A large scale map can be obtained from: Compagnie Générale de Géophysique (CGG), 50 rue Fabert, Paris 7<sup>e</sup>: Etude aéromagnétique, région du Jura Suisse. Etude 2680, feuille n° 9 (1970).
- BOLLIGER, J. (1967): Die Projektionen der Schweizerischen Plan- und Karten-Werke. Druckerei Winterthur A.G., 130 + 13 pages, Winterthur.
- BONANOMI, J. and SCHUMACHER, P. (1976a): Synchronisation d'Horloges par Signaux Horaires. *La Suisse Horlogère*, n° 11 (11 mars, 1979) pp. 229–235.
- BONANOMI, J. and SCHUMACHER, P. (1976b): Quartz Clocks Synchronized by LF Time Signals. *Proc. Eighth Annual Precise Time and Time Interval (PTTI) Meeting*, US Naval Res. Lab., pp. 135–146, Washington D. C.
- BRIGGS, I. C. (1974): Machine Contouring Using Minimum Curvature. *Geophysics*, Vol. **39**, pp. 39–48.
- BRÜCKMANN, W. (1913): Beobachtungen in den Schweizer Hochalpen über die Änderung der Erdmagnetischen Kraft mit der Höhe. *Abh. des Preuss. Meteorol. Inst.*, Vol. **4**, n° 9, 25 pages.
- BRÜCKMANN, W. (1930): Erdmagnetische Vermessung der Schweiz. I. Allgemeines – Deklination. *Ann. der Schweiz. Meteorol. Zentralanst.*, Jahrgang 1930, n° 7, 24 pages and one map.
- BRÜCKMANN, W. (1931): Erdmagnetische Vermessung der Schweiz. II. Horizontalintensität, Inklination. *Ann. der Schweiz. Meteorol. Zentralanst.*, Jahrgang 1931, n° 6, 10 pages and three maps.
- BRÜCKMANN, W. (1933): Karte der Magnetischen Deklination in der Schweiz für Mitte 1935, bei Beziehung auf Kartennord im Rechtwinkligen Koordinatensystem. *Ann. der Schweiz. Meteorol. Zentralanst.*, Jahrgang 1933, n° 6, 2 pages and one map.
- CADISCH, J. (1932): Über die Vornahme der Kompasskorrektur. Bemerkungen zur Neuen Isogonenkarte der Schweiz. *Eclogae Geol. Helv.*, Vol. **25**, pp. 33–38.
- COX, A. (1975): The Frequency of Geomagnetic Reversals and the Symmetry of the Nondipole Field. *Rev. Geophys. Space Phys.*, Vol. **13**, pp. 35–51.
- DE LORIO, J.-P. (1962): L'Anomalie Magnétique du Jorat, son Extension sur la Côte Française du Léman (Etude de la Composante Verticale). *C.R. Soc. Phys. Hist. Nat. Genève*, Vol. **15**, pp. 384–388.
- DE VUYST, A., KOENIGSFELD, L., and LAHAYE, E. (1962): La Distribution du Champ Magnétique Terrestre en Belgique à l'Epoque 1960.5. *Publications de l'Institut Royal Météorologique de Belgique, Série A*, n° 30: A set of 8 maps.
- ELMIGER, A. (1971): Astronomisch-Geodätische Lotabweichungen in der Schweiz. Zusammenstellung 1867–1970. Bericht an die Schweiz. Geodätische Kommission (June 1971). This publication can be obtained from: Institut für Geodäsie und Photogrammetrie, ETH-Hönggerberg, CH-8093 Zürich.
- FARKAS, T. (1973): Bestimmung der Magnetischen Deklination und deren Säkularänderung in Baden-Württemberg. *Deutsche Geodätische Kommission, Reihe C (Dissertationen)*, Heft n° 190 (München).
- FISCHER, G. (1973): An Inexpensive Portable Vector-Magnetometer. Abstract No. SI-6, p. 247 of *IAGA Bulletin* n° 34: Program and Abstracts for the Second General Scientific Assembly, Kyoto (Japan), 1973.
- FISCHER, G. (1975): Un Magnétomètre Vectoriel d'un Nouveau Type. *Zeitschrift für Angewandte Mathematik und Physik*, Vol. **26**, p. 136.
- FISCHER, G. (1979): Electromagnetic Induction Effects at an Ocean Coast. *Proc. IEEE*, Vol. **67**, pp. 1050–1060.
- FISCHER, G. and SCHNEGG, P.-A. (1977): Le Nouveau Levé Géomagnétique de la Suisse. *Vermessung, Photogrammetrie, Kulturtechnik (Mensuration, Photogrammétrie, Génie Rural)*, n° 8–77, pp. 253–261. This paper has been reprinted with the authors' permission by the review *Géomètre*, July 1978 issue, pp. 14–23.
- FISCHER, G., SCHNEGG, P.-A., and USADEL, K. D. (1978): Electromagnetic Response of an Ocean Coast Model to E-Polarization Induction. *Geophys. J. R. astr. Soc.*, Vol. **53**, pp. 599–616.
- GALLAY, Cl. (1975): Etude Géomagnétique de la Zone d'Ivrée (Italie du Nord). *Diplom Thesis*, Département de Minéralogie, Université de Genève, CH-1211 Genève 4.
- GARLAND, G. D. (1971): Introduction to Geophysics. *Mantle Core and Crust*, W. B. Saunders Co., Philadelphia.
- GRÜTER, M. (1964): Der Erdmagnetische Dienst. Jubiläumsschrift "Hundert Jahre Meteorologie in der Schweiz 1864–1963". Published by the Swiss Institute of Meteorology, pp. 39–41, Zürich.
- GRÜTER, M. (1965): Maps of Declination, and of Horizontal and Vertical Intensities for 1962.5. *Atlas of Switzerland*, Sheet n° 10, Geophysics. Published by the Topographical Survey of Switzerland, Wabern-Bern.



- GURTNER, W. (1978): Das Geoid in der Schweiz. Published by Schweiz. Geodätische Kommission. This publication can be obtained from: Institut für Geodäsie und Photogrammetrie, ETH-Hönggerberg, CH-8093 Zürich.
- HERZIG, H. (1977): Magnetische Messungen im Val Poschiavo. Diplom Thesis, Institut für Geophysik, ETH-Hönggerberg, CH-8093 Zürich.
- HUMBOLDT, A. and GAY-LUSSAC, J.-L. (1808): Beobachtungen über die Stärke und die Neigung der Magnetischen Kräfte, angestellt in Frankreich, der Schweiz, Italien und Deutschland. Gilbert's Annalen der Physik, Vol. **28**, Halle, pp. 257–276.
- MALIN, S.R.C. (1975): Measurements of the Geomagnetic Field Direction in London since 1576 to the Present. Paper SM 20–1, p. 41 of IAGA Bulletin n° 36: Program and Abstracts XVI IUGG General Assembly, Grenoble, 1975, and private communication.
- MAURER, J. (1885a): Einfluss der Höhe auf die Täglichen Variationen der Magnetischen Deklination. Zeitschrift der österreichischen Ges. für Meteorol., Vol. **20**, pp. 180–183.
- MAURER, J. (1885b): Influence de l'Altitude sur la Variation Diurne de la Déclinaison Magnétique. Arch. des Sciences Phys. et Nat., Genève, 3rd Period, Vol. **13**, pp. 339–345.
- MAURER, J. (1907): Unsere Erdmagnetischen Verhältnisse im Spiegel ihrer Literatur. Wissenschaftliche Nachrichten, Beiblatt zu den Neuen Denkschriften der S.N.G., 1. Jahrgang, Serie A, n° 1, pp. 9–15.
- MAURER, J. (1934): Die Schwankungen der Kompassnadel in der Umgebung unserer Alpen nach Langjährigen Aufzeichnungen. Vierteljahrsschrift der Naturf. Ges. in Zürich, Vol. **79**, pp. 24–28.
- MERCANTON, P.-L. and WANNER, E. (1943): Die Magnetische Anomalie im Jorat (Kanton Waadt). (I. Teil. Die Verteilung der Vertikalintensität). Ann. der Schweiz. Meteorol. Zentralanst., Jahrgang 1943, Addendum, 9 pages and two maps.
- MERCANTON, P.-L. and WANNER, E. (1945): L'Anomalie Magnétique du Jorat (Vaud), I. La composante verticale. Bull. Soc. Vaudoise des Sc. Nat., Vol. **63**, No. 264, pp. 1–14, and one map.
- MERCANTON, P.-L. and WANNER, E. (1946): Die Magnetische Anomalie im Jorat, Kanton Waadt. (II. Teil. Horizontalintensität und Deklination). Ann. der Schweiz. Meteorol. Zentralanst., Jahrgang 1946, n° 6, 9 pages and one map.
- MERCANTON, P.-L. and WANNER, E. (1948): L'anomalie Magnétique du Jorat (Vaud). II. Composante Horizontale. Déclinaison. Champ Perturbateur. Esquisse d'une Interprétation. Bull. Soc. Vaudoise des Sc. Nat., Vol. **63**, n° 270, pp. 15–24, and one map.
- MEYER DE STADELHOFEN, C., SIGRIST, W., and DONZÉ, A. (1973): L'anomalie Magnétique du Jorat. Bull. des Laboratoires de Géol., Minéral., Géophys. et du Musée géolog., Univ. de Lausanne, n° 202, 8 pages.
- NESS, N.F. (1970): Magnetometers for Space Research. Space Science Reviews, Vol. **11**, pp. 459–554.
- NIETHAMMER, Th. (1921): Die Schwerebestimmungen der Schweizerischen Geodätischen Kommission und ihre Ergebnisse. Verhandl. der Schweiz. Naturf. Ges., Schaffhausen, 102. Jahresversammlung, Part II, pp. 50–64.
- PRIMDAHL, F. (1970): Bibliography of Fluxgate Magnetometers. Publication of the Earth Physics Branch, Dept. of Energy, Mines and Resources, Ottawa (Canada), Vol. **41**, n° 1, pp. 1–14.
- PÜHRINGER, A., SEIBERL, W., TRAPP, E., and PAUSWEG, F. (1975): Die Verteilung der Erdmagnetischen Elemente in Österreich zur Epoche 1970.0. Arbeiten aus der Zentralanstalt für Meteorologie und Geodynamik, Heft 14, Publikation n° 205: A set of 9 maps.
- SCHWAB, R.F. (1960): Einige Ergebnisse einer Aeromagnetischen Studie im Gebiet des Waadtländerjuras. Bull. Ver. Schweizer. Petrol.-Geol. u. -Ing., Vol. **26**, pp. 31–32.
- SCHWENDENER, H. (1978): Magnetische und Seismische Messungen an Gesteinen der Zone Ivrea-Verbano und Strona-Ceneri. Diplom Thesis, Institut für Geophysik, ETH-Hönggerberg, CH-8093 Zürich.
- SCHWENDENER, R. (Wild-Heerbrugg, CH-9435 Heerbrugg, Switzerland): Private communication.
- SERSON, P.H. and PRIMDAHL, F. (1972): Bibliography of Magnetometers. Publication of the Earth Physics Branch, Dept. of Energy, Mines and Resources, Ottawa (Canada), Vol. **43**, n° 8, pp. 501–506.
- STAUB, G. (1950): Erdmagnetismus und Bussolenmessung. Schweiz. Zeitschrift für Vermessung, Vol. **48**, pp. 4–11.
- USHER, M.J. and REID, J.P. (1975): An absolute Vector Magnetometer. Abstract SM-13, p. 133 of IAGA Bulletin n° 36: Program and Abstracts XVI IUGG General Assembly, Grenoble, 1975. A paper was published in 1978: J. Physics E (Scientific Instruments), Vol. **11**, pp. 1169–1172.
- VAN RIJCKEVORSEL, E. and VAN BEMMELEN, W. (1896): Magnetische Beobachtungen in der Schweiz im Jahre 1895 Ausgeführt. J. van Boekhoven, 20 pages, Utrecht.
- VAN RIJCKEVORSEL, E. and VAN BEMMELEN, W. (1899): Magnetische Beobachtungen in der Schweiz. Ausgeführt in den Jahren 1896 und 1897. H. G. Bom, 47 pages, Amsterdam.
- WAGNER, J.-J., CHESSEX, R., DUMORTIER, St., ESPINOSA, A., GALLAY, Cl., NERI, Ph., and WEBEL, S. (1978): The Total Field Magnetic Anomalies of the Ivrea Zone: Tentative Model. Abstract on p. 51 of Programme and Abstracts for the 2nd Symposium IVREA-VERBANO. Varallo Sesia (Italy), 1978.
- WANNER, E. (1939): Die Erdmagnetische Station Regensberg. Ann. der Schweiz. Meteorol. Zentralanst., Jahrgang 1939, n° 8, 2 pages.
- WANNER, E. (1947): Die Deklinationskarte der Schweiz für die Epoche 1948.0 Bezogen auf Kartennord (Meridian von Bern). Ann. der Schweiz. Meteorol. Zentralanst., Jahrgang 1947, addendum inserted between n°s 5 and 6, 2 pages.
- WEAVER, J.T. and THOMSON, D.J. (1972): Induction in a Non-Uniform Conducting Half-Space by an External Line Current. Geophys. J. R. astr. Soc., Vol. **28**, pp. 163–185.
- WEBEL, S. (1973): Geomagnetism of Northwestern Italy: Magnetic and Tectonic Interpretation of the Total Field Anomaly of the Ivrea Zone. Diplom Thesis, Département de Minéralogie, Université de Genève, CH-1211 Genève 4.
- WEBER, E.K., GASSMANN, F., NIGGLI, E., and RÖTHLISBERGER, H. (1949): Die Magnetische Anomalie Westlich von Locarno. Schweiz. Mineralog. und Petrograph. Mitteil., Vol. **29**, n° 2, pp. 492–510.
- WIENERT, K.A. (1970): Notes on Geomagnetic Observatory and Survey Practice. UNESCO Publication, Paris.
- WILD, H. and SIDLER, G. (1859): Bestimmungen der Elemente der Erdmagnetischen Kraft in Bern. Mitteil. der Naturf. Ges. in Bern, n°s 430–434, pp. 49–88.
- WOLF, R. (1858): Über die Deklination in Basel, nach einem Manuskript von Daniel Huber. Vierteljahrsschrift der Naturf. Ges. in Zürich, Vol. **3**, pp. 175–176.
- WOLFENBERGER, R. (1977): Magnetische Intensitätsmessungen im Südwesten von Graubünden. Diplom Thesis, Institut für Geophysik, ETH-Hönggerberg, CH-8093 Zürich.

**TABLE VI** – This table lists the survey sites. The various column headings are, from left to right:

the site number.  
the site name and Canton.  
the x-coordinate in meters.  
the y-coordinate in meters.  
the altitude in meters.  
the declination D in degrees and minutes.\*  
the inclination I in degrees and minutes.\*  
the field amplitude or total intensity F in nT<sup>10</sup>.  
the X-component of the field in nT<sup>10</sup>.  
the Y-component of the field in nT<sup>10</sup>.  
the Z-component of the field in nT<sup>10</sup>.  
the horizontal component or intensity H in nT<sup>10</sup>.  
the declination with respect to map North D<sub>K</sub> in degrees and minutes.\*

\* To save space, degrees (D), minutes (M) and tenths of minutes (m) are here written as DD.MMm

TABLE OF SURVEY SITES

TABLE VI

EPOCH 1978.0

1

NO	SITE	L	CANTON	X COORD	Y COORD	ALT	DECL	INCL	TOT F	X	Y	Z	M	UK
1	LE MONT	VD		156779	538770	742.	2.374	62.420	46705.	21399.	980.	41503.	21421.	2.024
2	NOVILLE	VD		136744	557628	374.	2.510	62.057	46542.	21755.	1083.	41130.	21782.	2.269
3	CHAMPERY	VS		112485	555465	1057.	2.462	61.537	46440.	21852.	1057.	40964.	21877.	2.209
4	L ETIAVZ	VD		140175	580750	1378.	2.431	62.878	46513.	21719.	1031.	41118.	21743.	2.321
5	LES PLANS	VD		122757	573770	1105.	2.495	61.576	46464.	21816.	1077.	41010.	21842.	2.346
6	MOLESON-VILLAGE	FR		156979	569187	1110.	2.537	62.170	46568.	21631.	1094.	41225.	21659.	2.361
7	LE MOURET	FR		175908	579110	755.	2.414	62.252	46624.	21562.	1013.	41326.	21586.	2.294
8	UBERBARM	BE		191372	595505	770.	2.372	62.336	46683.	21490.	983.	41431.	21512.	2.346
9	MUNTHEOD	VD		150465	518014	595.	2.482	62.152	46562.	21652.	1060.	41208.	21678.	2.014
10	COPPET	VD		131662	502194	439.	3.002	62.821	46496.	21774.	1142.	41067.	21803.	2.045
11	AVULLY	GE		113538	488424	400.	3.066	62.819	46439.	21747.	1182.	41015.	21779.	2.033
12	ZWEISELBERG	BE		173270	614007	600.	2.304	62.249	46653.	21583.	945.	41350.	21603.	2.384
13	REICHENBACH	BE		163119	595380	835.	2.369	62.198	46610.	21622.	988.	41280.	21645.	2.343
14	LENK	BE		143750	600959	1067.	2.297	62.890	46544.	21723.	947.	41153.	21743.	2.302
15	KIENTAL	BE		159335	621955	427.	2.307	62.173	46583.	21641.	949.	41240.	21662.	2.433
16	GRINDELWALD	BE		163619	643924	960.	2.212	62.197	46622.	21633.	889.	41290.	21651.	2.464
17	UMBACH	BE		184893	635599	950.	2.267	62.309	46678.	21523.	919.	41410.	21543.	2.472
18	SIGNAU	BE		195962	620807	712.	2.321	62.358	46708.	21476.	951.	41467.	21497.	2.441
19	ETZELKOFEN	BE		213856	602968	550.	2.386	62.465	46740.	21360.	986.	41562.	21383.	2.403
20	SAICOURT	BE		232573	581633	776.	2.459	62.533	46770.	21289.	1028.	41631.	21314.	2.353
21	HEMBETSCH	BE		237972	611323	528.	2.321	62.566	46827.	21279.	942.	41702.	21300.	2.387
22	IFENTHAL	SO		247255	632150	688.	2.313	63.017	46855.	21230.	935.	41759.	21251.	2.500
23	NIEDERLENZ	AG		250188	656422	415.	2.223	63.837	46886.	21223.	879.	41794.	21241.	2.551
24	SISSLEHOF	AG		267012	640000	305.	2.339	63.101	46908.	21152.	948.	41858.	21173.	2.572
25	ANLESMER	BL		259122	612227	307.	2.367	63.849	46902.	21211.	968.	41820.	21233.	2.436
26	RIEMEN	BS		270753	617508	360.	2.317	63.142	47058.	21170.	935.	42017.	21191.	2.419
27	LOEWENBURG	BE		253654	590703	576.	2.451	63.816	46868.	21234.	1021.	41770.	21258.	2.397
28	CHEVENEZ	BE		250146	566055	525.	2.528	63.814	46863.	21231.	1068.	41764.	21258.	2.331
29	LES JORATS	VD		171573	521634	993.	2.584	62.238	46558.	21543.	1119.	41259.	21573.	2.135
30	MEZERY	VD		156283	501778	1200.	2.589	62.181	46540.	21603.	1125.	41207.	21633.	2.927
31	VILLARANON	FR		163944	557738	785.	2.505	62.250	46571.	21538.	1069.	41278.	21564.	2.263
32	MURG	SG		219125	733962	618.	1.536	62.481	46837.	21396.	707.	41658.	21408.	3.110
33	GRUSCH	OM		204760	767934	605.	1.483	62.417	46811.	21463.	676.	41595.	21473.	3.251
34	TSCMUGGENMEDEH	GM		185100	769130	1908.	1.390	62.305	46703.	21550.	621.	41429.	21559.	3.277
35	SUM EN	GM		183167	809143	1408.	1.299	62.325	46732.	21541.	563.	41467.	21548.	3.360
36	MANTINA	GM		146297	830025	1050.	1.258	62.358	46772.	21520.	537.	41524.	21527.	3.362
37	FULDERA	GM		166326	824470	1610.	1.254	62.230	46740.	21663.	538.	41420.	21669.	3.343
38	SUSANA	GM		188154	796163	1660.	1.359	62.251	46644.	21591.	602.	41347.	21599.	3.263
39	BENNINGAPASS	GM		143545	800352	2140.	1.328	62.107	46447.	21670.	585.	41078.	21678.	3.271
40	BRUSIO	GM		127649	806869	940.	2.324	62.236	47313.	21903.	972.	41926.	21945.	4.301
41	STAMPA	GR		134386	765856	1045.	1.506	62.891	46570.	21743.	700.	41177.	21754.	3.251
42	SEGL I.I	GM		145149	778525	1800.	2.342	62.817	46680.	21873.	982.	41227.	21895.	4.161
43	BERGUM	GM		166364	776529	1407.	1.422	62.206	46701.	21668.	644.	41365.	21677.	3.233
44	MALIX	GM		186417	759867	1107.	1.496	62.318	46754.	21556.	687.	41483.	21567.	3.215
45	WEISSTANNEN	SG		206015	744775	1008.	1.503	62.424	46806.	21452.	689.	41595.	21463.	3.138
46	MATT	GL		198095	719676	738.	1.586	62.378	46773.	21490.	742.	41537.	21503.	3.075
47	MEGENSDORF	ZH		252845	678569	528.	2.184	63.036	46914.	21237.	855.	41823.	21255.	3.041
48	KUMMBACH	BE		220443	620042	581.	2.319	62.479	46794.	21370.	945.	41619.	21391.	2.481
49	UFFIRON	LU		228569	644294	497.	2.225	62.532	46815.	21318.	884.	41670.	21336.	2.481
50	MUMI	AO		234564	669139	485.	2.186	62.566	46854.	21295.	859.	41726.	21313.	2.587
51	UNTERWAGELI	ZG		221328	685547	760.	2.130	62.500	46821.	21362.	827.	41656.	21378.	3.025
52	MEICHENBURG	SZ		226454	715652	410.	2.050	62.526	46855.	21347.	777.	41702.	21362.	3.119
53	THINGI	SZ		209725	704025	985.	2.072	62.429	46781.	21431.	793.	41576.	21445.	3.072
54	SEUDORF	UR		194188	689154	434.	2.077	62.372	46756.	21488.	799.	41518.	21503.	2.590
55	ADLIGENSWIL	LU		214000	670413	548.	2.179	62.453	46803.	21409.	859.	41611.	21426.	2.586
56	WOLFENSCHIESSEN	GM		193425	672099	533.	2.163	62.349	46739.	21506.	853.	41489.	21523.	2.578
57	ENTLEBACH	LU		203944	647020	718.	2.231	62.398	46762.	21455.	894.	41540.	21474.	2.502
58	BALDINGEN	AG		267639	665572	567.	2.229	63.118	46938.	21147.	880.	41895.	21166.	3.011
59	BEGGINGEN	SH		290579	681853	610.	2.159	63.244	47007.	21026.	832.	42034.	21043.	3.038
60	DICKIMOF	TO		278262	696132	460.	2.111	63.180	47011.	21108.	805.	41998.	21123.	3.072
61	LAMPERSWIL	TG		274412	720532	445.	2.021	63.168	46987.	21113.	750.	41969.	21127.	3.124
62	KESSEL	SG		272224	741461	445.	1.594	63.156	46996.	21133.	734.	41970.	21145.	3.219
63	BECKEN	SG		254997	765163	405.	1.502	63.062	46955.	21231.	681.	41876.	21242.	3.262
64	PLANZEN	FL		227975	758754	478.	1.536	62.548	46858.	21325.	705.	41719.	21336.	3.255
65	GUTTANNEN	BE		167313	664823	1066.	2.173	62.205	46649.	21637.	865.	41318.	21654.	2.544
66	ANDEHMATT	UR		165613	687970	1433.	2.090	62.259	46645.	21572.	810.	41349.	21588.	2.594
67	FAIDU	TI		148203	705200	753.	2.045	62.105	46568.	21722.	787.	41184.	21737.	3.046
68	USOGNA	TI		129524	719110	265.	2.103	62.096	46568.	21732.	824.	41178.	21747.	3.181
69	TAVERNE	TI		103248	715562	368.	2.075	61.497	46505.	21941.	814.	40996.	21956.	3.130
70	GENESTERIO	TI		79088	718747	340.	2.011	61.401	46384.	21999.	775.	40828.	22013.	3.081
71	SOMLENT	TI		139028	684299	810.	2.086	62.076	46568.	21756.	814.	41165.	21771.	2.567
72	MOHEGNO	TI		121400	698262	305.	1.593	62.084	46469.	21702.	753.	41083.	21716.	2.552
73	LOSONE CASERNE	TI		114453	701044	227.	2.108	62.259	46562.	21534.	820.	41275.	21549.	3.082
74	LOSONE CENTRE	TI		113311	702965	210.	2.357	62.190	46790.	21716.	984.	41434.	21738.	3.342
75	ARCEGNO	TI		113074	701020	430.	2.575	62.353	46857.	21543.	1113.	41596.	21572.	3.548
76	ASCONA	TI		112054	704898	198.	2.355	62.005	46727.	21909.	992.	41261.	21931.	3.350
77	MAGADINO	TI		114333	710273	146.	2.159	62.016	46587.	21835.	864.	41144.	21852.	3.185
78	LUSTALLO	GM		129712	734814	413.	1.567	62.056	46567.	21782.	740.	41152.	21795.	3.134
79	MEDELS	GR		156145	740810	1510.	1.561	62.163	46630.	21684.	733.	41275.	21696.	3.166
80	ANDELM	GR		163875	752500	975.	1.482	62.221	46674.	21636.	681.	41351.	21647.	3.155
81	SCHLEUTS	GM		182342	736073	702.	1.526	62.125	46735.	21538.	706.	41470.	21550.	3.108
82	YRIN	GM		168806	727163	1461.	1.527	62.227	46666.	21624.	709.	41347.	21636.	3.056
83	DISENTIS	GR		173180	704383	1113.	1.594	62.283	46647.	21547.	749.	41360.	21560.	3.016
84	MUNTWIL	AN		247745	741628	783.	1.556	63.026	46944.	21740.	715.	41827.	21772.	3.178
85	KIMCHBERG	SO		251448	720264	740.	2.807	63.043	46949.	21747.	746.	41855.	21760.	3.106

NO	SITE	&	CANTON	X COORD	Y COORD	ALT	DECL	INCL	TOT F	X	Y	Z	H	OK
86	LIDBERG		ZH	259174	701637	555.	2.065	63.088	46936.	21187.	780.	41875.	21201.	3.056
87	HEUGMEILEN		ZH	237625	694055	706.	2.120	62.581	46879.	21290.	818.	41758.	21306.	3.065
88	WITZIL		BE	203228	571000	432.	2.426	62.371	46713.	21460.	1016.	41779.	21484.	2.259
89	MUNTMAIGNY		VD	197180	567000	565.	2.452	62.356	46686.	21465.	1032.	41446.	21490.	2.262
90	GLETTEHENS		FM	194024	560674	454.	2.498	62.343	46664.	21469.	1061.	41418.	21495.	2.272
91	CHABLES		FR	185932	552332	607.	2.502	62.305	46657.	21511.	1066.	41388.	21538.	2.228
92	FRUCHAUX		NE	210250	567099	615.	2.443	62.404	46758.	21440.	1025.	41540.	21465.	2.253
93	MOOS		BE	217250	573075	817.	2.457	62.459	46819.	21401.	1032.	41629.	21426.	2.301
94	OMVIN		BE	223699	584090	658.	2.429	62.505	46743.	21312.	1011.	41590.	21336.	2.337
95	COMUEMONT		BE	224600	577250	1145.	2.534	62.531	46768.	21289.	1075.	41628.	21316.	2.402
96	ST IMIER		BE	221699	566625	815.	2.485	62.506	46822.	21345.	1047.	41660.	21371.	2.292
97	CEHNIER		NE	211460	559875	778.	2.464	62.404	46759.	21440.	1039.	41541.	21465.	2.232
98	GRANGES		VD	178449	557700	478.	2.451	62.258	46628.	21556.	1036.	41333.	21581.	2.208
99	CHESELAUX		VD	182300	542924	515.	2.484	62.270	46627.	21540.	1056.	41340.	21566.	2.156
100	OGENS		VD	172500	545125	635.	2.500	62.239	46547.	21540.	1066.	41249.	21566.	2.185
101	GOMUEENS		VD	168880	535540	615.	2.520	62.256	46518.	21505.	1077.	41234.	21532.	2.151
102	MATHUO		VD	178274	532375	452.	2.557	62.255	46589.	21538.	1102.	41297.	21566.	2.169
103	LES MATTES		NE	204412	553549	818.	2.505	62.379	46700.	21442.	1064.	41473.	21468.	2.237
104	SOM MARTEL		NE	208603	548152	1294.	2.533	62.401	46696.	21413.	1080.	41483.	21440.	2.234
105	LES MOULET		NE	213975	553045	1100.	2.489	62.417	46737.	21414.	1053.	41529.	21440.	2.218
106	CHAUX D ABEL		BE	223074	560979	1050.	2.474	62.513	46801.	21327.	1039.	41646.	21353.	2.248
107	LES MUEULEUX		NE	228385	568115	988.	2.481	62.550	46792.	21278.	1041.	41661.	21304.	2.246
108	LE BEMONT		BE	234399	570889	1021.	2.523	62.581	46785.	21236.	1065.	41674.	21263.	2.354
109	COMHE PELLATON		NE	201853	541262	1164.	2.537	62.382	46688.	21432.	1084.	41644.	21459.	2.199
110	CHEUX DU VAN		NE	199119	546332	980.	2.509	62.379	46687.	21436.	1067.	41461.	21462.	2.200
111	ST SULPICE		NE	197319	533895	1119.	2.574	62.346	46666.	21464.	1109.	41422.	21443.	2.193
112	L AUBERSON		VD	184127	526637	1230.	3.004	62.280	46606.	21515.	1130.	41328.	21544.	2.183
113	MULLET		VD	188800	535277	1223.	2.565	62.306	46628.	21495.	1105.	41363.	21523.	2.193
114	MT AUBERT		VD	192404	541650	1145.	2.524	62.328	46659.	21484.	1078.	41405.	21511.	2.188
115	VUILLEHENS		VD	159912	526680	548.	2.467	62.223	46536.	21555.	1046.	41230.	21580.	2.047
116	MT TENDRE		VD	158827	515229	1273.	2.557	62.194	46531.	21585.	1104.	41207.	21613.	2.072
117	PHEVENEGES		VD	151596	530240	375.	2.294	62.245	46672.	21597.	939.	41364.	21617.	1.945
118	ST CENGUE		VD	145524	503444	1043.	2.577	62.099	46528.	21696.	1122.	41145.	21725.	2.026
119	ST URSANNE		BE	245060	578742	678.	2.457	62.583	46839.	21260.	1026.	41723.	21265.	2.334
120	BONFOL		BE	258895	578915	457.	2.472	63.053	46899.	21202.	1032.	41820.	21227.	2.344
121	BONCOURT		BE	259579	570064	428.	2.502	63.062	46906.	21193.	1050.	41832.	21219.	2.326
122	WALLENBACH		FM	198177	583387	509.	2.407	62.366	46708.	21464.	1004.	41472.	21488.	2.311
123	MUTTEN		FM	195853	574220	440.	2.448	62.352	46690.	21472.	1030.	41447.	21496.	2.300
124	PAYEMNE		VD	187247	562319	440.	2.510	62.317	46664.	21500.	1070.	41402.	21527.	2.293
125	GULLEY		FM	187430	571836	500.	2.441	62.304	46660.	21516.	1028.	41390.	21540.	2.279
126	COTTENS		FM	178010	569915	718.	2.473	62.270	46638.	21546.	1049.	41350.	21571.	2.300
127	TAFENS		FM	186104	584614	688.	2.417	62.299	46662.	21523.	1013.	41389.	21547.	2.329
128	MUNTSCHENIER		BE	204393	576830	433.	2.430	62.382	46734.	21456.	1018.	41505.	21480.	2.296
129	MOENISWIL		BE	205149	593825	625.	2.408	62.398	46734.	21438.	1003.	41515.	21461.	2.372
130	HARDERN		BE	215350	591580	490.	2.391	62.403	46748.	21366.	990.	41568.	21389.	2.342
131	GRANDVAL		BE	236560	599529	635.	2.392	62.561	46809.	21275.	986.	41683.	21298.	2.369
132	COMFAIVRE		BE	241800	588599	500.	2.422	62.570	46829.	21273.	1004.	41706.	21246.	2.356
133	FRANZY		F	95739	482750	515.	3.035	61.437	46775.	21934.	1172.	40843.	21963.	1.571
134	LELEA		F	128539	483870	855.	3.075	62.803	46464.	21778.	1189.	41027.	21810.	2.014
135	MIDOUX		F	138470	491170	1035.	3.031	62.861	46490.	21722.	1158.	41087.	21753.	2.011
136	MOBBIER		F	156000	492770	938.	3.049	62.145	46527.	21638.	1165.	41173.	21670.	2.036
137	MOUTHE		F	173949	505629	950.	3.015	62.228	46572.	21561.	1139.	41265.	21541.	2.074
138	METABIEF		F	178750	515610	1038.	3.010	62.250	46587.	21542.	1135.	41292.	21572.	2.126
139	LES FOURGS		F	188250	521139	1092.	3.023	62.296	46633.	21507.	1142.	41361.	21538.	2.170
140	GOUX		F	204500	510260	728.	3.071	62.362	46703.	21458.	1169.	41465.	21490.	2.154
141	LA FRESSE		F	200939	524540	1037.	2.599	62.359	46679.	21453.	1124.	41442.	21483.	2.164
142	GRAND COMBE		F	207000	533000	798.	2.578	62.388	46693.	21426.	1109.	41472.	21454.	2.192
143	VILLES		F	212739	540319	935.	2.550	62.412	46715.	21408.	1091.	41507.	21435.	2.205
144	LE BARBOUX		F	219324	544724	955.	2.540	62.452	46747.	21374.	1083.	41560.	21402.	2.221
145	BRETONVILLES		F	229750	537970	715.	2.587	62.507	46815.	21337.	1110.	41655.	21366.	2.228
146	CHAMQUEMONT		F	229420	554080	868.	2.543	62.517	46777.	21309.	1081.	41627.	21337.	2.277
147	CHAMMAUVILLENS		F	232569	561430	860.	2.520	62.552	46783.	21271.	1065.	41654.	21247.	2.297
148	INDEUILLENS		F	239930	564259	785.	2.516	62.563	46804.	21267.	1062.	41680.	21243.	2.309
149	AUTCHAUX		F	250199	553599	555.	2.541	63.819	46870.	21228.	1076.	41773.	21255.	2.271
150	BOUMOGNE		F	268000	559500	390.	2.510	63.115	46924.	21137.	1052.	41881.	21163.	2.274
151	HAGENBACH		F	276625	578450	305.	2.460	63.165	46961.	21094.	1019.	41944.	21119.	2.334
152	BANTENHEIM		F	276000	606450	239.	2.381	63.174	47006.	21106.	971.	41990.	21128.	2.419
153	MEZIEHENS		VD	161725	548319	756.	2.508	62.409	46601.	21360.	1062.	41404.	21387.	2.212
154	MT PELERIN		VD	149149	551200	805.	3.121	62.101	46640.	21741.	1216.	41245.	21775.	2.442
155	LES AVANTS		VD	146524	561125	1018.	3.056	62.090	46550.	21715.	1173.	41158.	21746.	2.434
156	CHATEL ST DENIS		FR	155140	559950	845.	3.008	62.151	46588.	21661.	1140.	41230.	21691.	2.379
157	MAKSENS		FR	167510	569459	898.	2.475	62.213	46579.	21587.	1053.	41262.	21612.	2.300
158	LA VALSAINTE		FR	166100	582860	1178.	2.435	62.211	46585.	21593.	1028.	41266.	21617.	2.337
159	CHATEAU D OEX		FR	145250	574099	948.	2.462	62.102	46548.	21706.	1050.	41164.	21731.	2.314
160	VANIL MOIX		FR	151039	579330	1175.	2.438	62.133	46545.	21668.	1033.	41181.	21692.	2.320
161	GSTAAD		BE	145579	588779	1165.	2.393	62.899	46537.	21706.	1007.	41152.	21729.	2.329
162	WEISSENHURG		BE	166475	603569	878.	2.334	62.212	46605.	21604.	965.	41284.	21626.	2.354
163	GIMMIALP		BE	154659	604900	1375.	2.322	62.139	46565.	21673.	960.	41203.	21645.	2.350
164	GUMNUELBAD		BE	178250	601000	1270.	2.504	62.276	46669.	21552.	1069.	41381.	21578.	2.510
165	GUGGISHEM		BE	177279	590200	840.	2.396	62.263	46636.	21555.	1001.	41343.	21579.	2.340
166	AMUNTIENES		F	91474	560114	1235.	2.493	61.415	46360.	21958.	1042.	40816.	21985.	2.267
167	TANIGUES		F	105900	534544	604.	2.492	61.480	46419.	21902.	1074.	40913.	21928.	2.121
168	NANT BRILE		F	101844	550844	830.	2.458	61.455	46425.	21942.	1059.	40944.	21944.	2.140
169	MONTJINE		F	115175	547170	1200.	2.500	61.540	46441.	21945.	1041.	40944.	21944.	2.140
170	LA CHAPELLE		F	127044	548750	905.	2.524	61.540	46444.	21807.	1045.	41017.	21944.	2.140

TABLE OF SURVEY SITES  
\*\*\*\*\*

TABLE VI

EPOCH 1978.0

3

NO	SITE	A	CANTON	X COORD	Y COORD	ALT	DECL	INCL	TOT F	X	Y	Z	M	DM
171	JAMBAZ	F		123360	530549	850.	2.527	61.576	46486.	21825.	1097.	41029.	21852.	2.132
172	LUGNIN	F		138399	539549	550.	2.549	62.007	46621.	21851.	1113.	41168.	21879.	2.204
173	THONON	F		139100	527875	385.	2.462	62.035	46608.	21814.	1055.	41175.	21839.	2.051
174	YVOIRE	F		134074	515020	440.	2.526	62.031	46526.	21778.	1094.	41100.	21806.	2.042
175	LES FONTAINES	F		120099	512900	535.	2.504	61.555	46461.	21837.	1122.	40994.	21866.	2.069
176	MENTHONNEX	F		100099	502450	820.	2.587	61.463	46394.	21914.	1140.	40876.	21944.	2.034
177	SIEMME	GE		114489	503125	400.	2.596	61.535	46425.	21843.	1142.	40950.	21873.	2.046
178	MINDENBACH	BE		211784	620084	680.	2.305	62.431	46752.	21409.	938.	41551.	21429.	2.421
179	MOMNBACH	BE		208824	633150	910.	2.271	62.410	46743.	21431.	918.	41530.	21451.	2.462
180	DAIWIL	LU		215949	643750	580.	2.224	62.465	46788.	21386.	886.	41605.	21405.	2.477
181	SOEHENBERG	LU		184600	646540	1220.	2.228	62.310	46682.	21525.	895.	41414.	21543.	2.495
182	LOMBACH	LU		196199	637400	870.	2.261	62.361	46712.	21476.	913.	41472.	21466.	2.476
183	UTZIGEN	BE		200560	609360	680.	2.336	62.383	46720.	21451.	959.	41493.	21473.	2.390
184	WICHTACH	BE		188199	611110	595.	2.310	62.327	46691.	21506.	945.	41432.	21527.	2.374
185	OBENLANGNEG	BE		184670	623349	940.	2.285	62.306	46686.	21530.	931.	41415.	21550.	2.419
186	ISELWALD	BE		173600	640700	570.	2.200	62.240	46661.	21600.	880.	41351.	21618.	2.433
187	GUENHUEETTE	BE		173850	625025	1150.	2.267	62.233	46643.	21598.	922.	41331.	21618.	2.411
188	LAUTERBUNNEN	BE		156489	635750	850.	2.247	62.160	46596.	21665.	912.	41243.	21684.	2.451
189	SAALETEN	BE		165119	630369	1120.	2.241	62.209	46613.	21614.	907.	41289.	21633.	2.415
190	HUETI	BE		181074	600270	820.	2.345	62.283	46663.	21545.	969.	41380.	21567.	2.347
191	GANTWISCH	BE		174274	599849	1430.	2.369	62.242	46626.	21577.	985.	41321.	21599.	2.368
192	FRUTIGEN	BE		157050	614849	1035.	2.269	62.158	46592.	21665.	926.	41238.	21684.	2.354
193	KANDENSTEG	BE		149225	618500	1190.	2.292	62.120	46559.	21694.	942.	41185.	21714.	2.398
194	WULFWIL	SO		236524	625775	437.	2.306	62.585	46838.	21262.	932.	41724.	21282.	2.455
195	HEKSWIL	SO		224284	615209	490.	2.315	62.503	46790.	21339.	941.	41630.	21360.	2.403
196	MOEDSDORF	SO		259399	600310	370.	2.386	63.050	46911.	21214.	979.	41829.	21236.	2.388
197	WIKON	LU		234335	639799	449.	2.237	62.582	46828.	21263.	889.	41713.	21281.	2.408
198	ZEIZWIL	AG		238500	654200	630.	2.226	62.583	46847.	21270.	883.	41730.	21289.	2.540
199	SUMM	AG		245489	647525	425.	2.259	63.009	46864.	21246.	902.	41762.	21265.	2.535
200	GRINDEL	SO		247720	605865	615.	2.368	63.006	46857.	21243.	970.	41754.	21265.	2.402
201	HEIGOLDSWIL	BL		249000	619814	630.	2.343	63.013	46864.	21239.	954.	41764.	21260.	2.458
202	MUSSHOF	BL		260559	628029	590.	2.281	63.068	46912.	21195.	914.	41841.	21215.	2.444
203	WOLFLINSWIL	AG		257034	643119	480.	2.249	63.064	46899.	21195.	894.	41827.	21214.	2.500
204	MOLNTHAL	AG		262659	654669	430.	2.212	63.099	46923.	21164.	870.	41870.	21182.	2.530
205	MEUENTHAL	AG		273625	658830	313.	2.183	63.150	46957.	21118.	850.	41932.	21135.	2.526
206	OBENHRENDINGEN	ZH		260924	668700	502.	2.166	63.093	46925.	21174.	842.	41868.	21140.	2.566
207	MAFZ	ZH		273239	681900	412.	2.127	63.151	46965.	21122.	816.	41939.	21138.	3.005
208	STEINMAH	ZH		261190	676020	465.	2.153	63.094	46922.	21171.	834.	41866.	21168.	2.545
209	PFUNGEN	ZH		264384	691279	397.	2.090	63.105	46945.	21170.	795.	41893.	21185.	3.022
210	KAMSEN	SH		285620	703134	415.	2.064	63.209	47026.	21080.	778.	42029.	21094.	3.072
211	HALLAU	SH		282370	676935	424.	2.152	63.198	46981.	21071.	829.	41983.	21087.	3.001
212	MAULBURG	D		276825	626000	355.	2.398	63.167	46945.	21086.	981.	41931.	21109.	2.550
213	KAPELLEBUHL	D		291260	638724	1025.	2.312	63.225	46953.	21022.	925.	41974.	21042.	2.539
214	GOESWIL	D		277000	647325	710.	2.278	63.164	46940.	21091.	907.	41925.	21111.	2.554
215	GOESCHWEILER	D		301799	666299	900.	2.208	63.292	47014.	20970.	859.	42070.	20987.	2.598
216	WATTEHNINGEN	D		301534	694689	790.	2.114	63.307	47051.	20970.	802.	42112.	20985.	3.064
217	SCHLATT	D		292219	694900	518.	2.089	63.244	47036.	21041.	789.	42060.	21056.	3.044
218	KRUTTENBUHL	D		299440	715740	475.	2.057	63.291	47042.	20987.	768.	42094.	21001.	3.135
219	SALEM	D		292575	738540	440.	2.033	63.255	47042.	21032.	755.	42072.	21045.	3.243
220	BAVENSODORF	D		291674	757200	505.	1.522	63.247	47050.	21047.	687.	42074.	21058.	3.241
221	OBERDUMF	D		277409	761599	425.	1.513	63.176	47017.	21119.	684.	42001.	21131.	3.256
222	MUEHNWEILER	A		273239	775865	495.	1.462	63.161	47012.	21136.	653.	41987.	21147.	3.288
223	MEININGEN	A		239329	761599	430.	1.478	62.599	46911.	21288.	668.	41797.	21298.	3.215
224	THUEINGEN	A		230375	777064	610.	1.446	62.347	46887.	21341.	650.	41744.	21351.	3.271
225	SCHRUNZ	A		215524	789209	690.	1.392	62.458	46866.	21440.	619.	41670.	21449.	3.285
226	PARTENEN	A		204824	800500	1090.	1.363	62.381	46788.	21498.	602.	41552.	21506.	3.319
227	GALTUER	A		205935	809490	1560.	1.357	62.398	46804.	21485.	598.	41577.	21493.	3.365
228	KAPPL	A		215779	822209	1190.	1.312	62.460	46856.	21434.	564.	41662.	21442.	3.395
229	PFUNDS	A		204909	833900	980.	1.288	62.429	46815.	21454.	554.	41606.	21461.	3.437
230	PRUTZ	A		219699	844900	870.	1.225	62.505	46871.	21388.	513.	41703.	21344.	3.440
231	ARLBENGPASS	A		224300	806240	1390.	1.323	62.501	46863.	21388.	574.	41694.	21346.	3.316
232	SCHNEPPAU	A		247449	789924	750.	1.411	63.034	46943.	21261.	625.	41848.	21270.	3.314
233	LIODLINGENDE	NE		217869	561330	1135.	2.466	62.467	46807.	21386.	1037.	41623.	21411.	2.243
234	CHUFFORT	NE		216680	568919	1035.	2.446	62.444	46791.	21407.	1026.	41594.	21432.	2.286
235	PNE MONSIEUR	BE		214484	574740	795.	2.459	62.429	46787.	21423.	1035.	41581.	21448.	2.313
236	MELCHSEE	OW		180925	666229	1980.	2.170	62.297	46657.	21530.	858.	41383.	21547.	2.550
237	STALDEN	OW		193329	657259	990.	2.190	62.347	46717.	21497.	870.	41468.	21515.	2.519
238	ENNETBUERGEN	OW		205050	675450	505.	2.151	62.412	46776.	21447.	843.	41561.	21463.	2.586
239	EIGENTAL	LU		203500	659090	1110.	2.186	62.398	46754.	21453.	865.	41533.	21470.	2.527
240	SEMPACH	LU		218024	657509	520.	2.191	62.482	46827.	21385.	866.	41650.	21402.	2.523
241	BEROMUNSTER	LU		229479	658930	735.	2.218	62.551	46838.	21305.	874.	41703.	21323.	2.559
242	ROTKREUZ	ZG		223560	675794	445.	2.178	62.494	46834.	21374.	857.	41664.	21391.	3.016
243	ALBIS	ZH		236810	682389	735.	2.124	62.577	46861.	21287.	820.	41739.	21302.	3.002
244	EGGENWIL	AB		246470	668119	365.	2.180	63.015	46876.	21246.	853.	41776.	21261.	2.575
245	GO ST BERNARD	VS		82570	580450	2020.	2.291	61.408	46244.	21917.	951.	40709.	21938.	2.181
246	CHANNION	VS		88659	593930	1990.	2.261	61.483	46047.	21736.	924.	40583.	21756.	2.227
247	CHAMPSEC	VS		100360	585189	915.	2.357	61.439	46315.	21912.	993.	40791.	21935.	2.273
248	ROISAN	I		71474	589950	770.	2.040	61.222	46484.	22258.	803.	40801.	22273.	1.583
249	BLONAZ	I		81125	600799	1620.	2.146	61.477	46484.	21953.	860.	40965.	21970.	2.151
250	ENTREVES	I		77420	567049	1635.	2.405	61.363	46305.	21996.	1028.	40734.	22020.	2.214
251	PREUIL	I		87260	614500	2015.	2.289	63.026	46229.	20956.	176.	41206.	20956.	2.371
252	ANTRY	I		72949	611619	1025.	1.544	61.307	46538.	22184.	771.	40903.	22198.	2.080
253	CHAMPOLUC	I		77449	623006	1598.	3.546	61.299	46495.	22135.	1513.	40860.	22187.	4.076
254	GNESSUNET	I		77869	629125	1740.	2.515	60.520	46118.	22244.	1120.	40744.	22447.	3.040
255	UMY	I		60599	613400	1000.	2.225	61.298	46141.	22000.	912.	40548.	22014.	2.413

TABLE OF SURVEY SITES  
\*\*\*\*\*

TABLE VI

EPOCH 1978.0

4

NO	SITE	&	CANTON	X COORD	Y COORD	ALT	DECL	INCL	TOT F	X	Y	Z	M	OK
256	VARALLO	I		74049	660250	480.	2.381	61.463	46520.	21980.	1012.	40987.	22003.	3.121
257	ALAGNA	I		77030	639099	1120.	2.352	61.333	46309.	22035.	995.	40718.	22058.	2.573
258	MIGLIANDONE	I		93300	673224	210.	1.272	61.441	46426.	21978.	558.	40890.	21985.	2.086
259	VANZONE	I		91375	650439	690.	2.152	61.406	46373.	21984.	865.	40821.	22002.	2.437
260	VILLADOSSOLA	I		101550	664669	235.	2.181	61.526	46338.	21825.	877.	40867.	21842.	2.547
261	CREVOLA	I		111650	667625	305.	1.578	61.581	46427.	21806.	748.	40981.	21819.	2.362
262	AREUSE	NE		200149	556534	435.	2.504	62.363	46695.	21459.	1065.	41458.	21485.	2.254
263	BEVAIX	NE		197300	552810	455.	2.545	62.360	46673.	21451.	1090.	41437.	21479.	2.273
264	GONGIER	NE		195210	548700	608.	2.523	62.359	46708.	21469.	1077.	41467.	21496.	2.226
265	LUESCHENZ	BE		210125	578650	515.	2.393	62.417	46771.	21432.	994.	41560.	21455.	2.270
266	AUTAVAX	FR		189989	556630	481.	2.529	62.329	46676.	21490.	1082.	41420.	21518.	2.280
267	NALPS	GR		164135	701400	1950.	2.255	62.090	46670.	21783.	922.	41264.	21802.	3.236
268	BRIGELS	GR		181114	724044	1265.	2.023	62.302	46705.	21550.	767.	41429.	21564.	3.135
269	LEVMELIA	GR		158600	725770	1865.	2.001	62.170	46616.	21668.	757.	41267.	21681.	3.120
270	SAFIENPLATZ	GR		172125	743729	1308.	1.506	62.252	46695.	21608.	695.	41389.	21619.	3.130
271	ANDSA	GR		182515	770020	1750.	1.503	62.335	46760.	21538.	691.	41499.	21549.	3.280
272	STWASSBENG	GR		191675	777619	1980.	1.481	62.362	46737.	21495.	676.	41495.	21506.	3.303
273	PRATVAL	GR		177414	753810	710.	1.556	62.282	46729.	21587.	726.	41438.	21599.	3.239
274	JOF	GR		146229	763924	2115.	1.536	62.171	46556.	21640.	715.	41215.	21652.	3.272
275	INNERFENNERA	GR		154069	754000	1510.	1.573	62.179	46608.	21654.	739.	41266.	21667.	3.253
276	TIEFENCASTEL	GR		170939	764604	1150.	1.500	62.249	46693.	21611.	692.	41385.	21622.	3.244
277	RUNA	GR		158475	767924	1415.	.211	62.237	46624.	21604.	133.	41316.	21604.	1.572
278	VAL MOSEG	GR		148135	787659	1905.	1.443	62.091	46554.	21737.	660.	41162.	21747.	3.315
279	BEVER	GR		158399	789034	1710.	1.486	62.193	46749.	21704.	686.	41399.	21715.	3.367
280	UMHAIL	GR		159050	829790	2445.	1.319	62.180	46673.	21688.	580.	41324.	21696.	3.434
281	IL FUORN	GR		171750	811935	1790.	1.325	62.264	46735.	21615.	582.	41432.	21623.	3.340
282	ZENNEZ	GR		177725	802450	1610.	1.430	62.326	46665.	21507.	645.	41409.	21516.	3.392
283	RAMOSCH	GR		190800	824790	1145.	1.279	62.395	46797.	21487.	550.	41569.	21494.	3.372
284	S-CHAML	GR		177970	821020	1790.	1.313	62.316	46776.	21572.	573.	41501.	21579.	3.382
285	SENTIG	GR		176619	784634	1890.	1.442	62.293	46689.	21557.	654.	41409.	21567.	3.301
286	S ANTONIEN	GR		204630	788490	1408.	1.419	62.435	46792.	21434.	636.	41590.	21443.	3.260
287	SANDASCA	GR		193015	795599	1638.	1.420	62.360	46841.	21547.	639.	41586.	21556.	3.345
288	UNTERVAZ	GR		200625	760465	530.	1.457	62.398	46798.	21480.	661.	41572.	21490.	3.181
289	BALZERS	FL		215939	756860	472.	1.543	62.493	46835.	21381.	711.	41664.	21392.	3.249
290	OBENWALD	VS		153444	669950	1375.	2.106	62.150	46544.	21656.	823.	41191.	21672.	2.506
291	NUFEMEN	TI		147396	676139	1443.	2.027	62.083	46506.	21720.	776.	41115.	21734.	2.462
292	PIUTTA	TI		152055	695627	991.	2.111	62.110	46596.	21728.	829.	41212.	21744.	3.057
293	SEMENTINA	TI		115599	714316	214.	2.098	62.022	46563.	21818.	824.	41127.	21834.	3.176
294	CASTELHOTTO	TI		93619	708990	208.	2.085	61.456	46439.	21958.	821.	40912.	21773.	3.102
295	LE SEPER	VO		135750	571945	1335.	2.487	62.052	46509.	21746.	1068.	41098.	21773.	2.327
296	MUKAZ	VS		125039	561450	390.	2.470	61.586	46533.	21837.	1062.	41077.	21863.	2.251
297	DOHEMAZ	VS		111940	569259	450.	2.471	61.548	46464.	21850.	1063.	40992.	21876.	2.297
298	ANDON	VS		117920	587979	488.	2.382	61.564	46444.	21824.	1005.	40985.	21847.	2.314
299	SANETSCH	VS		132909	588580	4078.	2.418	62.037	46476.	21751.	1024.	41059.	21775.	2.353
300	TSANFLEUNGOM	VS		126565	590974	1385.	2.400	61.591	46471.	21804.	1016.	41026.	21828.	2.349
301	PHAZ JEAN	VS		110909	601090	1050.	2.350	61.471	46461.	21944.	990.	40940.	21966.	2.356
302	MUHEL	VS		132939	646509	1120.	2.046	62.024	46473.	21769.	789.	41052.	21783.	2.311
303	ZEHMATT	VS		44275	623029	1840.	4.388	60.432	47105.	22462.	1866.	41087.	23038.	4.518
304	GNAECHEN	VS		114809	629985	1568.	2.236	61.538	46439.	21857.	914.	40964.	21876.	2.406
305	MATTMARK	VS		96820	640639	2220.	2.213	61.453	46380.	21893.	900.	40787.	21911.	2.443
306	SEMBAENCHER	VS		103014	579264	745.	2.467	61.457	46413.	21934.	1064.	40889.	21960.	2.350
307	THIENT	VS		99375	565549	1345.	2.456	61.455	46373.	21918.	1057.	40853.	21943.	2.261
308	SCHWYZ	SZ		209938	692229	670.	2.081	62.439	46769.	21424.	799.	41594.	21439.	3.013
309	BISISTAL	SZ		201955	705645	798.	2.050	62.293	46789.	21469.	781.	41543.	21483.	3.059
310	SUSTEN	UN		177204	680788	1658.	2.097	62.268	46651.	21564.	814.	41360.	21580.	2.561
311	REALP	UR		160122	679724	1963.	1.597	62.246	46623.	21580.	752.	41321.	21593.	2.453
312	AMSTEG	UR		180372	697000	838.	2.081	62.279	46647.	21549.	803.	41363.	21564.	3.038
313	KLAUSEN	UN		194010	711139	1375.	2.021	62.351	46726.	21501.	764.	41478.	21514.	3.061
314	ELM	GL		198000	732435	988.	1.556	62.386	46775.	21482.	723.	41544.	21444.	3.119
315	ENGI	GL		205319	729764	775.	1.540	62.353	46762.	21516.	714.	41512.	21528.	3.088
316	KLOENTAL	GL		208863	711244	1130.	2.011	62.435	46780.	21424.	755.	41579.	21437.	3.053
317	SIMPLON	VS		121780	645288	1975.	2.158	61.598	46454.	21794.	861.	41015.	21811.	2.415
318	GONDOD	VS		115387	654082	1001.	2.100	61.522	46445.	21882.	828.	40959.	21898.	2.407
319	FORMAZZA	I		134939	676194	1259.	2.067	62.095	46479.	21692.	800.	41099.	21707.	2.501
320	BACENO	I		123855	668639	780.	2.211	61.529	46442.	21869.	898.	40961.	21888.	3.001
321	CANNOBIO	I		101505	696150	227.	2.075	61.424	46549.	22048.	818.	40988.	22064.	3.020
322	CUVIO	I		84389	701310	272.	2.071	61.419	46447.	22006.	814.	40895.	22021.	3.043
323	BINAGO	I		71190	714060	373.	2.035	61.404	46418.	22011.	791.	40860.	22025.	3.078
324	MONTEFANO	I		71840	734400	389.	1.562	61.381	46381.	22022.	745.	40812.	22035.	3.129
325	S FEDELE	I		92559	726560	750.	1.578	61.446	46435.	21970.	753.	40902.	21983.	3.094
326	BENE LARIO	I		98885	735909	348.	1.557	61.475	46476.	21956.	739.	40956.	21968.	3.127
327	SORICO	I		115210	750500	208.	1.502	61.583	46508.	21843.	700.	41053.	21854.	3.157
328	MADESIMO	I		145720	747965	1605.	1.490	62.117	46564.	21709.	689.	41188.	21720.	3.135
329	GORDONA	I		127739	749755	248.	1.491	61.468	46753.	22096.	701.	41190.	22108.	3.143
330	VAL MASIMO	I		120375	769875	820.	1.363	61.517	46479.	21911.	614.	40986.	21920.	3.129
331	VAL MALENCO	I		123954	786200	745.	1.397	59.515	47104.	23643.	686.	40735.	23653.	3.256
332	TEGLIO	I		114789	802424	367.	1.338	61.451	46735.	22111.	603.	41169.	22119.	3.287
333	MALGHE GRUA	I		116699	818040	874.	1.477	61.518	46686.	22005.	690.	41169.	22016.	3.516
334	SUNUALO	I		134399	822264	870.	1.370	61.579	46602.	21895.	618.	41134.	21903.	3.436
335	VALDIDENTO	I		152104	821479	1320.	1.298	62.158	46621.	21690.	567.	41264.	21698.	3.364
336	LIVIGNO	I		155529	806273	1450.	1.357	62.151	46634.	21704.	604.	41271.	21712.	3.336
337	PRATTO	I		167783	842378	908.	1.244	62.238	46744.	21652.	535.	41423.	21654.	3.438
338	NESTA	I		189875	840637	1060.	1.272	62.378	46773.	21496.	545.	41537.	21503.	3.446
339	MESOCO	GR		140444	737402	842.	1.540	62.094	46544.	21724.	721.	41154.	21740.	3.176
340	VAL CALANCA	GR		142188	730187	1334.	1.572	62.101	46570.	21730.	741.	41183.	21742.	3.115

TABLE OF SURVEY SITES  
\*\*\*\*\*

TABLE VI

EPOCH 1978.0

5

NO	SITE	A	CANTON	X COORD	Y COORD	ALT	DECL	INCL	TOT F	X	Y	Z	M	DK
341	ROVEMEDO	GM		121320	728009	269.	1.568	62.025	46516.	21795.	741.	41087.	21808.	3.096
342	LAVENTIZZO	TI		124375	707259	560.	2.056	62.093	46486.	21698.	793.	41104.	21713.	3.066
343	SOMOGNO	TI		135529	704474	971.	2.046	62.069	46532.	21749.	789.	41129.	21763.	3.041
344	SOMELO	TI		126630	694194	378.	2.061	62.044	46499.	21763.	799.	41084.	21777.	2.597
345	CIMALOTTO	TI		126193	680869	1390.	2.082	61.593	46511.	21829.	814.	41062.	21844.	2.542
346	FUSIO	TI		144904	694459	1390.	2.082	62.117	46558.	21703.	810.	41182.	21718.	3.021
347	MONETO	TI		111855	691189	690.	1.427	62.130	46234.	21541.	644.	40904.	21551.	2.345
348	BRISSAGO	TI		108650	696573	910.	2.225	61.373	46776.	22213.	921.	41155.	22232.	3.173
349	SEMIONE	TI		140704	718130	378.	2.012	62.102	46589.	21737.	767.	41200.	21750.	3.086
350	PIZ MEDEL	TI		160603	714705	1670.	2.004	62.171	46568.	21644.	758.	41225.	21658.	3.060
351	TORRE	TI		149984	715895	760.	2.015	62.139	46592.	21694.	767.	41226.	21707.	3.077
352	BISINON	ZM		251521	694507	528.	2.105	63.060	46905.	21206.	805.	41830.	21221.	3.054
353	JUCKENEN	ZM		248789	706656	677.	2.000	63.031	46912.	21247.	742.	41818.	21260.	3.019
354	WALD	ZM		239511	710676	888.	2.076	62.583	46876.	21287.	790.	41756.	21302.	3.118
355	EINSIEDELN	SZ		223171	699935	936.	2.096	62.504	46833.	21363.	806.	41669.	21378.	3.074
356	VONDEKTHAL	SZ		219380	711205	765.	2.056	62.484	46822.	21383.	782.	41647.	21347.	3.099
357	NAEFELS	GL		216149	723174	443.	2.026	62.462	46827.	21413.	764.	41637.	21426.	3.137
358	SCHILSTAL	SG		213024	740237	1139.	1.581	62.465	46828.	21410.	736.	41640.	21423.	3.191
359	KUNKELS	SG		194350	751145	1068.	1.522	62.375	46667.	21447.	700.	41441.	21458.	3.192
360	VUKALP	SG		225649	747651	1165.	1.565	62.525	46857.	21351.	724.	41703.	21364.	3.219
361	MESSLAU	SG		231432	733204	756.	2.041	62.350	46867.	21324.	770.	41728.	21338.	3.212
362	WATTWIL	SG		240939	725759	838.	2.024	62.593	46881.	21279.	758.	41767.	21242.	3.153
363	UMHAESCH	AM		239774	738520	859.	1.546	62.562	46901.	21327.	711.	41766.	21339.	3.149
364	WASSCHAUEN	AI		238829	750273	877.	1.581	62.571	46883.	21307.	732.	41755.	21320.	3.252
365	TRUGEN	AR		251890	752700	908.	1.533	63.041	46932.	21245.	700.	41842.	21257.	3.220
368	MOHN	TO		262344	751437	402.	1.544	63.091	46971.	21202.	706.	41908.	21214.	3.225
367	EDLISCHWIL	SG		260837	741665	573.	1.569	63.095	46971.	21196.	721.	41910.	21209.	3.193
368	FLAWIL	SG		251579	732779	654.	2.023	63.025	46941.	21267.	757.	41840.	21280.	3.195
369	ISTIGHOFEN	TG		266690	728694	444.	2.050	63.125	46963.	21154.	770.	41922.	21168.	3.200
370	BOTTIGSHOFEN	TG		276817	733427	456.	2.018	63.182	46994.	21100.	748.	41984.	21113.	3.197
371	ANETSCHWIL	TG		262649	716240	526.	2.035	63.124	46940.	21146.	760.	41900.	21159.	3.112
372	UESSLINGEN	TO		271620	705573	492.	2.059	63.151	46965.	21123.	774.	41939.	21138.	3.074
373	ROSSENGES	VD		167590	549277	709.	2.482	62.260	46489.	21488.	1052.	41211.	21514.	2.191
374	LE CMET	FR		162265	558810	908.	3.019	62.236	46586.	21558.	1142.	41282.	21588.	2.363
375	MAU PACCOT	VD		155340	549099	743.	3.164	62.205	46792.	21685.	1240.	41445.	21721.	2.473
376	BOTTENS	VD		163412	540005	726.	2.509	62.285	46475.	21451.	1067.	41214.	21478.	2.166
377	APPLES	VD		155569	521764	658.	2.484	62.199	46528.	21579.	1058.	41208.	21605.	2.037
378	CHUVILLY	VD		165738	525955	593.	2.512	62.239	46534.	21533.	1073.	41238.	21560.	2.088
379	UNTERHEID II	DE		176890	653240	580.	2.199	62.308	46676.	21525.	876.	41407.	21543.	2.505
380	FURKA	UR		160090	676430	1964.	2.283	62.181	46494.	21591.	932.	41166.	21611.	3.120
381	BEDRETTO	TI		150069	681525	1460.	2.078	62.073	46579.	21765.	810.	41173.	21780.	2.544
382	BLITZINGEN II	VS		143729	658939	1255.	2.176	62.078	46552.	21744.	871.	41152.	21762.	2.512
383	BINN II	VS		135625	658860	1478.	2.133	62.068	46492.	21729.	843.	41093.	21745.	2.468
384	TERMEN	VS		131180	645200	965.	2.079	62.123	46500.	21668.	807.	41135.	21683.	2.336
385	VISP II	VS		127619	632279	646.	2.204	62.008	46530.	21817.	892.	41089.	21835.	2.368
386	SAAS BALEN	VS		111829	637689	1475.	2.246	61.495	46387.	21883.	921.	40891.	21902.	2.460
387	FAPLEKALP II	VS		142220	631619	1688.	2.258	62.076	46564.	21750.	923.	41162.	21770.	2.438
388	TUKTMANNAL	VS		118139	620790	1810.	2.254	61.525	46372.	21840.	924.	40896.	21860.	2.372
389	LEUKERBAD II	VS		135574	614139	1328.	2.282	62.043	46517.	21767.	939.	41099.	21787.	2.363
390	ILLGNABEN II	VS		126664	614869	854.	2.317	61.569	46485.	21839.	964.	41024.	21860.	2.402
391	RAMIL	VS		133810	598580	1810.	2.355	62.031	46481.	21762.	985.	41060.	21784.	2.347
392	ZINAL II	VS		108119	614965	1688.	2.247	61.448	46323.	21909.	923.	40804.	21928.	2.332
393	SATANNA II	VS		99125	603779	1838.	2.301	61.437	46193.	21859.	955.	40683.	21879.	2.322
394	GRANGES II	VS		123139	602110	503.	2.317	61.564	46489.	21847.	965.	41024.	21868.	2.329
395	CLEUSON LAC	VS		106039	591310	2190.	2.361	61.459	46328.	21895.	995.	40816.	21917.	2.312
396	BRANCHE II	VS		90079	574650	1408.	2.421	61.410	46309.	21942.	1035.	40768.	21966.	2.278
397	SALES	FR		164010	563955	842.	2.526	62.206	46576.	21592.	1085.	41254.	21619.	2.320
398	MOILLERTSON	FR		153255	563959	1134.	2.519	62.135	46581.	21680.	1085.	41214.	21707.	2.313
399	BLUNAY	VD		150125	558619	826.	2.556	62.085	46571.	21734.	1111.	41174.	21762.	2.320
400	LUTRY	VD		151314	543959	658.	3.048	62.167	46902.	21786.	1172.	41518.	21818.	2.328
401	SULLENS	VD		160685	533974	600.	2.470	62.268	46531.	21499.	1045.	41253.	21524.	2.092
402	NAZ	VD		168045	543194	663.	2.541	62.234	46510.	21527.	1091.	41214.	21555.	2.215
403	GRANCHEN II	SO		225720	596220	463.	2.364	62.094	46782.	21345.	972.	41617.	21367.	2.342
404	GRANCHEN III	SO		224885	597069	429.	2.357	62.502	46782.	21335.	967.	41622.	21357.	2.340
405	ALTREU	SO		226859	601709	428.	2.364	62.505	46780.	21331.	971.	41622.	21353.	2.374
406	RHEINFELDEN	AG		268950	633095	343.	2.297	63.102	46942.	21167.	922.	41889.	21187.	2.490
407	BAUMA	ZM		247220	709830	650.	2.029	63.029	46904.	21245.	760.	41810.	21259.	3.067
408	LEGGENSWIL	SG		258614	727220	527.	1.596	63.084	46954.	21202.	738.	41888.	21214.	3.136
409	NESSLAU II	SG		230909	734715	850.	1.585	62.547	46871.	21331.	736.	41730.	21343.	3.165
410	MAIENFELD	GR		207960	759955	572.	1.510	62.440	46810.	21434.	692.	41609.	21445.	3.233
411	GINZEN	GL		206539	727200	628.	1.596	62.424	46800.	21447.	746.	41590.	21460.	3.130
412	KALTBRUNN	SG		231850	719889	571.	2.004	62.546	46863.	21328.	747.	41722.	21341.	3.098
413	KONKORDIA	VS		150479	644729	2750.	2.175	62.132	46534.	21671.	867.	41171.	21688.	2.442
414	AARGLETSCHE	BE		157500	656779	2400.	2.134	62.152	46561.	21661.	841.	41207.	21677.	2.459
415	CRESTA	GM		148824	759415	1950.	1.508	62.161	46589.	21668.	697.	41238.	21679.	3.216
416	VAL MADRIS	GR		141747	758668	1964.	1.490	62.143	46544.	21669.	687.	41186.	21680.	3.195
417	MAHMURERA	GM		150448	769244	1713.	3.070	62.233	46109.	21339.	1162.	40858.	21370.	4.437
418	TGAVHETGA	GM		146449	770465	1943.	4.432	62.140	46264.	21551.	271.	40937.	21553.	2.205
419	JULIENPASS	GM		149074	774793	2015.	1.481	62.194	46674.	21668.	682.	41334.	21679.	3.279
420	PLAUN DA LEJ	GM		143680	775744	1820.	1.532	61.120	46823.	22545.	743.	41031.	22557.	3.335
421	VAL FORNO	GM		138670	774488	1911.	1.330	62.109	46434.	21661.	586.	41068.	21669.	3.125
422	CASACCIA	GM		140108	771080	1470.	1.525	62.124	46510.	21675.	710.	41144.	21687.	3.301
423	ST MORITZ	GM		151707	783387	1965.	2.008	62.168	46720.	21718.	763.	41358.	21732.	3.456
424	VIANO	GM		125670	808753	1330.	2.090	62.079	47086.	21494.	826.	41625.	22010.	4.078
425	PHAUDA	GM		130755	801744	1360.	4.286	65.054	45996.	14314.	1512.	41717.	14373.	6.235

NO	SITE	L	CANTON	X COORD	Y COORD	ALT	DECL	INCL	TOT F	X	Y	Z	M	OK
426	RAVISCÉ	GM		136560	802680	1242.	1.234	62.207	46163.	21420.	520.	40889.	21426.	3.189
427	SFAZU	GM		140670	802965	1548.	1.261	62.171	46386.	21566.	540.	41064.	21573.	3.214
428	VAL CHAMUEHA	GM		158750	794330	1938.	1.374	62.194	46698.	21682.	614.	41355.	21690.	3.246
429	ALBULAPASS	GM		161220	781055	2068.	1.425	62.249	46568.	21554.	643.	41274.	21564.	3.261
430	ANTROPIANA	I		100420	651474	1088.	2.308	61.540	46855.	22048.	968.	41332.	22069.	2.600
431	CESANA	I		74789	672770	568.	2.076	61.401	46401.	22006.	817.	40843.	22021.	2.486
432	FOHNO	I		86849	666189	808.	1.462	62.804	46429.	21782.	673.	40997.	21792.	2.236
433	FOBELLO	I		84659	653959	1108.	2.046	61.423	46226.	21897.	794.	40703.	21912.	2.351
434	VALDUGGIA	I		63400	667439	354.	2.314	61.480	46307.	21861.	963.	40811.	21882.	3.094
435	INVOMIO	I		67469	682810	315.	2.144	61.344	46387.	22065.	863.	40794.	22082.	3.010
436	ALBIZZATE	I		64940	705229	340.	2.120	61.353	46384.	22053.	847.	40797.	22070.	3.112
437	VEDDASCA	I		103519	703598	1186.	2.308	61.543	46466.	21861.	960.	40991.	21882.	3.295
438	LUINO	I		92875	701508	206.	2.138	61.445	46508.	22002.	857.	40965.	22019.	3.112
439	BISUSCHIO	I		82500	711543	345.	2.092	61.405	46413.	22006.	827.	40856.	22022.	3.122
440	MASNAGO	I		75969	705029	378.	2.114	61.382	46383.	22019.	842.	40815.	22035.	3.106
441	TRAVEDONA	I		74193	694715	212.	2.133	61.384	46393.	22021.	854.	40825.	22037.	3.067
442	STRESA	I		79119	683770	648.	2.136	61.416	46402.	21987.	855.	40853.	22003.	3.009
443	CICOGNA	I		95255	681950	648.	2.142	61.407	46430.	22011.	860.	40872.	22027.	3.006
444	PIANCOMPRA	I		95454	691974	1202.	2.111	61.474	46518.	21973.	838.	40993.	21989.	3.032
445	FINERO	I		106644	685334	838.	1.434	62.879	46314.	21639.	651.	40943.	21649.	2.318
446	BUTTOGNO	I		110019	677569	895.	1.594	61.572	46344.	21777.	757.	40902.	21790.	2.434
447	NIVASCO	I		130158	672927	835.	2.204	62.054	46640.	21813.	891.	41215.	21831.	3.019
448	CRODO	I		117434	668215	418.	2.120	62.012	46448.	21776.	837.	41019.	21792.	2.508



## Map Captions

The following applies to Maps 1 to 9:

The data are always reduced to epoch 1978.0. In the small areas bordered with a broken line the data are unreliable: these are highly perturbed zones which have not been surveyed with a network of stations sufficiently dense to permit the correct contour pattern to be traced. The maps are all to the scale of 1:1 250 000, one centimeter thus represents 12.5 km. The contour parameters are in sexagesimal degrees and/or minutes, or in  $nT^{10}$ .

**Map 1.** Isogonic chart, i.e. contours of equal declination  $D$  with respect to geographic North.

**Map 2.** Isoclinic chart, i.e. contours of equal inclination  $I$ .

**Map 3.** Isodynamic chart, i.e. contours of equal field amplitude or total intensity  $F$ .

**Map 4.** Chart of declination  $D_K$  with respect to kilometric grid North, sometimes also called map North.

**Map 5.** Chart of horizontal component  $H$ , sometimes called horizontal intensity.

**Map 6.** Chart of vertical component  $Z$ , sometimes called vertical intensity.

**Map 7.** Chart of declination anomalies  $\Delta D = D - D_{\text{normal}}$ . This is often called residual declination.  $D_{\text{normal}}$  is specified in Table Va.

**Map 8.** Chart of inclination anomalies  $\Delta I = I - I_{\text{normal}}$ . This is often called residual inclination.  $I_{\text{normal}}$  is specified in Table Va.

**Map 9.** Chart of amplitude anomalies  $\Delta F = F - F_{\text{normal}}$ . This is often called residual amplitude or residual total intensity.  $F_{\text{normal}}$  is specified in Table Va.

**Map 10.** Location of survey stations.

Achevé d'imprimer sur les presses  
de l'imprimerie Paul Attinger SA, à Neuchâtel.  
le 20 octobre 1979.

# Contributions to the Geology of Switzerland Beiträge zur Geologie der Schweiz Matériaux pour la Géologie de la Suisse

Geophysics – Geophysik – Géophysique

No.		Fr.
1	<b>H. Röthlisberger.</b> Zur seismischen und petrographischen Charakterisierung einiger Molassegesteine, einschliesslich der Beschreibung von Methoden der Korngrössenbestimmung in Festmaterial. 91 Seiten, 31 Figuren. 1957 . . . . .	14.–
2	<b>O. Friedenreich.</b> Eine grossräumige Widerstandskartierung nordwestlich von Zürich und ihre geologische Deutung. 47 Seiten, 22 Textfiguren, 9 Karten. 1959 . . . . .	20.–
3	<b>F. Gassmann.</b> Schweremessungen in der Umgebung von Zürich. 70 Seiten, 24 Textfiguren, 2 Tafeln. 1962 . . . . .	24.–
4	<b>E. Poldini.</b> Les Anomalies gravifiques du canton de Genève. Avec 63 pages, 25 figures et 3 planches. 1963 . . . . .	24.–
5	<b>L. Rybach.</b> Refraktionssismische Untersuchungen im Raum Aare-, Limmat- und Surbtal. 49 Seiten, 42 Figuren. 1962 . . . . .	14.–
6	<b>O. Gonet.</b> Etude gravimétrique de la plaine du Rhône. Région Saint-Maurice–Lac Léman. 50 pages, 30 figures, 2 planches. 1965 . . . . .	14.–
7	<b>C. Meyer de Stadelhofen.</b> Carte des résistivités de la plaine du Rhône. 8 pages, 2 figures, 2 planches. 1966 . . . . .	8.–
8	<b>O. Gonet.</b> Etude gravimétrique du lac Léman à bord du mésoscaphe «Auguste Piccard». 20 pages, 8 figures, 1 planche. 1969 . . . . .	8.–
9	<b>J.-J. Wagner.</b> Elaboration d'une carte d'anomalie de Bouguer. Etude de la vallée du Rhône de Saint-Maurice à Saxon (Suisse). 91 pages, 32 figures, 2 planches. 1970 . . . . .	22.–
10	<b>H. Lazreg.</b> Etude géophysique, géologique et hydrogéologique de la région de Concise à Pompaples (pied du Jura vaudois). 51 pages, 16 figures, 7 planches. 1971 . . . . .	22.–
11	<b>M. Petch.</b> Contribution à l'étude hydrogéologique de la plaine de l'Orbe. 95 pages, 23 figures, 15 planches. 1970 . . . . .	22.–
12	<b>P.-A. Gilliand.</b> Etude géoélectrique du Klettgau (Suisse), canton de Schaffhouse. 85 pages, 47 figures, 10 annexes, 5 planches. 1970 . . . . .	22.–
13	<b>P. Corniche.</b> Application des méthodes géophysiques à la recherche hydrogéologique. 65 pages, 25 figures. 1973 . . . . .	22.–
14	<b>F. Heller.</b> Magnetische und petrographische Eigenschaften der granitischen Gesteine des Albignagebietes (Nördliches Bergeller Massiv). 66 Seiten, 24 Textfiguren. 1972 . . . . .	22.–
15	<b>E. Klingelé.</b> Contribution à l'étude gravimétrique de la Suisse romande et des régions avoisinantes. 94 pages, 6 figures, 35 planches. 1972 . . . . .	22.–
16	<b>W. Sigrist.</b> Contribution à l'étude géophysique des fonds du lac Léman. 56 pages, 28 figures, 1 planche. 1974 . . . . .	22.–
17	<b>R. Olivier.</b> Elaboration d'un système de traitement gravimétrique géré par l'ordinateur. Etude gravimétrique du plateau romand de Versoix (GE) à Concise (VD). 56 pages, 21 figures, 10 planches. 1974 . . . . .	22.–
18	<b>H. Buchli, R. Paquin, A. Donzé.</b> Etude géoélectrique et gravimétrique du Chablais entre Anières et Evian. 170 pages, 81 figures, 4 planches. 1976 . . . . .	32.–
19	<b>G. Fischer, P.-A. Schneegg, J. Sesiano.</b> A new geomagnetic survey of Switzerland. 44 pages, 15 figures, 8 tables, 10 cartes. 1979 . . . . .	28.–

## MAP CAPTIONS

The following applies to Maps 1 to 9:

The data are always reduced to epoch 1978.0. In the small areas bordered with a broken line the data are unreliable: these are highly perturbed zones which have not been surveyed with a network of stations sufficiently dense to permit the correct contour pattern to be traced. The maps are all to the scale of 1:1 250 000, one centimeter thus represents 12.5 km. The contour parameters are in sexagesimal degrees and/or minutes, or in  $nT^{10}$ .

**Map 1.** Isogonic chart, i.e. contours of equal declination  $D$  with respect to geographic North.

**Map 2.** Isoclinic chart, i.e. contours of equal inclination  $I$ .

**Map 3.** Isodynamic chart, i.e. contours of equal field amplitude or total intensity  $F$ .

**Map 4.** Chart of declination  $D_K$  with respect to kilometeric grid North, sometimes also called map North.

**Map 5.** Chart of horizontal component  $H$ , sometimes called horizontal intensity.

**Map 6.** Chart of vertical component  $Z$ , sometimes called vertical intensity.

**Map 7.** Chart of declination anomalies  $\Delta D = D - D_{\text{normal}}$ . This is often called residual declination.  $D_{\text{normal}}$  is specified in Table Va.

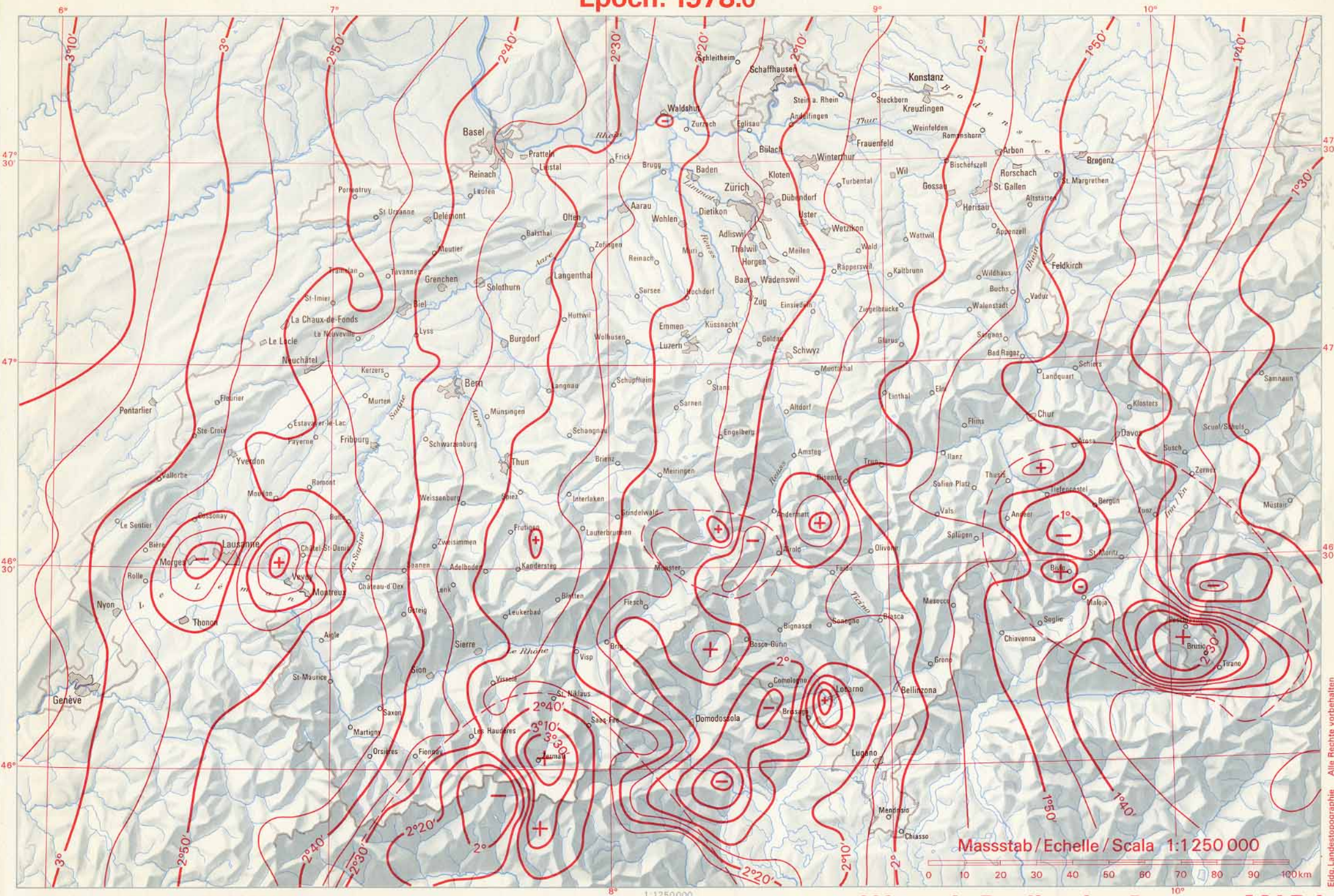
**Map 8.** Chart of inclination anomalies  $\Delta I = I - I_{\text{normal}}$ . This is often called residual inclination.  $I_{\text{normal}}$  is specified in Table Va.

**Map 9.** Chart of amplitude anomalies  $\Delta F = F - F_{\text{normal}}$ . This is often called residual amplitude or residual total intensity.  $F_{\text{normal}}$  is specified in Table Va.

**Map 10.** Location of survey stations.

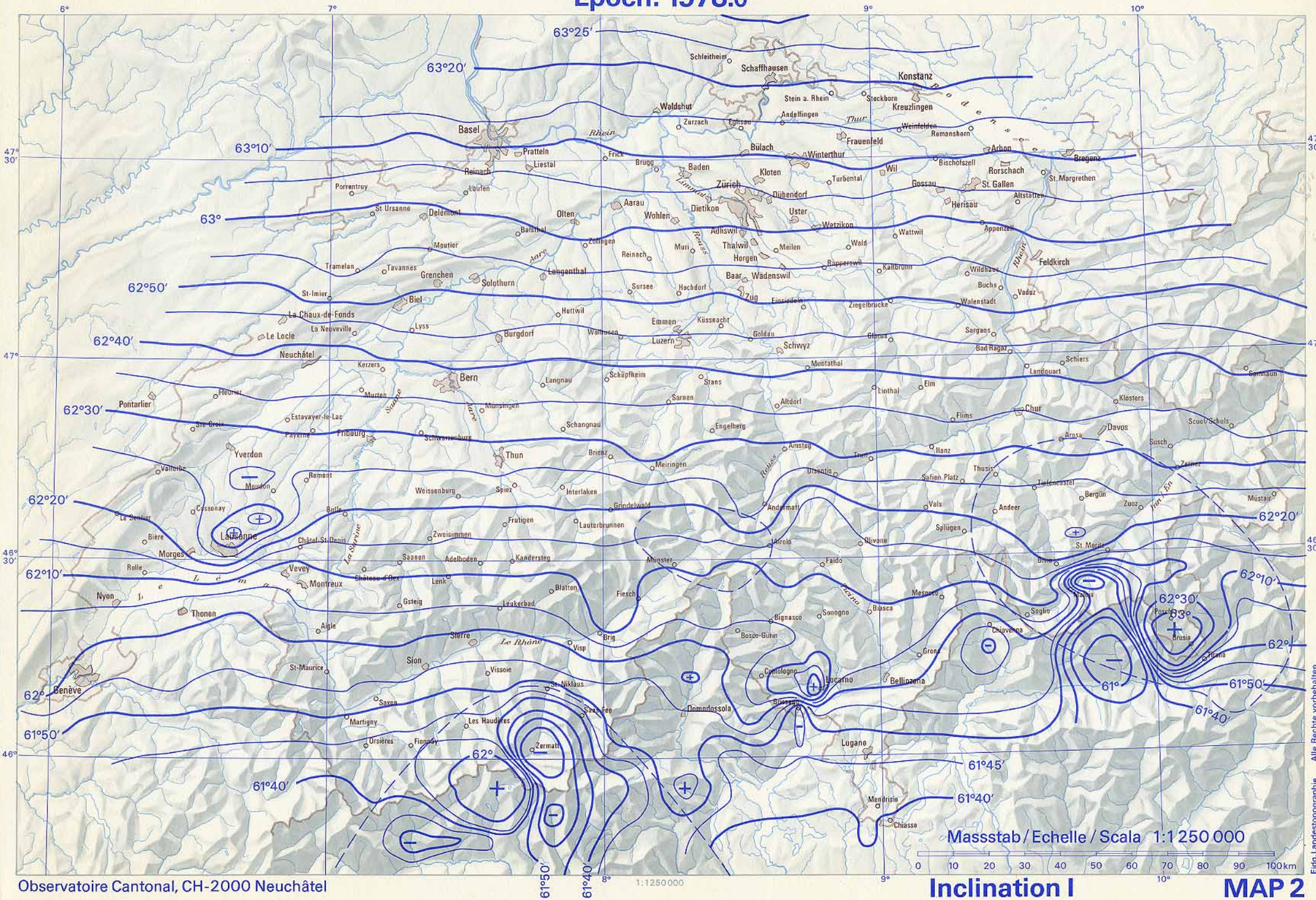


Epoch: 1978.0



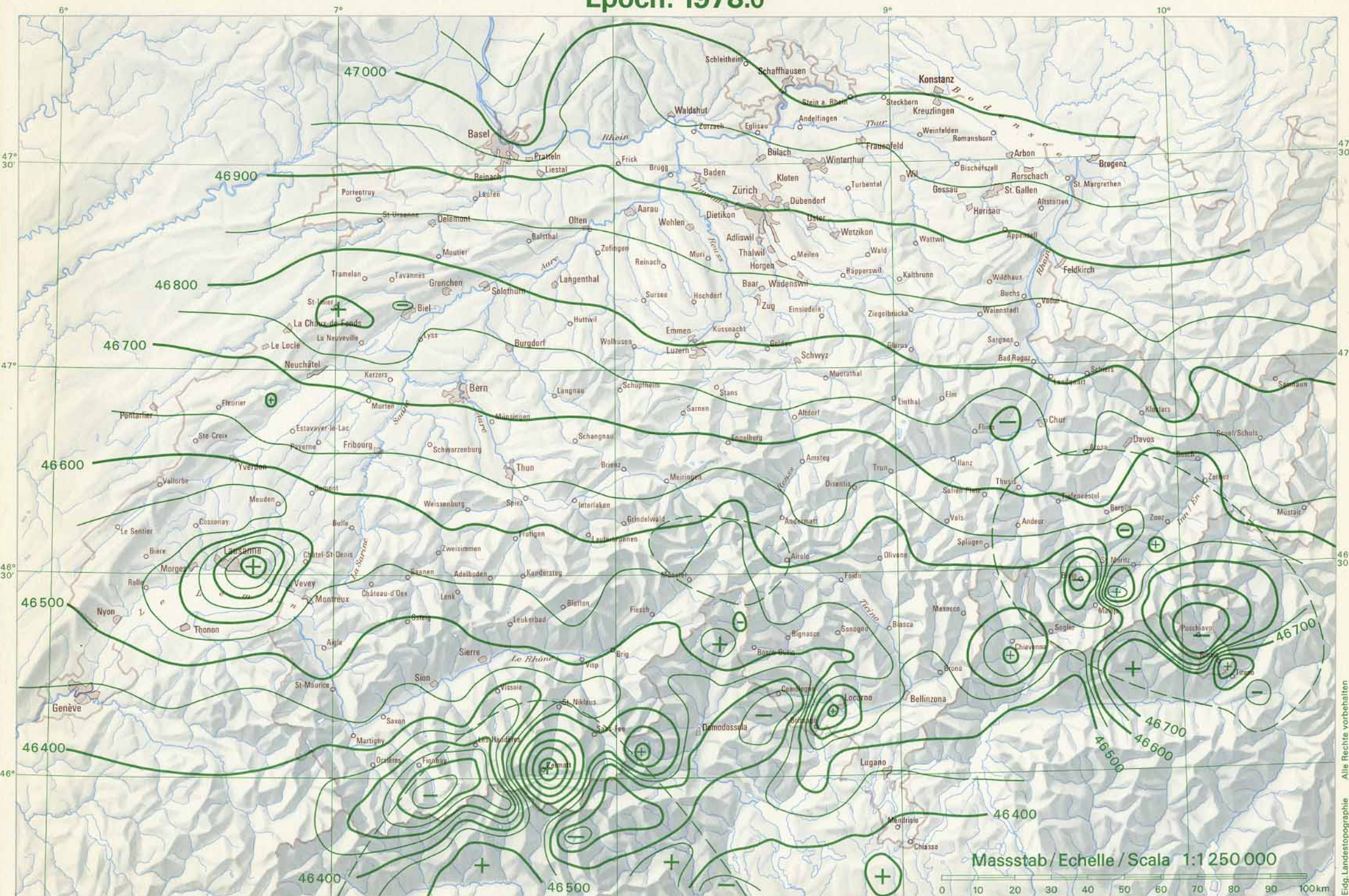


Epoch: 1978.0





Epoch: 1978.0

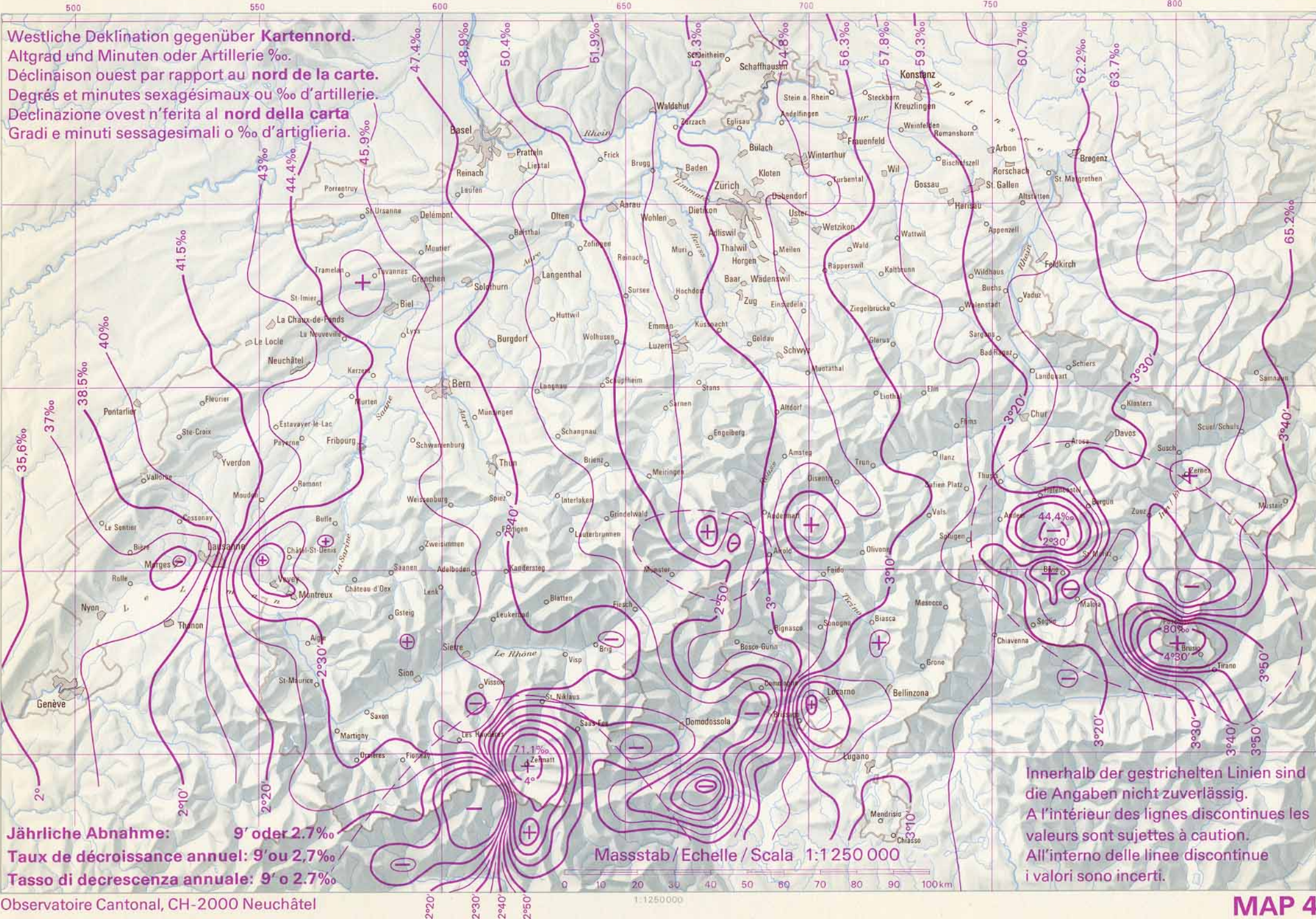




# Declination from Map North DK

Epoch: 1978.0

Westliche Deklination gegenüber Kartennord.  
Altgrad und Minuten oder Artillerie ‰.  
Déclinaison ouest par rapport au nord de la carte.  
Degrés et minutes sexagésimaux ou ‰ d'artillerie.  
Declinazione ovest n'ferita al nord della carta  
Gradi e minuti sessagesimali o ‰ d'artiglieria.



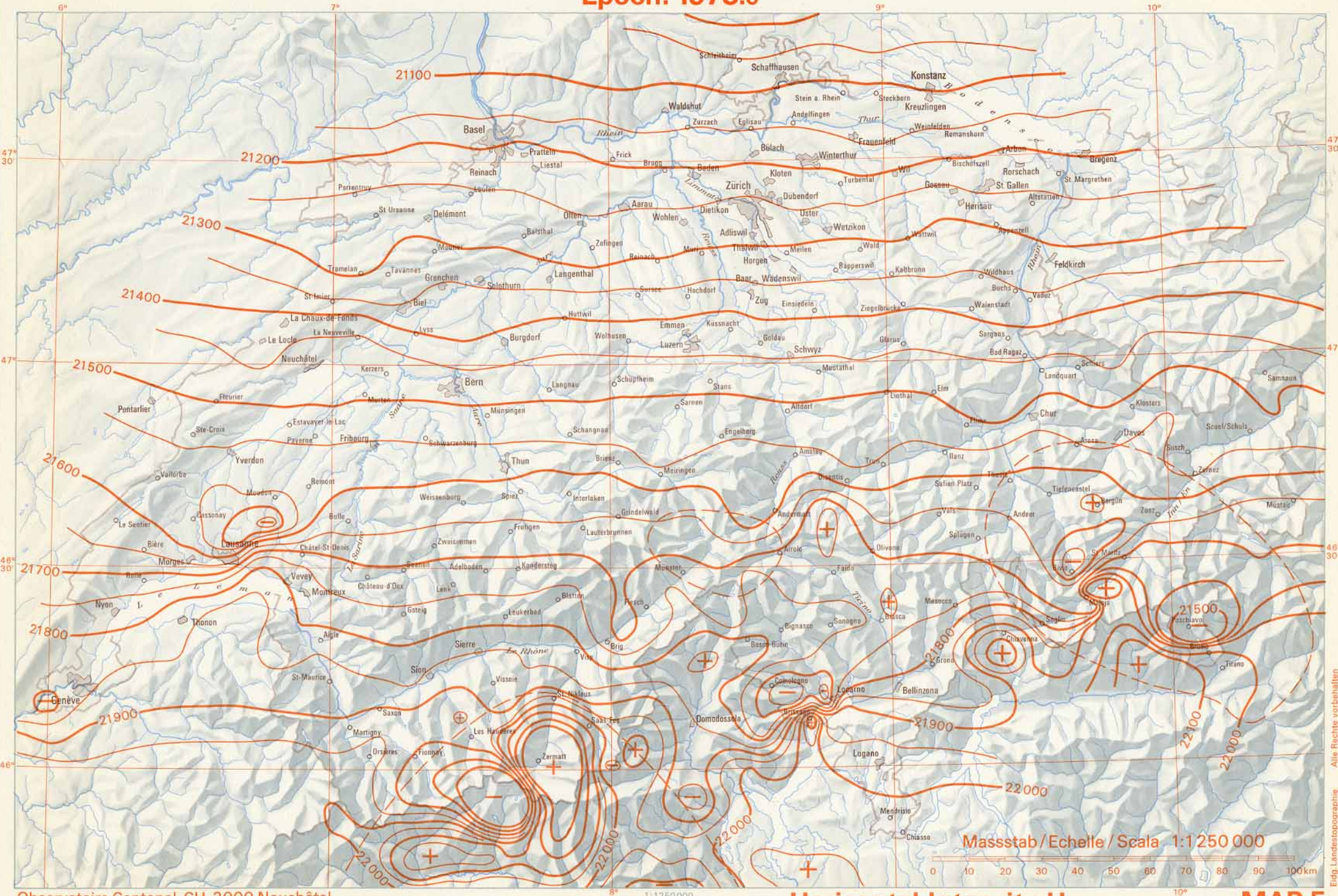
Jährliche Abnahme: 9' oder 2.7‰  
Taux de décroissance annuel: 9' ou 2.7‰  
Tasso di decrescenza annuale: 9' o 2.7‰

Masstab / Echelle / Scala 1:1 250 000

Innerhalb der gestrichelten Linien sind die Angaben nicht zuverlässig.  
A l'intérieur des lignes discontinues les valeurs sont sujettes à caution.  
All'interno delle linee discontinue i valori sono incerti.

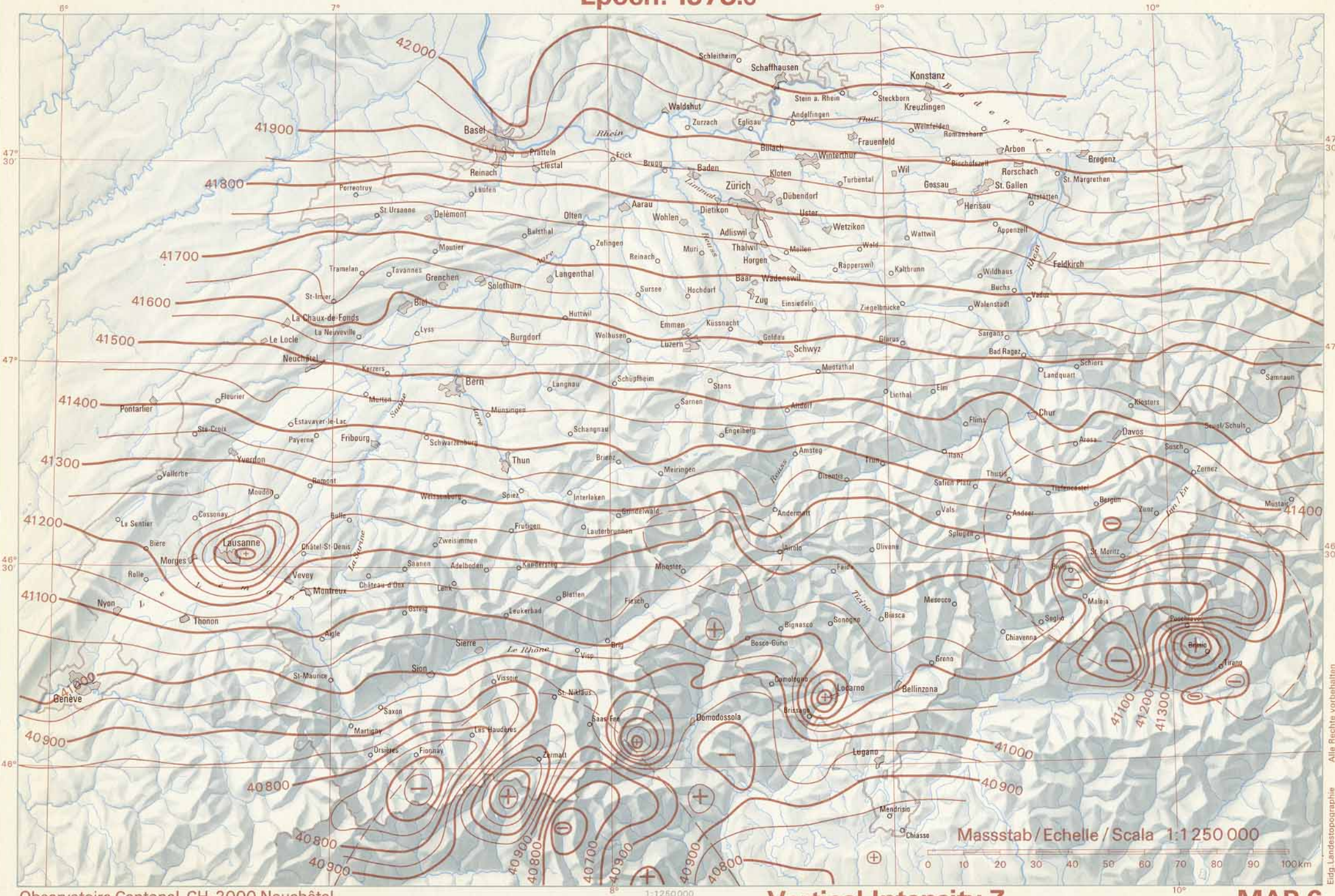


Epoch: 1978.0



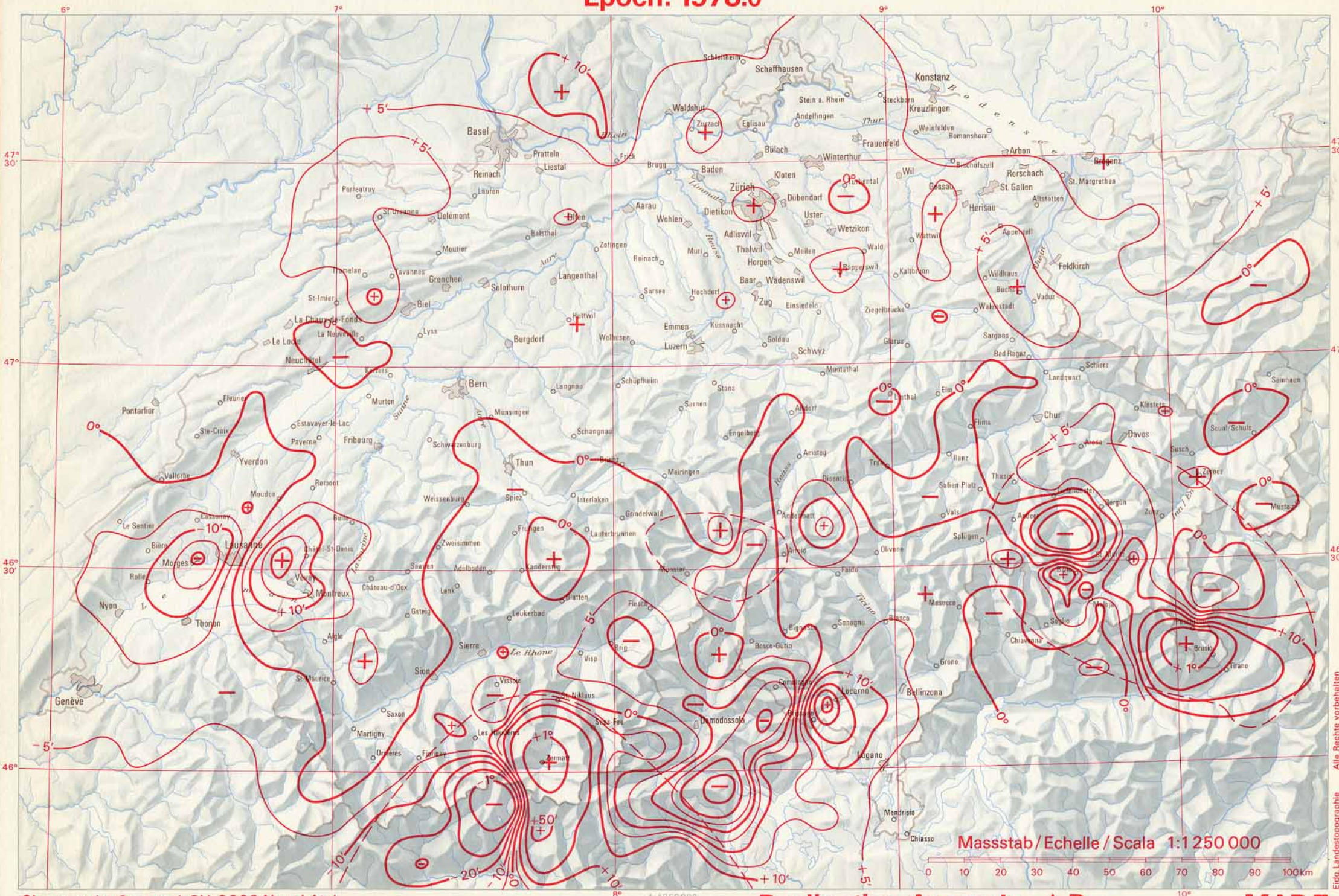


Epoch: 1978.0



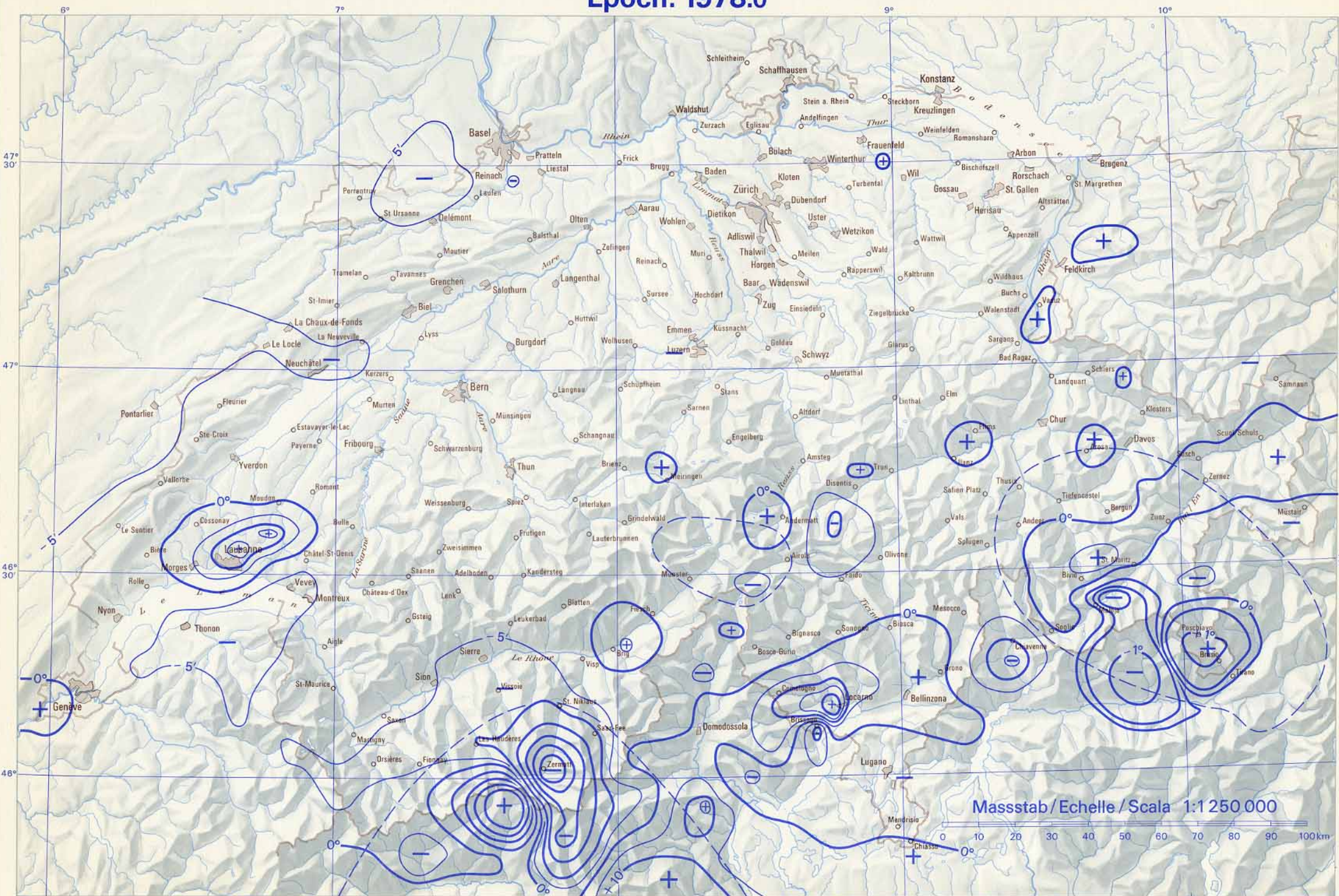


Epoch: 1978.0



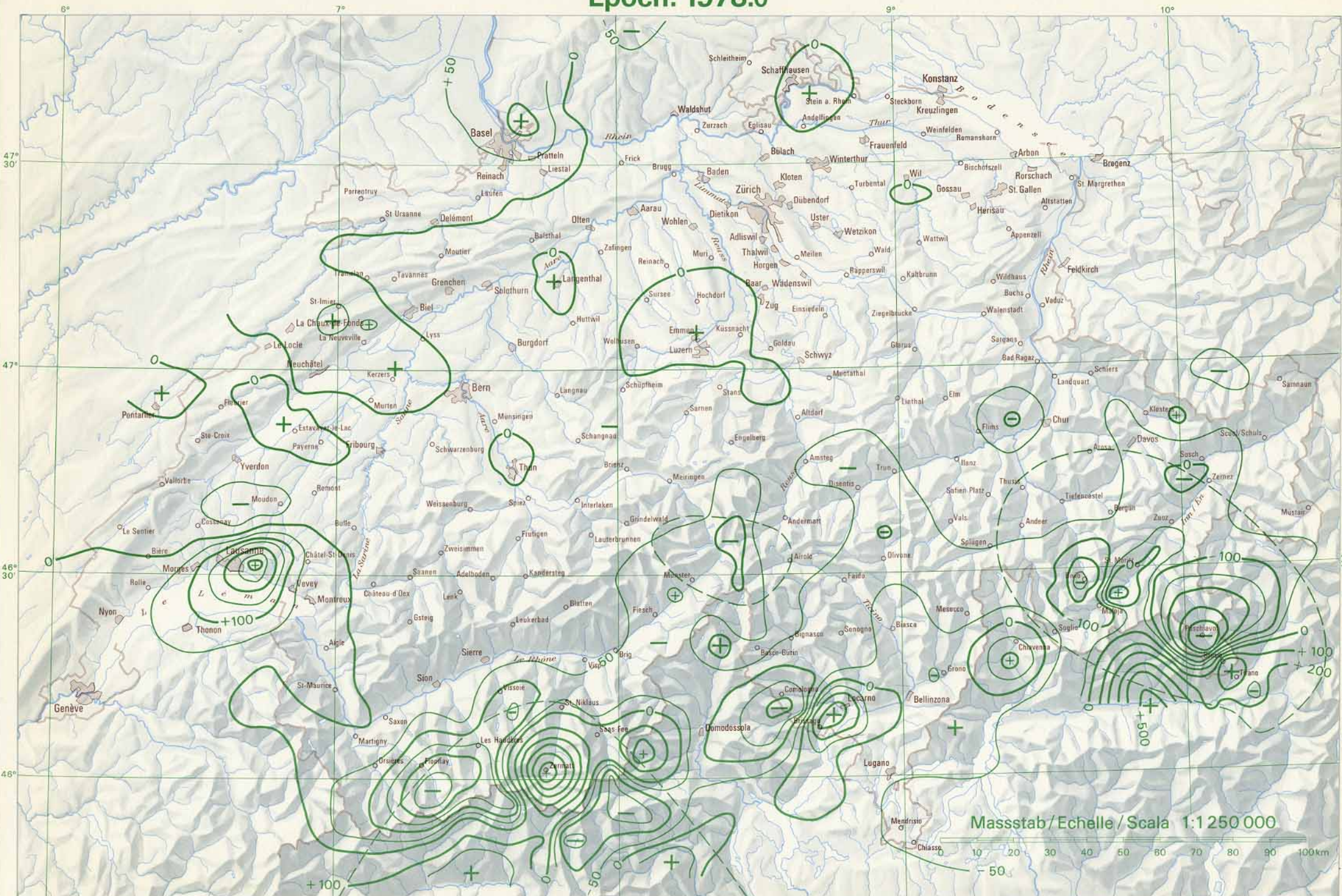


Epoch: 1978.0





Epoch: 1978.0





# Period of observations 1974–1977



Observatoire Cantonal, CH-2000 Neuchâtel

Massstab / Echelle / Scala 1:1250 000  
 0 10 20 30 40 50 60 70 80 90 100 km  
 Survey Stations (x, y) MAP 10